

From the Department of Medical Biochemistry and Biophysics
Karolinska Institutet, Stockholm, Sweden

IDENTIFICATION AND CHARACTERIZATION OF KIDNEY GLOMERULUS-ASSOCIATED GENES AND PROTEINS

Perisic Ljubica



**Karolinska
Institutet**

Stockholm 2012

Previously published papers were reproduced with permission from the publisher.
Published by Karolinska University Press. Box 200, SE-171 77 Stockholm, Sweden
Printed by Reproprint AB, Gårdsvägen 4, 169 70 Solna, www.reproprint.se
© Perisic Ljubica, 2012
ISBN 978-91-7457-804-1

To my father

SUMMARY

The kidney glomerulus is a micro-organ comprised of a molecular filtration barrier that prevents the loss of blood proteins into the primary filtrate. This function is dependent on the coordination of its three constituent layers: the endothelium, the glomerular basement membrane and the podocytes. While each of the three layers contributes to the permselectivity of the glomerular filtration barrier, the podocyte forms the final barrier to filtration.

Many glomerulus-enriched proteins have been implicated in the pathogenesis of renal diseases. We have identified over 300 glomerulus-upregulated genes using expressed sequence tag profiling and microarray analysis, in order to discover new genes with important roles in glomerular filtration. Two of the proteins were characterized further in this study.

Plekhh2 is an intracellular protein with two PH, MyTH and FERM domains, highly enriched in the podocytes and testes, for which no function has previously been ascribed. We studied by immunoelectron microscopy Plekhh2 distribution in the human glomerular filter and found that its expression was reduced in focal segmental glomerulosclerosis. Heterologously expressed Plekhh2 localizes to the peripheral regions of lamellipodia in cultured podocytes and its PH1 domain contains a PIP3 consensus-binding site. The N-terminal half of Plekhh2 is not required for targeting to lamellipodia but it rather mediates Plekhh2 self-association. By yeast two-hybrid analysis we identified two Plekhh2 interacting partners: Hic-5, a focal adhesion protein, and actin. Plekhh2 and Hic-5 coprecipitate and colocalize at the soles of podocyte foot processes *in situ* and endogenous Hic-5 partially relocates from focal adhesions to lamellipodia in Plekhh2-expressing podocytes. We

also found that Plekhh2 stabilizes the cortical actin cytoskeleton by attenuating actin depolymerization. Plekhh2, Hic5 and actin show parallel expression changes in two mouse models of glomerular damage.

Schip1 is a coiled-coil protein previously discovered through association studies with schwannomin (Nf2, merlin) in the mouse brain, shown to be responsive to PDGF β stimulation. We have identified Schip1 as a highly enriched kidney glomerulus transcript in the podocytes, and investigated its functions in this context. We show that Schip1 promotes migration of cells in response to PDGF β stimulation and accumulation of cortical actin. In cultured podocytes, Schip1 localizes to lamellipodia periphery, closely overlapping the cortical actin. Actin disassembly by latrunculin A treatment, could not be prevented by Schip1 expression, but the protein colocalized to remaining actin fibers. Strikingly, by yeast two-hybrid, coprecipitations and FRET we discovered that Schip1 interacts with Nherf2/ezrin. This is a well characterized podocyte protein complex, forming a supporting net for docking actin filaments in the foot processes by binding to podocalyxin and/or PDGFr β cytoplasmic tails. Furthermore, we show by comparative microarray studies, that the expression of Schip1 and its associated proteins is affected in a similar manner in several mouse models of human glomerular diseases.

Our experiments suggest that both Plekhh2 and Schip1 are involved in actin assembly dynamics at the leading edge of cellular extensions. We propose that these proteins are associated to the complex podocyte foot process actin network. The discovery and characterization of novel glomerular genes and proteins presented in this thesis, has contributed to our understanding of glomerular biology and pathophysiology of renal diseases.

LIST OF PUBLICATIONS

- I. Patrakka J, Xiao Z, Nukui M, Takemoto M, He L, Oddsson A, PERISIC L, Kaukinen A, Al-Khalili Szigarto C, Uhlén M, Jalanko H, Betsholtz C, Tryggvason K. **Expression and subcellular distribution of novel glomerulus-associated proteins dendrin, ehd3, sh2d4a, plekhh2 and 2310066E14Rik.** *J Am Soc Nephrol*, 18(3): 689-97, 2007.
- II. PERISIC L, Lal M, Hulkko J, Hultenby K, Önfelt B, Sun Y, Duner F, Patrakka J, Betsholtz C, Uhlén M, Brismar H, Tryggvason K, Wernerson A*, Pikkarainen T*. **Plekhh2, a novel podocyte protein downregulated in human FSGS, is involved in matrix adhesion and actin dynamics.** *Equal contribution. *Kidney International (in press)*
- III. PERISIC L, Hultenby K, Sun Y, Lal M, Betsholtz C, Uhlén M, Wernerson A, Pikkarainen T, Tryggvason K, Patrakka J. **Schip1 is a Nherf2 and ezrin interacting podocyte foot process protein involved in regulation of actin dynamics in response to PDGF stimulation.** *Submitted to Laboratory Investigations*

TABLE OF CONTENTS

1	Introduction- Review of literature.....	1
1.1	Kidney.....	1
1.1.1	General structure.....	1
1.1.2	Development.....	3
1.1.3	Human glomerular diseases and mouse proteinuria models.....	6
1.2	Glomerulus.....	10
1.2.1	Cell organization.....	11
1.2.2	Filtration barrier.....	13
1.2.3	Glomerular basement membrane.....	14
1.3	Podocytes.....	16
1.3.1	Cell biology and function.....	16
1.3.2	Podocyte proteins and involvement in kidney disease.....	21
1.3.2.1	Transcription factors.....	21
1.3.2.2	Apical surface proteins.....	23
1.3.2.3	Cell-matrix adhesion and basal surface proteins.....	24
1.3.2.4	Slit diaphragm.....	27
1.3.2.5	Major and foot process cytoskeleton.....	32
1.3.3	Podocytes <i>in vitro</i>	36
1.4	Glomerular gene expression changes in diseased kidney.....	39
2	Aims of the study.....	41
3	Material and methods.....	42
4	Results and discussion.....	51
4.1	Expression of novel glomerular genes (paper I).....	51
4.2	Plekhh2 (paper II).....	53
4.3	Schip1 (paper III).....	56
5	Conclusions.....	60
6	Acknowledgements.....	62
7	References.....	68

LIST OF ABBREVIATIONS

BSA	bovine serum albumin
coIP	coimmunoprecipitation
cDNA	complementary DNA
DAPI	4', 6'-diamidino-2-phenylindole
E	embryonic day
FRET	fluorescence resonance energy transfer
FN	fibronectin
F-actin	filamentous-actin
GBM	glomerular basement membrane
GlomBase	glomerular transcript database
GlomChip	glomerular cDNA microarray chip
GlomNet	glomerular protein-protein interaction network
GFP	green fluorescent protein
HRP	horseradish peroxidase
HEK	human embryonic kidney
HPC	human podocytes
ILK	integrin-linked kinase
ISH	<i>in situ</i> hybridization
MAP	microtubule associated proteins
mRNA	messenger ribonucleic acid
NHERF2	Na ⁺ /H ⁺ - exchanger regulatory factor 2
NB	northern blot
kD	kilo Daltons
kb	kilo base pairs
PCR	polymerase chain reaction
Plekhh2	pleckstrin homology domain containing 2
PFA	paraformaldehyde
PBS	phosphate buffered saline
PI3K	phosphoinositide 3-OH kinase
RT-PCR	reverse transcript PCR
RT	room temperature

1 INTRODUCTION- REVIEW OF LITERATURE

1.1 Kidney

Kidneys are paired excretory organs situated on the retroperitoneal side of the abdominal cavity, on both sides of the spine. Their primary function is filtration of toxic substances and waste products from circulating blood plasma. Kidneys are subject to extreme physiological conditions as they normally filtrate about 180 liters of primary urine each day and have the responsibility of maintaining the body fluids osmotic pressure. Almost 99% of the primary urine is resorbed back into the plasma, with final daily urine excretion being 1-1.5 liters. In healthy individuals, this urine is devoid of any proteins of the size of albumin or larger. In addition to the plasma filtration function, the kidneys ensure proper water and electrolytes balance important for regulation of blood pressure; they have a role in vitamin metabolism and account for the production of erythropoietin (a hormone essential for red blood cell production) [1].

1.1.1 General structure

Morphologically, the kidneys are bean-shaped organs supplied with blood by a single renal artery, that branches further into a renal microcirculation network. The filtered blood leaves the urinary system also by a single vein. A cross-section through the kidney reveals two distinct zones within the kidney parenchyma: cortical and medullar (Figure 1). The process of blood filtration

occurs in the outer zone (renal cortex), and resorption and modification of the primary urine continues in the tubules in the cortex and the medullar zone, in the basic functional units of the kidney, the nephrons, that span both the cortex and medulla. Each human kidney has about one million nephrons, composed of: the glomerulus, the proximal tubule, the loop of Henley, the distal tubule and the connecting tubule. Cortical zone contains glomeruli, proximal tubules and part of the distal tubules, while medullar pyramids contain ascending and descending thin limbs and collecting ducts. Blood is filtered under pressure in the glomerulus; the filtrate then enters the renal tubules and finally leaves the nephrons by means of the collecting duct into the renal pelvis.

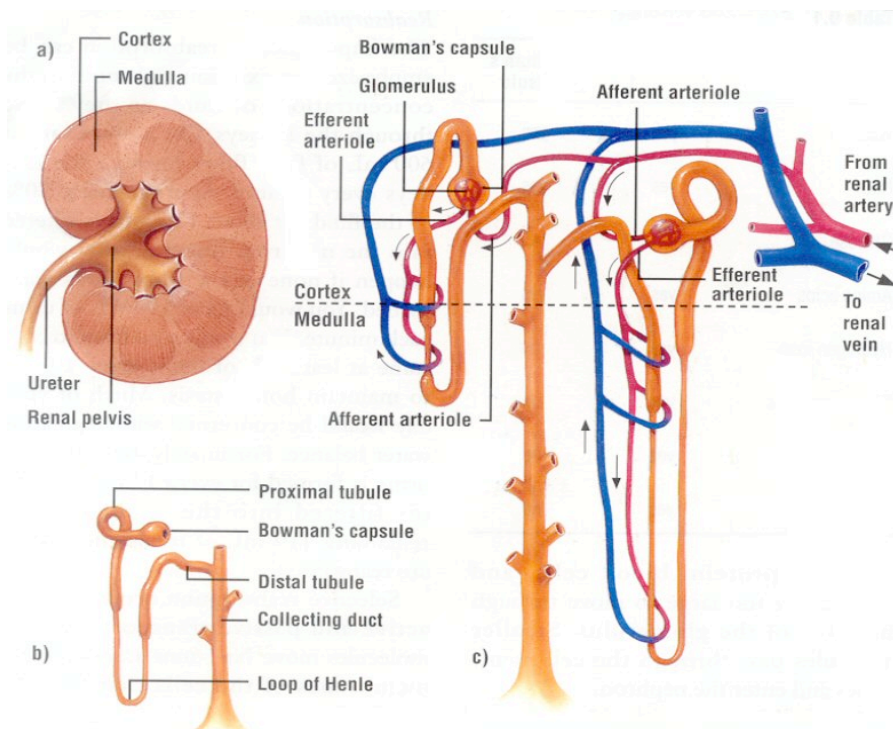


Figure 1. Schematic representation of the kidney structure showing its cortical and medullar zones (a), functional unit-nephron (b) and organization of nephron and vascular elements within the organ (c). Picture by Human Body Reviews.

1.1.2 Development

Embryonic development of the vertebrate urogenital system requires progressive formation of three stages of kidney structures by the intermediate mesoderm: the pronephros, the mesonephros and the metanephros. These three developmental kidney stages are depicted in Figure 2. The pronephros is the most primitive kidney and in humans, it is rapidly replaced already at day 24 *post coitum* (E9.5 in mice) by the mesonephros, which functions also shortly during embryonic development. In females, regression of mesonephros is complete, whereas in males it is partial and its remains will give rise to the genital organs [2]. Metanephric kidney development is initiated around midgestation, 28th day *post coitum* (E10.5 in mice) when the epithelial thickening called the ureteric bud forms and elongates to invade the adjacent metanephric mesenchyme, blastema [3].

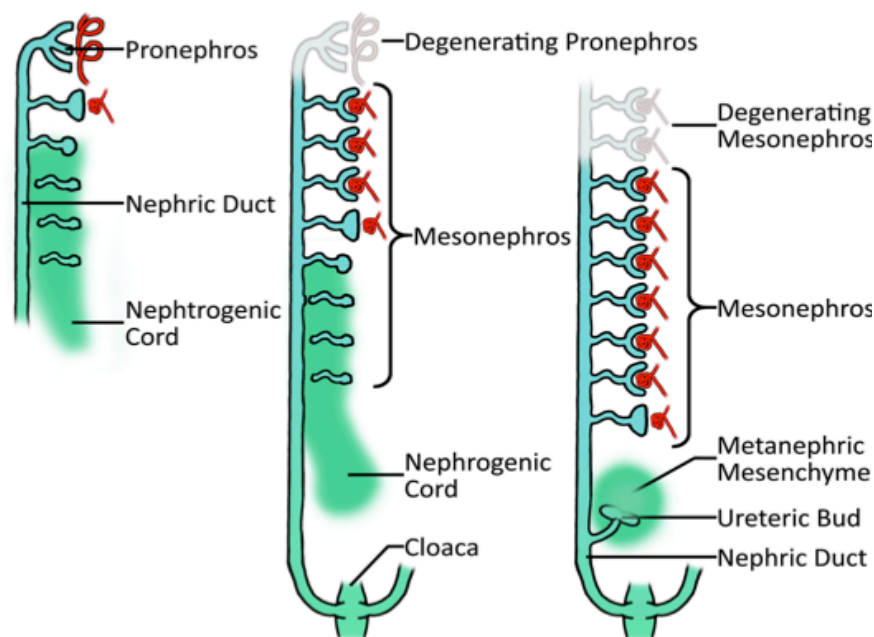


Figure 2. Embryonic stages of kidney organogenesis. Picture by Creative Commons Attribution.

Interactions between the ureteric bud and blastema lead to complex epithelial-mesenchymal signaling, critical for the initiation of outgrowth and branching of the ureteric bud on one side, and formation of nephron precursors on the other side [4] (Figure 3). These signaling events are regulated by a network of transcription and growth factors, and modulated by cell adhesion molecules [5]. Several branching steps take place successively until the characteristic tree-like structure of the mature collecting system is formed. In the first phase of ureteric bud branching, the primary cortex tubules are generated, in the second the branches elongate, and in the third phase the cortex tubules are finalized [5] .

The metanephric mesenchyme cells form a cap around the ureteric bud tip, and can be subdivided into the “capping” and “induced” mesenchyme. The capping mesenchyme contains the stem cell population for the entire nephron. How stemness is maintained in the metanephric mesenchyme and then lost after birth is one of the unsolved questions in nephrology. After proliferation these cells begin expressing epithelial markers and enter a succession of developments leading from comma-shaped bodies to S-shaped bodies. The proximal segment of S-shaped body gives rise to future glomerulus, middle portions develop into proximal tubule and the loop of Henley, whereas cells closest to the ureteric bud become the distal tubule [6] .

Comprehensive understanding of the mechanisms and processes involved in kidney development is crucial as urinary tract malformations represent about 1% of all birth defects in humans [7]. Improper metanephric kidney branching morphogenesis leads to decreased number of nephrons in the adult kidney and may be a predisposition to future chronic renal disease [8].

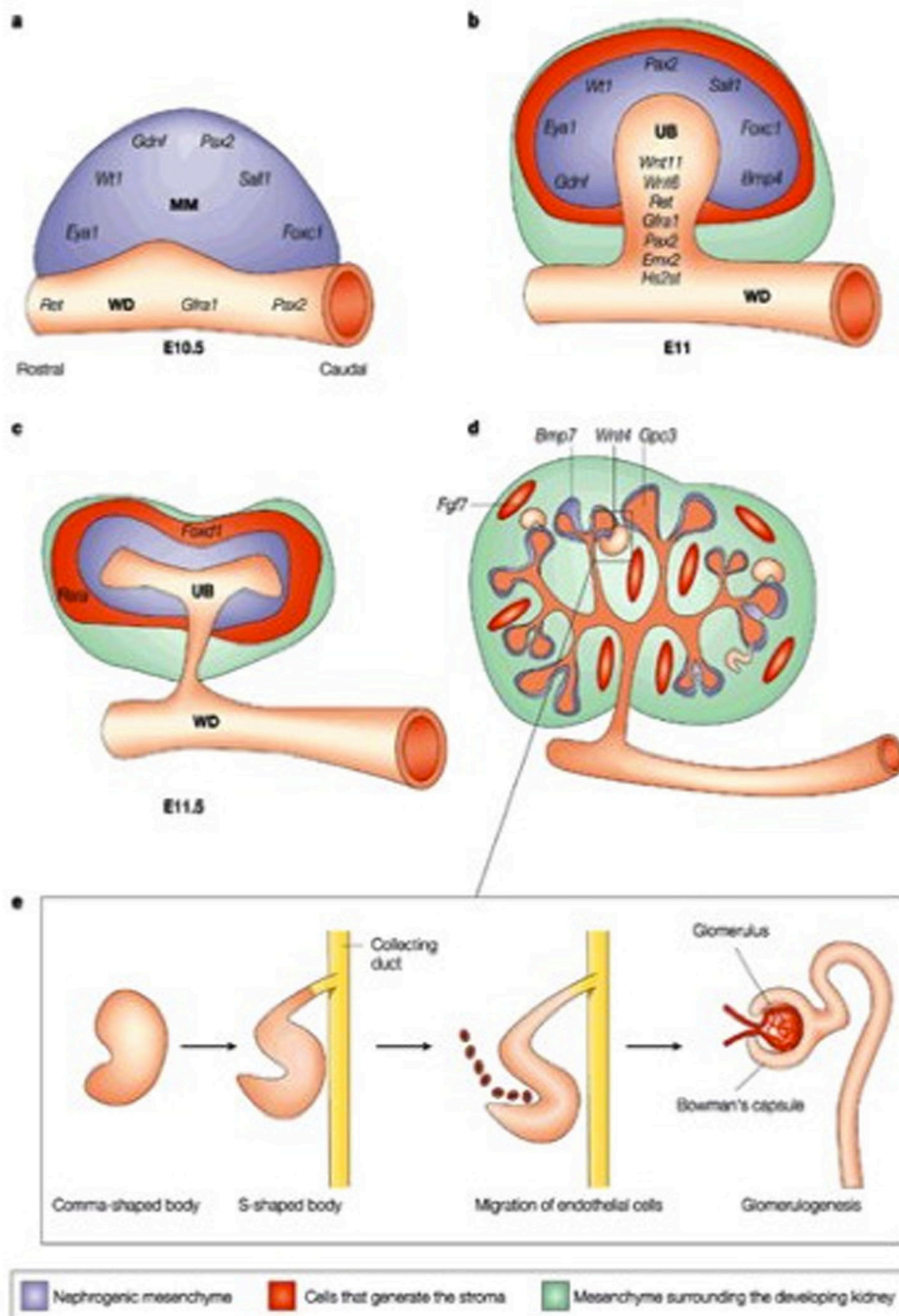


Figure 3. Kidney development starts by ureteric bud (UB) outgrowth (a, b) and branching (c, d), initiated by signaling between the Wolffian duct (WD) and metanephric mesenchyme (MM). Various signaling molecules are involved in the process. Different stages of glomerulogenesis (e). From Vainio and Lin, *Nature Reviews Genetics* 3, 533-543 (July 2002)

1.1.3 Human glomerular diseases and mouse proteinuria models

In glomerular disease, damage of cells and extracellular structure of the glomerular filter, allows large plasma proteins and sometimes erythrocytes to leak into the primary urine. Glomerular disease is characterized by: proteinuria (large amounts of protein in the urine; also called albuminuria if albumin is measured), reduced glomerular filtration rate (GFR), hypoproteinemia (low blood protein) and edema (swelling in parts of the body typical for kidney glomeruli dysfunction). GFR is generally considered as the best overall measure of kidney function and it is estimated as the clearance of an inert filtration marker filtered by the glomerulus, but neither absorbed nor excreted by the tubuli [9]. In practice, albumin excretion rate is more often used as a measure for proteinuria as it can easily be tested by probing the urine with a dipstick. The albumin passage of 30-300 mg/ 24h is defined as microalbuminuria, whereas values greater than that are referred to as macroalbuminuria [10]. Many studies have shown that microalbuminuria in diabetes patients represents an early diagnostic parameter for onset and progression of diabetic nephropathy [11].

Depending on the origin and histopathology, glomerular diseases have different classifications that often overlap with each other. In fact, nephrotic syndrome is an exceedingly heterogeneous group of disorders mainly classified as acquired and inherited. Many acquired diseases are immune-mediated:

Lupus nephritis is a kidney disease caused by systemic *lupus erythematosus*, occurring when autoantibodies are deposited in the glomeruli,

causing inflammation. **Goodpasture's syndrome** is also an autoimmune disease, involving an autoantibody targeting specifically the kidneys and lungs [12]. **IgA nephropathy** is a form of glomerular disease caused by immunoglobulin A deposition in glomeruli. **Membranous nephropathy** (MN) is the most common cause of nephrotic syndrome, and kidney biopsy shows deposits of immunoglobulin G and complement C3 in glomeruli as well as thickened glomerular basement membrane. **Minimal change nephrotic syndrome** (MCNS) is mostly diagnosed in children less than 10 years of age; it is likely mediated by abnormality in T-cells and in turn, causes changes in some resident cells of glomerulus. **Alport syndrome** is a hereditary chronic glomerular disease caused by mutations in any of the three type IV collagen genes, *COL4A3*, *COL4A4* or *COL4A5*, the products of which are specifically found in the GBM and also the inner ear and lens capsule. Absence of or defective collagen results in distortion of the GBM structure with subsequent hematuria and development of renal insufficiency. Alport syndrome usually involves also hearing and vision impairment [13, 14]. In some cases, glomerular disease can be related to infection that induces the immune system to overproduce antibodies, which are circulated in the blood and finally deposited in glomerulus, causing permanent or reversible damage. This may happen both as a result of bacterial as well as viral infection (e.g. HIV), but is thought that it is anyway genetically predisposed.

In the past few decades, the genetic components of inherited nephrotic syndrome have been extensively studied. Mutations in genes coding for essential glomerular proteins often lead to dramatic changes in glomerular epithelial cells and/or basement membrane structure organization, ultimately

causing proteinuria. Glomerulosclerosis is a histopathological finding typical for many of these diseases. It involves scarring of the glomeruli caused by the activation of glomerular cells to produce and deposit extracellular material such as interstitial collagens. **Chronic kidney disease** (CKD), a progressive loss of renal function over a period of time, is one of the primary diabetes complications. In Canada it is estimated that 2.3 million people have CKD (2008), in the US about 17% of adults aged 20 years and older (2004) and in UK about 8.8% of the population have symptomatic CKD (World Health Organization webpage). **Diabetic nephropathy** (DN) is the most common kidney disease and the main cause of death in diabetes patients. Several studies have reported the existence of susceptibility genes for this disease found on chromosome 3q [13, 15, 16]. **Steroid-resistant nephrotic syndrome** is an autosomal recessive inherited disorder caused by mutations in the *NPHS2* gene [17], characterized by early childhood onset of proteinuria and rapid progression to end-stage renal disease. Another similar disease is **congenital nephrotic syndrome of the Finnish type** (CNF), caused by mutations in the gene *NPHS1* gene encoding nephrin. CNF is characterized by massive proteinuria already *in utero*, premature birth and edema [18]. **Focal segmental glomerulosclerosis** (FSGS) is characterized by scattered scarring in the kidney, typically limited to one part of the glomerulus and to minority of glomeruli in the affected region. It is mostly caused by mutations of genes coding for proteins associated to actin cytoskeleton of glomerular epithelial cells, *ACTN4* and *CD2AP* [19, 20]. Generally, the treatment of kidney diseases is composed of medication, hemodialysis and eventually renal replacement, presenting a public health issue with significant social and

economic burden on clinical practice [21]. Hence, studies of renal filtration system are of enormous importance for understanding the kidney function in normal and disease state.

To enable such studies, many experimental proteinuric rodent models have been developed. For example, in the ADR model, adriamycin (the trade name of Doxorubicin, anthracycline antibiotic that intercalates DNA) is the compound that causes progressive glomerular pathological features that mimic human FSGS. This is achieved by a single intravenous injection of adriamycin, with overt proteinuria emerging after 4-5 days [22, 23]. A model mimicking immune-mediated glomerular diseases had also been developed and it involves administration of lipopolysaccharide (LPS, the major component of gram-negative bacteria outer membrane). LPS binds to Toll-like receptor 4 complex, triggering the secretion of pro-inflammatory cytokines. In contrast to adriamycin model, LPS causes milder proteinuria that reverts to baseline within 72 hours [24]. Diabetic nephropathy is usually studied in *db/db* mouse that has a mutation in the leptin receptor gene, leading to high insulin levels and severe obesity mimicking type II diabetes [25]. It is often noted that susceptibility to glomerular damage varies in all these models depending on the rodent substrain used [26]. Additionally, detailed investigations of all these and other models have revealed that they do not ideally correspond to human disease, and raised questions as to their relevance. Nevertheless, these models together, keeping in mind their limitations, today still present significant tools for studies of glomerular diseases.

1.2 Glomerulus

Glomerulogenesis starts at the proximal segment of the S-shaped body, at the tip of the developing nephron, where it involves cell differentiation simultaneously with vasculogenesis. The early capillary loop is observed within the glomerular cleft of the nascent glomerulus, and at one end of the S-shaped body a layer of visceral epithelial cells is also present, which latter will develop into podocytes. The basal aspect of these cells rests on the future glomerular basement membrane (GBM). On the other side of the visceral epithelial cells, overlying their apical surface is a lining of thin parietal epithelial cells that will form the Bowman's capsule. Expansion of the original capillary component into a plexus of six to eight individual capillary loops stimulates visceral epithelial cells to migrate and distribute around these loops (future capillary tuft). The GBM remains a constant barrier between the visceral epithelial cells and capillary endothelial cells. During further differentiation, components that will contribute to the glomerular capillaries, endothelial and mesangial cells, will invade the space on the side of the basement membrane opposite from visceral epithelial cells [27]. Differentiation of various cell types is strictly controlled by the microenvironment. Essentially, the glomerulus is a capillary tuft surrounded by the Bowman's capsule, on one side and urinary space on the other, with incoming blood entering through an afferent arteriole and filtration occurring in the capillary wall (Figure 4).

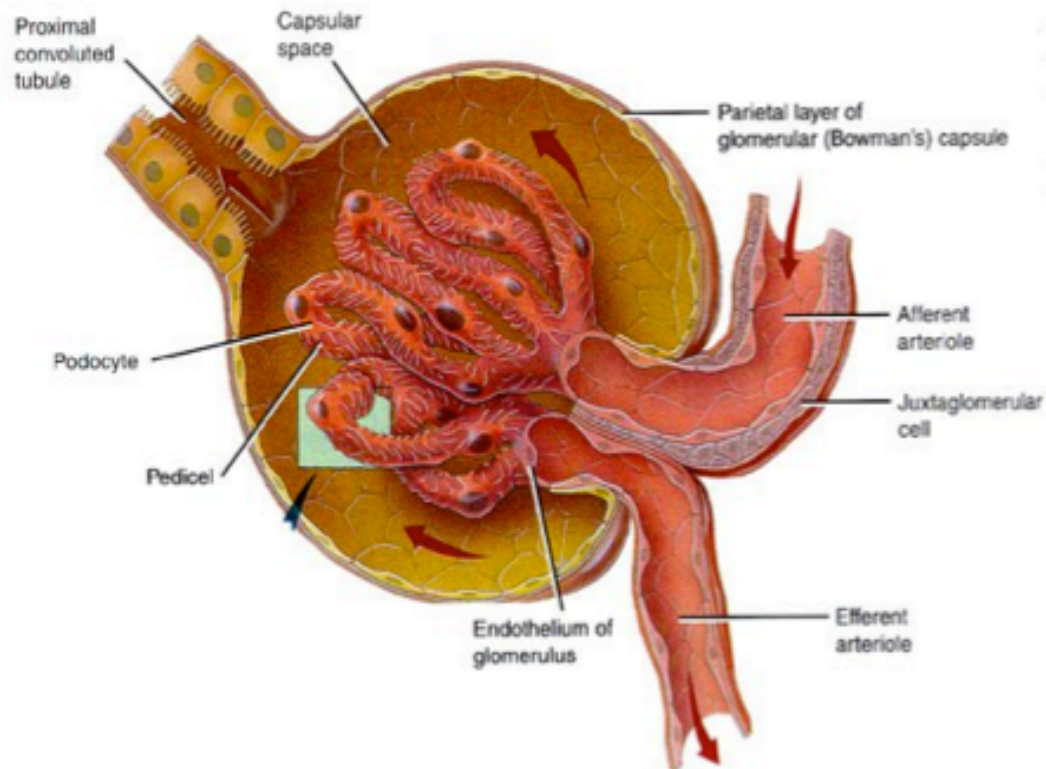


Figure 4. Glomerulus is a capillary tuft consisting of 6-8 capillary loops, surrounded by Bowman's space. Copyright © The McGraw-Hill Companies, Inc.

1.2.1 Cell organization

A mature glomerulus is a micro-organ that comprises three distinct cell types: endothelial, mesangial and visceral epithelial cells (podocytes), that are dedicated to an orchestrated function for filtration of plasma.

Glomerular endothelial cells (GECs) are specialized to support the selective filtration of massive volumes of plasma. They line the luminal surface of the entire glomerular vascular tuft, and are flat and perforated by dense arrays of trans-cellular pores, fenestrae. The size of the pores ranges

from 70-100 nm in diameter. An elaborate glycocalyx covers these cells and their fenestrae, forming a barrier that, together with other glomerular components, prevents loss of plasma proteins into the urine [28]. It is well known that in women with pre-eclampsia, GECs are markedly thickened and the size and density of fenestrae is reduced compared to normal pregnancy, causing reduced glomerular filtration rate [29].

Mesangial cells form the central region of glomerulus and provide support to the glomerular tuft. They constitute 30-40% of the total glomerular cell population and have several roles: they excrete mesangial matrix, secrete and act as targets for growth factors, clear circulating immune-complexes and may contribute to a contractile function of the filtration unit. Mesangial cells express PDGFr β and need PDGF β expressed by the endothelial cells, to be properly recruited to glomerulus [30]. Furthermore, they are also in direct contact with GECs within glomerulus. Typically, mesangial cells in the glomerulus are vascular smooth muscle-like cells containing smooth muscle actin and myosin, able to contract and constrict the capillary lumen causing alteration of blood flow into the tuft [31]. Glomerular pathology associated to mesangial cells is often seen in immune-mediated glomerular injury, such as IgA nephropathy or systemic *lupus nephritis*. In these conditions, deposition of immunoglobulins or immune-aggregates activates the mesangium to produce chemo-attractants for inflammatory cells, proliferate and change mesangial matrix [31].

The podocytes are positioned on the outside of the glomerular capillary loop and consist of a large cell body floating in the urinary space. These unique cells are anchored to the underlying basement membrane through

primary and secondary processes with long interdigitating foot processes that extend around the capillary loop. Between the foot processes of two neighboring podocytes are uniform 40 nm-wide slits bridged by a slit diaphragm, permeable to water and small solutes. The podocytes are terminally differentiated cells, indispensable for integrity of the filtration barrier thanks to their distinct morphological features and functions. In the adult human kidney, there are about 500-600 podocytes per glomerular tuft, and their rate of turnover is very slow. When podocytes are lost through apoptosis or detachment into the urinary space, there is a very limited ability for the remaining cells to proliferate and recover [32]. Podocytes and the novel proteins expressed by them are at the core of the study presented here and therefore they will be discussed further in more detail.

1.2.2 Filtration barrier

The filtration barrier is composed of three layers: the innermost fenestrated endothelial cells, the glomerular basement membrane and the outermost podocyte layer with slit diaphragms between the foot processes (Figure 5). All three layers have to be intact to maintain normal filtration function; injury to any of the components leads to proteinuria and progressive renal disease. Mutations in the genes for several podocyte and slit diaphragm proteins lead to malfunction of this barrier with proteinuria and renal insufficiency as result [13]. The glomerular filtration barrier is both size- and charge-selective in filtering blood plasma [33]. The blood flows through the capillaries under hydraulic forces generated by the isorhythmic contractions of

the heart, but the cells composing the filtration barrier also have the power to modulate this flow. The glomerular filtration rate is determined by the hydraulic conductivity of the glomerular capillary wall: the surface area available for filtration and forces acting across the wall.

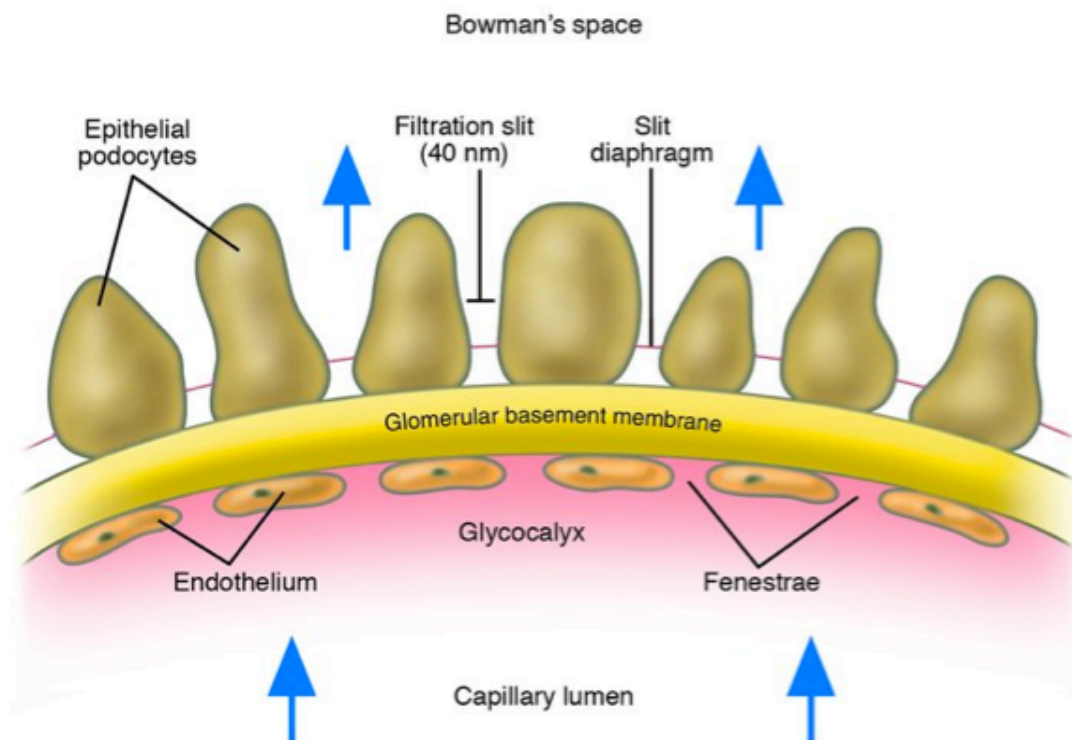


Figure 5. Glomerular filtration barrier is composed of the fenestrated endothelium, glomerular basement membrane and podocyte foot processes forming the modified cell-cell junction, slit diaphragm. Filtration direction is marked by arrows. Reproduced from Deen W, J Clin Invest, 2004; 114(10); 1412-1414

1.2.3 Glomerular basement membrane

The GBM is an amorphous extracellular lamina resulting from a fusion of basement membranes produced by the endothelial cells and podocytes. It is

about 300 nm in thickness, composed, like all basement membranes, of mainly collagen, laminin, proteoglycans and nidogen [33]. At the electron microscope level it is possible to distinguish three distinct layers of the GBM: a dense central *lamina densa*, an electronlucent *lamina rara interna* and a likewise electronlucent *lamina rara externa* [34]. Defects in the molecules composing the GBM have adverse effects on the glomerulus function but do not always lead to proteinuria. The GBM mainly serves as structural support to the capillaries.

As in other basement membranes, type IV collagen is the main structural component of the GBM. This collagen type forms a three-dimensional scaffold into which other proteins are embedded. During nephrogenesis the embryonic GBM type IV collagen heterotrimer ($\alpha 1$)₂ $\alpha 2$ is replaced by an adult $\alpha 3\alpha 4\alpha 5$ isoform. Mutations in any of the genes for the $\alpha 3\alpha 4\alpha 5$ heterotrimer cause Alport's syndrome characterized by mild proteinuria [33].

Laminins are heterotrimeric proteins indirectly cross-linked to the collagen IV network in the basement membrane. In the GBM, an embryonic laminin-511 is replaced after birth in a developmental shift by adult laminin-521 isoform. It has been shown that laminin $\beta 2$ chain-deficient mice exhibit massive proteinuria despite compensation with laminin $\beta 1$ [35]. Patients with mutations in the laminin $\beta 2$ gene develop Pierson's syndrome also characterized with massive perinatal proteinuria [36].

Entactin/ nidogen is a globular protein able to bind laminins, collagens and perlecan in the basement membrane. This protein that exists in two genetically different forms, contributes to a functional GBM meshwork. In entactin-1 knock-out mice, a morphological thickening of the basement

membrane is observed, changing the filtration properties and anionic charges of the GBM, but no abnormal reorganization of other GBM components was observed [37].

Heparan sulfate proteoglycans, such as perlecan, collagen XVIII and agrin, provide anionic charge to the GBM that is believed to be partially responsible for impermeability of the GBM to anionic plasma proteins. Proteoglycans bind water, thus keeping the GBM as a hydrated gel matrix [38]. However, the importance of proteoglycans for the filtration function has been questioned, as studies with genetically modified mice lacking agrin and heparan-sulfate deficient perlecan-mice have shown that they do not develop proteinuria, even when crossed with each other [39-41]. On the other hand, collagen XVIII deficient mice exhibit mild glomerular insufficiency [42]. More studies are obviously needed to elucidate the function of these proteins in the glomerular filter.

1.3 Podocytes

1.3.1 Cell biology and function

Podocytes are highly specialized cells that serve several functions in the kidney glomerulus. Briefly, they support the capillary loops structurally, participate in the synthesis and repair of the basement membrane, produce growth factors (VEGF and PDGF) that control functions of endothelial and mesangial cells, and they also have an immunological surveillance role [32].

Primitive podocytes are polygonal, proliferative cells. They are distinguished from other cells of the developing nephron during the transition

from the S-shaped body to distinct glomerulus. During the S-shaped body stage, they still express markers typical for proliferative cells such as PCNA and cyclins A/B1 [43]. Podocytes lose their ability to divide upon entry into the glomerular capillary loop stage, by the expression of cell cycle inhibitors p27Kip1 and p57Kip2 [44]. At this point they also start expressing also their specific markers and develop the characteristic architecture structurally subdivided to: the cell body, the major processes and the foot processes. Little is known about the molecular genetic basis for segmentation of the nephron and which genes act to define the podocyte vs other cell lineages, but a set of podocyte-specific transcription factors certainly plays a key role. An apicobasal polarity axis allows for podocyte orientation between the urinary space and the GBM. Conserved polarity complexes such as Par3, Par6, aPKC are essential regulators of podocyte morphology [45].

According to some theories, podocyte foot process formation starts with the selective detachment of the cell body from the GBM. Subsequently, cell polarization takes place with cytoplasmic extensions of the cells (resembling filopodia) appearing. They scaffold around the capillary loops, with adjacent foot processes always being derived from different podocytes. Finally, cells that begin as adjacent epithelial cells end up as cells with isolated bodies but interdigitated foot processes anchored at the GBM [27]. In proteinuric diseases, retraction of foot processes is often observed and this phenomenon is referred to as podocyte effacement. Between adjacent foot processes a specific structure is observed under the electron microscope, called the slit diaphragm. It is a complicated and sophisticated cell-cell adherens/tight junction, which is a major component of the protein barrier between the

circulation and Bowman's space. Its protein composition has been partially revealed and described.

At the subcellular level, it is observed that the voluminous cell body of podocytes contains a prominent nucleus, a well-developed Golgi system, abundant rough and smooth endoplasmic reticulum, lysosomes and many mitochondria. The density of organelles indicates a high level of metabolic activity and protein synthesis [46]. Interestingly, podocytes possess structures resembling neuronal synaptic vesicles, which contain glutamate, coexpress Rab3A and synaptotagmin 1, and undergo spontaneous and stimulated exocytosis and recycling, with glutamate release. The presence of a series of neuron- and synapse-specific molecules in normal human glomeruli has been described [47]. These data point toward a synaptic-like mechanism of communication among glomerular cells, which fits well with the molecular composition of the glomerular filter and suggests complex glomerular signaling dynamics.

Accumulated body of evidence shows common biological features of podocytes and neurons [48]:

- both cell types possess long and short cell processes equipped with highly organized cytoskeletal systems.
- both show cytoskeletal segregation: microtubules (MTs) of mixed polarity and intermediate filaments (IFs) in podocyte major processes and in neurites, while actin filaments (AFs) are abundant in podocyte foot processes and in neuronal synaptic regions.
- in both cell types, the processes formation is: mechanically dependent on MTs, assembled by various microtubule-associated proteins,

positively regulated by PP2A (a Ser/Thr protein phosphatase) and accelerated by laminins. The elongation of both podocyte processes and neuronal dendrites is supported by Rab8-regulated basolateral-type membrane transport.

- both podocyte processes and neuronal dendrites express synaptopodin, an actin-associated protein, in a development-dependent manner.

Mature podocytes are terminally differentiated cells whose phenotype properties are tightly regulated by upregulation and robust expression of CDK-inhibitors [46]. Cell survival is essential for podocytes, as these cells principally need to be functional for the whole lifespan of the individual. The podocyte properties are supported by proper attachment to the GBM, since it is known that when detached, podocytes susceptibility to apoptosis increases significantly. VEGF and IGF-1 signaling pathways have been implicated in reduction of podocyte apoptosis [49, 50]. Escape of the podocytes from the strict cell-cycle control is a disastrous event causing rapid glomerular destruction. Several pathways of podocyte injury are possible, sometimes involving the change of podocyte cell numbers, as summarized in Figure 6. This escape of podocytes from the cell-cycle control happens in a set of glomerular disorders such as HIV nephropathy, collapsing glomerulopathy and some variants of FSGS. In these diseases p27, p57 and cyclin D1 are lost, whereas an increase of the proliferation markers is seen in areas with podocyte proliferation [51, 52]. Normally, podocytes do not have proliferation as a regenerative possibility. It can be speculated that the complex cytoskeleton network effectively inhibits podocyte proliferation, because for

reentry into the cell cycle its deconstruction would be needed, leading to abolishment of glomerular permselectivity [46]. Conversely, podocyte loss caused by apoptosis is seen in Pima Indians with type II diabetes [53], and in other renal diseases as well as pyromycin-induced nephrosis in rats [54]. This could be the result of the critical process termed anoikis: detachment of podocytes from the GBM, which induces cell death [55]. Interestingly, recent studies have provided some evidence that podocytes can be regenerated from a resident population of renal progenitors localized within the parietal epithelium of Bowman's capsule of the human renal glomerulus [56]. Thus, podocyte cell cycle quiescence appears to be a necessity and a prerequisite for a functional glomerulus.

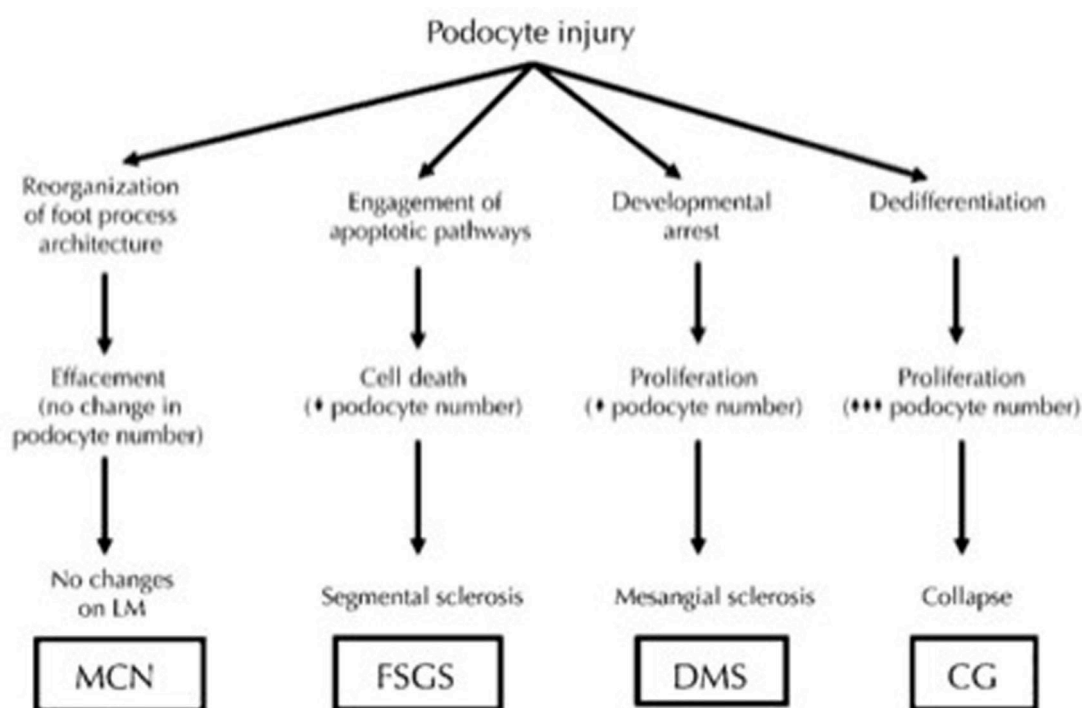


Figure 6. Podocyte injury results in several possible reaction pathways. MCN-minimal change nephrosis, DMS-diffuse mesangial sclerosis, CG-collapsing glomerulopathy. Taken from Barisoni et al, Arch Pathol Lab Med. 2009 February; 133(2): 201-216.

A vast number of “podocyte-specific” proteins have been identified in the past two decades (Figure 7, some of which will be mentioned further), especially since the identification of the gene causing congenital nephrotic syndrome of the Finnish type. The significance of this discovery brought attention to podocytes as being central in the glomerular pathology. Many research groups, including ours, have taken a mainly “podocentric” view when it comes to studies of the glomerulus and its diseases.

1.3.2 Podocyte proteins and involvement in kidney disease

1.3.2.1 Transcription factors

WT1

This is a zinc-finger transcription factor first identified as a suppressor gene for Wilm’s tumor, a tumor of the kidney observed in children. Its expression becomes restricted to the podocyte cell lineage in the S-shaped stage of glomerulogenesis and it is one of the markers of podocytes in the adult kidney. Denys-Drash syndrome results from mutations that affect the DNA-binding ability of the WT1 protein, and involves a diffuse mesangial sclerosis within glomeruli. Frasier’s syndrome, a rare disorder also caused by mutations in WT1, displays proteinuria and FSGS in early childhood. It is thought that WT1 might be responsible for directing the expression of growth factors that regulate development of glomerular vasculature, but also that it might regulate expression of podocyte cell surface protein podocalyxin [27].

FOXC2

Member of a forkhead/winged family of transcription factors, this protein is detected in developing and mature podocytes. Podocytes in *Foxc2*-knockout mice retain columnar shape and do not develop foot processes and slit diaphragms. The expression of other podocyte transcription factors, *Lmx1b* and *Pod1*, was found to be normal, suggesting that they function in independent pathways [57].

LMX1B

It is a LIM-domain transcription factor involved in regulation of expression of several key podocyte proteins: podocin, CD2AP, type IV collagens. Mutations in *LMX1B* cause Nail-patella syndrome, characterized by thickening and splitting of GBM accompanied by skeletal and nail dysplasia [58]. Knockout mice for this protein demonstrated reduced assembly of podocyte foot processes [59]. *Lmx1b* binding sites have been found upstream of its target genes, indicating that it has a major role in regulation of podocyte-specific gene expression [60].

Pod1

Also known as epicardin/capsulin, it is a helix-loop-helix transcription factor expressed from early stages of kidney development. In *Pod1*-knockput mice, glomerular development appears arrested at the single capillary loop stage, the podocytes loose their lateral cell-cell attachments but remain adhered to the GBM [61].

Kreisler

Kreisler (MafB) is a leucine zipper protein expressed in podocytes from capillary loop stage glomeruli. It is also expressed in brain where it participates in patterning of the hindbrain. Kreisler-deficient mice podocytes lose their lateral contacts and fail to form proper foot processes [62].

1.3.2.2 Apical surface proteins

Podocalyxin

It is a transmembrane sialoprotein located at the apical and lateral surface of podocytes, a major component of the podocyte glycocalyx. It carries 80% of the glomerular sialic acid content which provides negative charge [63]. Its negative charge has antiadhesive effect on podocytes: repels the adjacent foot processes away from each other, maintaining the filtration slits open. Indeed, Podocalyxin-knockout mice lack foot processes and slit diaphragms and are unable to filter primary urine [64]. Podocalyxin intracellular tail is connected to actin cytoskeleton via ezrin/Nherf2 and the dissociation of this complex leads to foot process effacement [65]. Of note, podocalyxin is also expressed in brain neurons and glomerular endothelial cells [66, 67].

Podoendin and Podoplanin

Both are negatively charged sialoglycoproteins, components of podocyte glycocalyx together with podocalyxin. Podoendin is a cell differentiation-dependant protein of podocytes, also found in lung endothelium [68]. Podoplanin-knockout mice have embryonic lethal phenotype [69], but it was

shown that this protein is downregulated in some mouse and rat proteinuria models [70]. Also, injection of anti-podoplanin antibodies in rats causes rapid transient proteinuria [71].

Glepp1

Glomerular epithelial protein 1 (or PTPRO) is found in the kidney exclusively on the apical surface of podocytes. It is a receptor tyrosin phosphatase with a large ectodomain, a transmembrane domain and a cytoplasmic segment. Glepp1 deficiency in mice causes broadening and shortening of podocyte foot processes in connection to altered distribution of cytoskeletal protein vimentin. Mice were without proteinuria, although with decreased glomerular filtration rate [72]. Recently, mutations in GLEPP1 gene were associated to childhood-onset nephrotic syndrome in Turkish population [73].

Megalin and Cubilin

These are synergistic endocytic receptors typically involved in albumin reabsorption in the proximal tubule [74], but they have been found also in glomerular podocytes. Cubilin revealed apical surface expression overlapping with megalin, but also intracellular expression in podocytes [75].

1.3.2.3 Cell-matrix adhesion and basal surface proteins

Integrin

The most abundant integrin isoform in podocytes is $\alpha3\beta1$, binding to several components of the GBM such as laminin, fibronectin, entactin and collagen IV

[76]. Mice lacking $\alpha 3$ integrin gene show defects in glomerular capillary tuft branching and failure to form proper foot processes [77]. Mice deficient for the integrin $\beta 1$ gene in podocytes develop massive proteinuria and a phenotype similar to that of $\alpha 3$ integrin knockouts [78]. The binding of integrins to GBM components generates “outside-in” signaling: receptor clustering and formation of focal adhesion points involving actin cytoskeleton-binding proteins. Integrin is linked to the podocyte foot process actin cytoskeleton *via* talin, paxilin and vinculin [46]. It is thought that integrin signaling at the basal aspect of podocytes is bridged with slit diaphragm signaling by ILK (integrin-linked kinase). Podocyte-specific knockout of ILK develops proteinuria and thickening of GBM [79]. Integrins can also be downstream effectors in cell responses in the framework of “inside-out” signaling.

Tetraspanins

CD151 is a member of the tetraspanin family localized to the sole of the foot processes and associated to $\alpha 3\beta 1$ integrin. It is thought that tetraspanins are involved in maturation of the GBM since the changes seen in CD151 knockout mice pointed to thickening and splitting of the GBM that precedes podocyte abnormalities [80]. Very recently it was shown that knockdown of CD151 in cultured podocytes reduces $\beta 1$ integrin expression and cell adhesion [81].

Dystroglycan

Similarly to integrins, dystroglycans are heterodimeric transmembrane proteins. They too function by connecting GBM components (laminin, agrin, perlecan) to the foot process actin cytoskeleton, but *via* utrophin [82].

Dystroglycan-null mice fail to form an extra-embryonic basement membrane and do not develop past E5.5 [83]. Blocking of dystroglycan-laminin binding causes disturbance in epithelial-branching morphogenesis [84]. However, recent studies with cell-lineage-specific dystroglycan deletions surprisingly show that it most likely does not contribute significantly to kidney development or function, in health or disease [85]. It appears that integrins are therefore the primary extracellular matrix receptors in glomerular epithelia. Otherwise, multiple forms of muscular dystrophy have been linked to dystroglycan glycozilation defects [86, 87].

uPAR

Podocytes express a urokinase receptor uPAR, required to activate the $\alpha v\beta 3$ integrin whose extracellular ligand in the GBM is vitronectin. The expression of uPAR, $\alpha v\beta 3$ integrin and vitronectin is increased in some proteinuric states and seems to have pathogenic roles in development of proteinuria. On the other hand, mice deficient for these proteins are protected from LPS-induced proteinuria [88].

Some of the abovementioned podocyte proteins are schematically depicted in Figure 7:

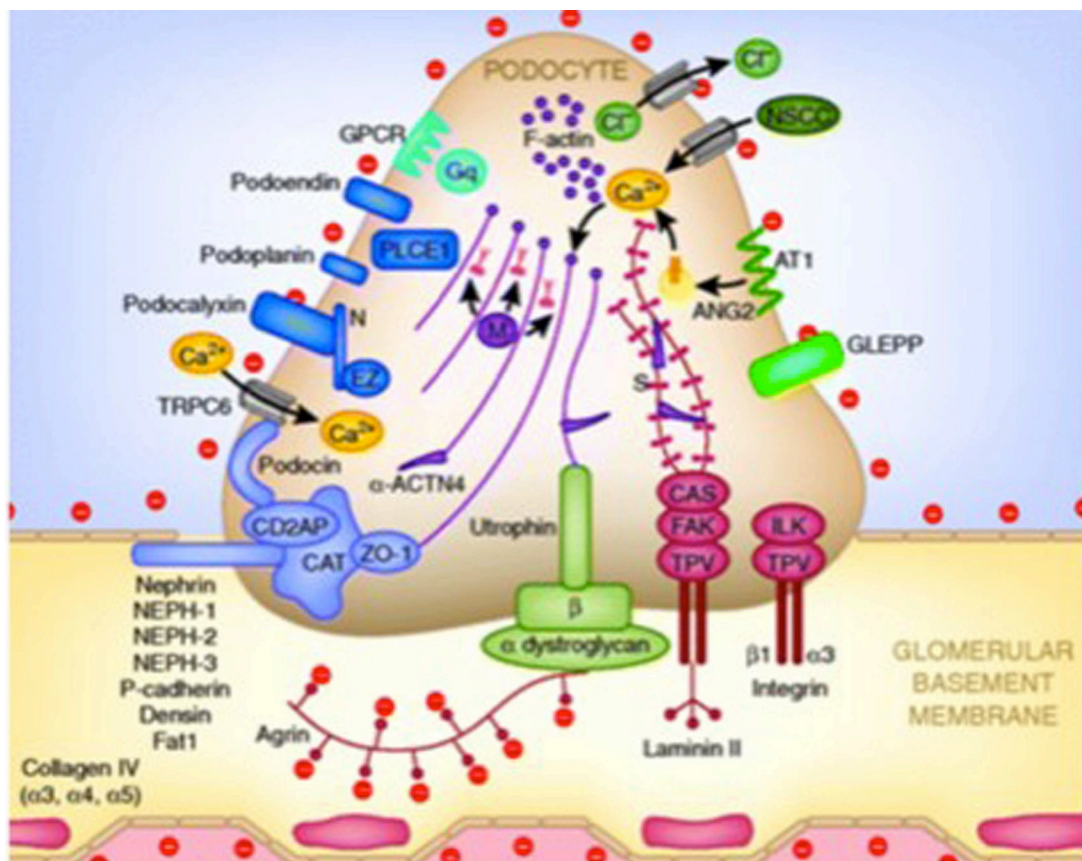


Figure 7. Some typical podocyte foot process and basement membrane proteins. Modified from Kobayashi et al, Anal Sci int, 2004. March; 79(1): 1-10

1.3.2.4 Slit diaphragm

In the early 1970s, the hypothesis of the slit diaphragm being the size-selective molecular sieve was raised [89]. The composition of the slit diaphragm began to unravel first in 1998 after the identification of the novel gene coding for nephrin protein, mutated in congenital nephrotic syndrome of the Finnish type (CNF) [18, 90]. Currently, the GBM is considered to function as a coarse filter whereas the podocyte slit diaphragm is the second ultrafilter that hinders the passage of proteins larger than albumin [13]. Many molecular components of the slit diaphragm have been identified, but many remain to be

discovered and characterized in order to assemble the mosaic of glomerular function. Importantly, although the slit diaphragm contains typical adherens/tight cell-cell junction proteins, it also comprises proteins not generally found elsewhere in the body.

Nephrin

This is a transmembrane protein, located in the kidney exclusively in the glomerular podocytes slit diaphragm. It has also been reported in regions of brain and pancreas [91]. It was discovered as the gene mutated in CNF, a rare disease with high incidence in Finland, characterized by massive proteinuria *in utero*, premature birth and edema. The only curative treatment available for children born with CNF is kidney transplantation [90]. A broad spectrum of mutations has been identified in the *NPHS1* gene [92, 93]. Inactivation of the gene in mice causes a similar phenotype as in humans, with neonatal death [91]. Extracellular domains of the nephrin proteins from adjacent foot processes interact in the center of the slit to form the zipper-like backbone. Besides a structural, nephrin also has a signaling function and through several mediator proteins it is connected to the actin cytoskeleton [13]. Participation of nephrin as a signaling molecule in the slit diaphragm has been described in many reports, showing the presence of lipid rafts in the slit to which nephrin and podocin are recruited. Lipid rafts are dynamic membrane microdomains that concentrate signal transduction molecules [94]. Nephrin and podocin recruit PI3K to the plasma membrane, and promote PI3K-dependent AKT signaling [95]. Nephrin phosphorylation results in recruitment of the adapter protein Nck and assembly of actin filaments in an Nck-

dependent fashion [96]. It had also been demonstrated that nephrin has a role in vesicular docking and insulin responsiveness of podocytes [97].

Podocin

Podocin was identified as the product of a gene *NPHS2* mutated in steroid resistant congenital nephrotic syndrome [98]. Mutations in *NPHS2* in humans lead to early childhood onset of proteinuria, whereas mouse knockout presents fused podocyte foot processes and lack of slits [99]. Podocin is a hairpin-shaped integral membrane protein with both ends directed into the intracellular space. It interacts directly with nephrin, Neph1, CD2AP and essentially recruits nephrin to the slit [94].

CD2AP, Nck, MAGI

These proteins are parts of the multiprotein adaptor complex bridging the junctional slit diaphragm with actin cytoskeleton and signaling cascades. CD2AP is an intracellular linker protein interacting both with nephrin and podocin, as well as actin. It was identified as a novel ligand interacting with the T-cell-adhesion protein CD2. It is a vital protein as CD2AP-deficient mice die due to massive proteinuria and foot process effacement, but exhibit also compromised immune system [100]. CD2AP mutations have been reported in some patients with FSGS [101]. Nck1 and Nck2 proteins interact with phosphotyrosines, and can recruit several other proteins involved in actin assembly regulation. In podocytes, nephrin phosphorylation stimulates Nck binding resulting in reorganization of actin cytoskeleton [96]. Podocyte-specific deletion of Nck1 and 2 leads to defects in foot process formation and

nephrotic syndrome [102]. MAGI-1 and 2 are membrane-associated scaffolding proteins, also interacting with nephrin and actin cytoskeleton proteins synaptopodin and α -actinin-4 [103].

Neph1, Neph2, Neph3

Nephs are transmembrane proteins structurally related to nephrin, with five extracellular IgG-like motifs. Through extracellular domains they also interact with nephrin [104], while interactions with podocin and ZO-1 occur *via* the intracellular domain [105, 106]. Neph1-knockout mice die perinatally due to massive proteinuria [107], but the roles of Neph2 and Neph3 are not known.

ZO-1, Claudins, CASK

Both ZO-1 and CASK are members of the MAGUK family of scaffolding proteins, specifically enriched at tight junctions of epithelia. In podocytes under nephrotic conditions, tight junctions are the main intercellular junctions [108]. ZO-1 is one of the key regulators of the tight junction assembly, known to associate with actin, catenin, claudin and Nephs [105, 109]. CASK is another tight junction protein and nephrin interacting partner [103], found also in synapses. It is believed that it has a role in maintenance of epithelial cell polarization [110]. Claudin-5 is the main claudin present in podocytes and it is suggested that the formation of tight junctions during nephrosis might be due to its local recruitment [108].

Cadherins, Catenin, FAT

Cadherins are essential transmembrane proteins mediating the assembly of adherens junctions. The newly established junctions are stabilized by linkage of cadherins to actin cytoskeleton through catenins [111]. Several cadherin proteins are present in the podocytes, one of them being VE-cadherin. It was identified as a slit diaphragm protein that links the coexpression and coregulation of nephrin and ZO-1 [112]. P-cadherin was also reported to be located in the slit but it is not considered to be of great importance [113]. Finally, FAT1/2 are large slit diaphragm proteins belonging to cadherin family. FAT1-knockout mice lack slit diaphragms and die 48 hours after birth, while FAT2-deficient mice do not show overt kidney phenotype (Sun Y, Tryggvason K, unpublished results).

TRPC6

Member of a family of nonselective cation channels, found in endothelial and mesangial cells as well as podocytes. It is involved in the regulation of calcium signaling, activated by G protein-coupled-receptors. Some human *Trpc6* gene mutations result in increased amplitude and duration of calcium influx after stimulation, causing the so-called “Trpc6 nephropathy” [114-116]. However, TRPC- knockout mice do not show any obvious renal phenotype [117, 118].

1.3.2.5 Major and foot processes cytoskeleton

The cytoskeleton, a cytoplasmic system of fibers, has to serve static and dynamic functions. Podocytes have a limited motility and a contractile role on the glomerulus [119]. In the podocyte, the cytoskeleton of the major processes has to maintain contact with the metabolic machinery of the cell body, and allow protein and vesicles transport along the processes. The foot process cytoskeleton responds to unique challenges of the filtration barrier: it is coupling the slit membrane molecular complexes to the podocyte-GBM complexes, and counteracts the distensible forces of the capillary wall. Different functions of the podocyte processes are represented by the different cytoskeleton composition: foot processes are rich in actin filaments, whereas major processes contain microtubules and intermediate filaments [46].

Microtubules are heterodimeric polymers of globular α - and β -tubulin subunits, building a polar 24 nm-thick structure. Microtubular-associated proteins, MAPs, are required for their elongation and maintenance. Process-bearing cells, like podocytes and neurons, show a mixed microtubular polarity, not typical for other cells. A major role of microtubules is the trafficking of proteins from the Golgi apparatus into the cell periphery. This directed membrane transport machinery is of importance in securing an adequate supply of podocyte foot processes with cargo synthesized in the perinuclear zones. [120]. Mature podocytes also express intermediate filaments with associated proteins (vimentin, tubulin, desmin and plectin) in their major processes and cell body [46].

Actin filaments are predominant in the foot processes, being highly dynamic and allowing for rapid growth, branching and disassembly in normal and disease conditions. They are bundled in closely packed parallel arrays or in loose networks by a unique assembly of linker molecules [121]. Effacement is a pathological process of retraction and fusion of podocyte foot processes, and it affects three aspects of the podocytes: it is initiated by cytoskeleton changes, but alters also the slit diaphragm and GBM contacts [122]. It is accompanied by an increase in actin filament density at the soles of the foot processes. Also, proofs that podocytes are somewhat motile cells come from timelapse *in vivo* and *in vitro* imaging, showing the constant reorganization of cell edges and processes [123]. Since the cytoskeletal organization is tightly regulated, many proteins have been studied to address this process. Small GTPases like RhoA, Rac1 and Cdc42, positive regulators of actin bundling, could be some of the key players [124]. These proteins are molecular switches that relay signals from the plasma membrane to the cytoskeleton. Additionally, intracellular calcium signaling is critical for actin polymerization and its variations significantly affect cytoskeletal function [125].

The characteristic pattern of actin-associated proteins in podocytes has been at least partially unraveled (Figure 8):

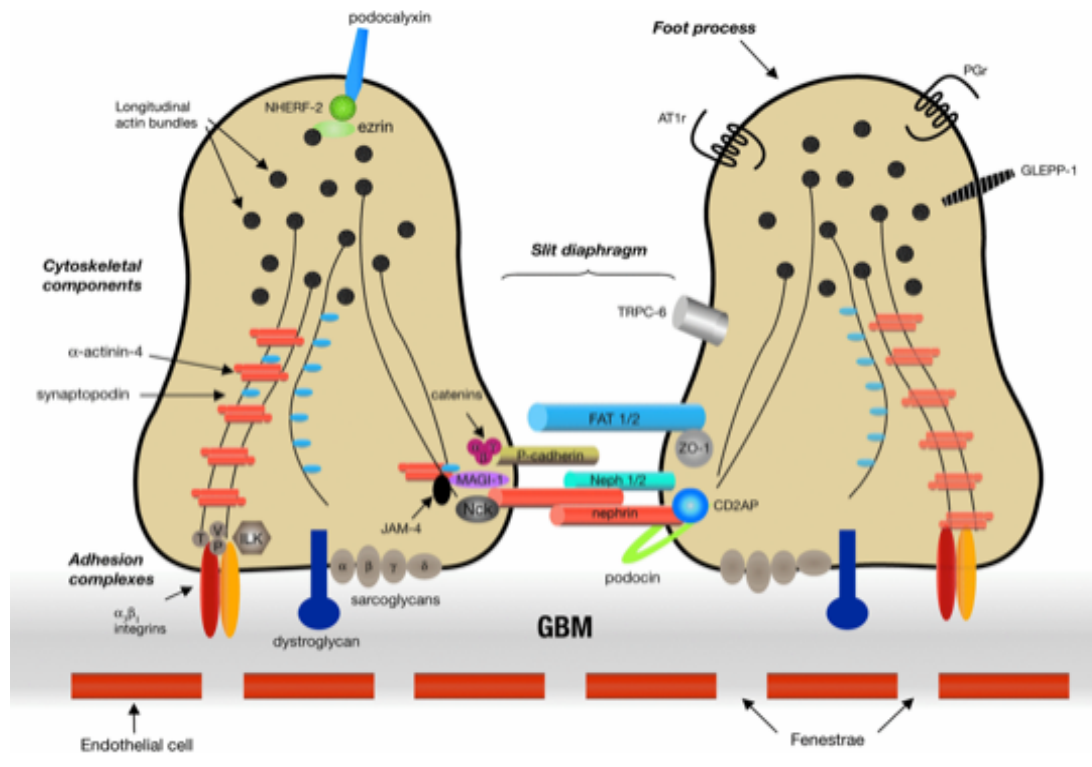


Figure 8. A schematic drawing showing the main components of podocyte foot process cytoskeleton and slit diaphragm. Reproduced from Michaud and Kennedy, *Clinical Science* (2007) 112, 325-335

α -Actinin-4

It is an actin bundling protein, specifically expressed in the glomerular podocytes. Mutant α -actinin-4 shows increased F-actin bundling activity [126]. Mutations in the *ACTN4* gene, encoding α -actinin-4, have been shown to cause a late-onset FSGS leading to end-stage renal disease [20]. Mice knockout for *ACTN4* have FPE, proteinuria and glomerulosclerosis, resembling the human FSGS disease. The podocytes also show impaired adhesion to the GBM that causes their shedding into urine [127]. It is likely that altered binding to actin somehow impairs the cytoskeleton dynamics in α -actinin-4 mutants, resulting in FPE.

Synaptopodin

This is another actin-associated protein expressed only by podocyte foot processes and telencephalic dendrites [128]. It interacts with α -actinin-4 and induces actin filaments elongation, typical for mature podocytes [129]. Synaptopodin expression levels are significantly reduced in some glomerulopathies, and knockout mice exhibit impairment in recovering from induced proteinuria challenge [129, 130].

Myosins

There is a growing interest in expression and function of myosins in the glomerular podocytes. Mutations in myosin IIA (MYH9) are associated with glomerulonephritis [131] and FSGS [132]. It has also been shown that disruption of myosin 1e function promotes podocyte injury in knockout mice [133] and childhood familial FSGS in humans [134]. Both proteins are non-muscle myosins, with a motor-head domain binding to ATP and F-actin, a calmodulin-binding neck domain, and a tail domain. Myosins appear to be important for podocyte motility and stabilization of actin cytoskeleton, but their exact function in podocytes still remains to be determined [134].

Cofilin-1

Cofilin-1 is an actin depolymerization protein shown to be important for maintenance of the podocyte cytoarchitecture in both zebrafish and mouse models. It has redundant roles with the other member of the same protein family, ADF, which can partially compensate for the lack of cofilin-1. It has

been shown that nephrin regulates cofilin-1 action by stabilizing it in either phosphorylated or dephosphorylated form [135].

Cortactin

It was identified as a molecular scaffold for actin assembly, important in cell migration and neurite outgrowth. It was also specifically localized to the cortical actin network of the podocyte foot processes, interacting with podocalyxin. Cortactin promotes F-actin nucleation and branch assembly, playing an active role in the formation of cortical actin network. Cortactin is a known substrate for tyrosine kinase, and its phosphorylation leads to dissociation of podocalyxin from actin filaments, and podocyte morphology change. This is in contrary to ezrin whose dephosphorylation has the same effect on podocalyxin [136].

1.3.3 Podocytes *in vitro*

There is a large body of literature describing the use of cells in culture for cardiac and nervous system, liver, blood and other organs research. Each cell-culture system has unique properties and kidney podocytes are no exception. Cultured podocytes were first introduced *in vitro* in the mid-seventies, following isolation of glomeruli from the kidney cortex [137]. However, in primary cultures, differentiated podocytes outgrown from isolated or micro dissected glomeruli, show very little proliferative activity and the possibility of contamination with other glomerular cell types, so it is difficult to perform experiments that require a large number of cells [46]. A major

problem with culturing podocytes *in vitro* has been the rapid dedifferentiation that accompanies the loss of specific architecture and results in the cobblestone morphology. Such podocytes resemble the immature podocyte precursor cells during early glomerular development, including the lack of synaptopodin expression [138].

For the purpose of mechanistic empirical studies, several podocyte cell lines of both murine and human origin have been developed. A conditionally immortalized murine podocyte cell line has been propagated from a transgenic mouse expressing a temperature-sensitive SV40 large T antigen [139, 140]. Cells under nonpermissive conditions, at 37°C, stop growing and exhibit many properties of differentiated podocytes: they are arborized and express WT1 and synaptopodin. The proper temperature is imperative, as the T antigen driving podocyte proliferation will be only partially degraded at even slightly lower temperature, thereby preventing the cells from exiting cell-cycle. A human podocyte cell line has been established by transfection with a temperature-sensitive SV40-T gene [141]. At the permissive temperature of 33°C, these cells proliferate and grow in cobblestone morphology, while a temperature switch to 37°C initiates growth arrest, cell differentiation and expression of typical podocyte markers: nephrin, podocin, CD2AP, synaptopodin. Synaptopodin is the key marker of a differentiated podocyte phenotype, because *in vivo* the expression of synaptopodin is specific to postmitotic differentiated podocytes. Moreover, these cells even form the slit-diaphragm-like cell-cell contacts [142].

Like other postmitotic cells in culture, such as neurons or cardiac myocytes, podocytes present many practical problems for researchers. In

general, successful culturing of podocytes requires a lot of attention as they quickly dedifferentiate and lose their specific markers. It is very important that they are maintained at 80-90% confluency to prevent multilayering and loss of cell-cell and cell-matrix contacts. The coating material mimicking the GBM would also be important, as podocytes grow faster and better and overall appear healthier, but type I collagen that is usually recommended is not a normal GBM component. Typically, podocytes in culture show low transfection efficiency ranging between 10-20% for undifferentiated cells. Transient transfection, even though simple and fast, does not provide incorporation of DNA of interest into the genome and is not ideal for differentiated podocytes. Stable transfections result in genome incorporation, but take much longer time. To overcome this problem, viral transduction is recommended, providing higher efficiency and continuous expression of the DNA of interest, even in differentiated podocytes [138]. However, in our hands, transfection of differentiated podocytes has proven as an exceptionally difficult task in spite of various methods that were tested.

Many published [140] and unpublished observations about podocytes *in vitro* have cleared the fact that they can not mimic completely the complex *in vivo* characteristics: they often lack expression of central podocyte-specific proteins, do not have the same morphology and are not continuously exposed to hemodynamic effects that exist in glomerulus. There is a need in the field of glomerular studies, for development of an *in vitro* 3-dimensional filtration system model, with endothelial cells growing on one side of the coating “GBM” surrounding the capillary tube (possibly made of some biomaterial), and podocytes on the other. Nevertheless, the existing podocyte cultures are

widely used in mechanistic studies of podocyte function, protein-protein interactions, *etc.* This may be a valid and valuable system in some regards, but the results obtained must be interpreted with care and combined with animal models and human studies.

1.4 Glomerular gene expression changes in diseased kidney

During the last decade we have seen an explosion of large-scale profiling methods utilized also for characterization of glomerular expression signatures in normal and diseased states. This was accelerated by the novel methods for massive glomeruli isolation coupled with proteomics and transcriptomics developments. Our group was one of the first to contribute to this modern approach of glomerulus analysis [57, 143].

Glomerulus expression profiles have so far been reported for several mouse or human disease states: murine LPS-induced nephrosis [144], *Lupus nephritis* mice [145], murine Adriamycin-induced nephrosis (Nukui M. et al, manuscript), nephrin-knockout mice model for CNF [146], db/db mice (Norlin J. et al, manuscript), human diabetic nephropathy [147], as well as human FSGS and minimal change disease [148]. In their study, Done et al [146] have shown that nephrin is involved in maturation but not development of podocytes, as the nephrin-knockout mice strikingly show very little expression changes compared to normal controls. Although proteinuria is the common denominator for all mentioned disease states, the profiling results depict their expression variability. Only two genes were downregulated in five of the aforementioned diseases: NEBL (nebulette)-an actin binding protein involved

in the organization of cytoskeletal network, and THSD7A (thrombospondin type 1, domain 7A)- an endothelial protein that interacts with components of the GBM. Only one gene was upregulated in four diseases: CDKN1A (cyclin dependant kinase inhibitor A)-a protein that promotes apoptosis during acute kidney injury (Tryggvason S. et al, manuscript). Pathway analysis shows that inflammation and fibrosis are common to all disease models: the db/db mice exhibit acute inflammatory signs already at 2 months of age, whereas human diabetic nephropathy patients show a decrease in integrin actin cytoskeleton signaling and increase in leukocyte extravasation (Tryggvason S. et al).

Clearly, large-scale profilings present a significant aspect of glomerular studies. A recently developed method, RNA sequencing, is an even more sophisticated and accurate tool that allows for sequencing and quantification of rare RNAs even in a single isolated glomerulus. One can imagine that the development of novel profiling techniques will take us yet further-into comparisons of expression signatures among cells of glomerulus *in situ*.

2 AIMS OF THE STUDY

The overall goal of this study was to identify and characterize novel genes and proteins possibly involved in the origin and progression of kidney glomerulus diseases. In addition, this study also aims to provide a deeper insight into the role of podocytes in maintenance of normal glomerular filtration and help us to understand some of the basic molecular mechanisms underlying the pathological states of glomerular filter.

The specific aims of this project were:

1. To identify transcripts of genes that have previously not been associated with renal glomerulus and its failure.
2. To characterize the general expression pattern of these transcripts and particularly localize the protein products of these genes in the kidney glomerular filter.
3. To identify interaction partners of the novel podocyte proteins, as these interactions are likely to shed light to the proteins physiological functions.
4. To examine the functional role of these proteins in cultured podocytes and study their possible involvement in mouse and human glomerular diseases.

3 MATERIAL AND METHODS

Expression constructs

Expression constructs were generated by cloning of PCR-amplified fragments into various expression vectors using established molecular biological methods. Inserts were amplified from kidney cDNA (Mouse MTCTM Panel I, Clontech) with Long PCR Enzyme Mix (Fermentas), and sequenced to confirm absence of PCR-generated mutations. The PCR program used was: 1 cycle of 95°C/4 min, 30 cycles of 95°C/1 min, 51°C/1 min, 72°C/2-4 min, and 1 cycle of 72°C/10 min. For yeast two-hybrid screening, inserts were cloned into the vector pGBKT7 (Clontech) in frame with the Gal4 DNA-binding domain. For expression in mammalian cells, cDNAs were cloned into pcDNA3.1 (Invitrogen), or vectors with various N-terminal tags (pCMV-Myc, pCMV-HA, or pEGFP-C; all from Clontech).

Antibodies

Commercial antibodies or antibodies from the Swedish Human Protein Resource project were used in all experiments. Proteins were visualized with secondary antibodies conjugated to various Alexa Fluor dyes (488, 546, 568; all from Invitrogen) or HRP (GE Healthcare). Phalloidin and DAPI reagents were purchased from Molecular Probes.

Human material

Normal renal tissue was taken from unaffected kidneys surgically removed because of localized carcinoma. Patients who fulfilled criteria for FSGS,

MCNS, MN and DN, were chosen for studies. All biopsies were taken for diagnostic purposes and re-examined to confirm diagnosis. Biopsy material has been saved prospectively and embedded in a low-temperature resin allowing immunoelectronmicroscopy (IEM). All material was used in agreement with the local Board of Ethics.

Reverse transcription (RT) and RT-PCR

For generating glomerular and “rest of kidney” cDNA, mouse glomeruli and kidney tissue devoid of glomeruli (rest of kidney) were isolated as previously described [57]. Fluorescently labeled podocytes were derived by FACS sorting of cells from glomeruli obtained from bitransgenic R26-stop-EYFP mice harboring the Cre transgene driven by the podocin promoter. Total RNA was then isolated by RNeasy mini Kit (QIAGEN) and 1 µg was reverse transcribed by Superscript III Reverse Transcriptase (Invitrogen). The generated cDNA was diluted 10-fold with Tris-EDTA buffer for freezer storage. For studies on tissue distribution, multiple mouse tissue cDNAs were used as templates for RT-PCR (Mouse MTC™ Panel I, Clontech). The PCR reactions were done by HotStartTaq polymerase (Qiagen) with gene-specific primers to amplify around 500 bp products. The PCR products were analyzed in 1% TBE agarose gel and photographed.

Northern blot

To study tissue distribution at the RNA level, specific 500 bp PCR products obtained from amplification of glomerular cDNA were used as probes. The probe was ³²P-dCTP labeled with Prime-It® RmT Random Primer Labeling Kit

(Stratagene) and hybridized with Mouse MTN® Blot (Clontech). Hybridizations were also performed on blots containing mRNA isolated from two kidney fractions, either only glomerular tufts or the kidney excluding glomeruli. The blots were exposed to a PhosphorImager SF screen (Molecular Dynamics) and analyzed with ImageQuant software (Molecular Dynamics).

***In situ* hybridization**

To localize gene expression in the kidney, *in situ* hybridization experiments were carried out on mouse cryosections. Gene-specific probes were transcribed by T7 or SP6 polymerases and labeled with ³⁵S. The procedure has been described previously [149].

Transient and stable transfections

Human podocytes were grown at 33°C/5% CO₂ in RPMI supplemented with 10% fetal bovine serum (Invitrogen), 1x insulin-transferrin-selenium-A supplement (Invitrogen), and antibiotics (100 U/ml penicillin and 100 µg/ml streptomycin) (Invitrogen), as previously described. HEK293, COS7, NIH3T3 and CHO cells were cultured at 37°C/5% CO₂ in DMEM containing the same supplements, except ITS-A. Cells were transiently transfected with Lipofectamine 2000 (Invitrogen) according to the manufacturer's recommendations. For generation of stable-expressing HEK293 clones, cells were selected and maintained in medium containing 500 µg/ml of G418. Stable transfectants were characterized by GFP immunofluorescence and Western blotting for GFP expression.

Immunofluorescence (IFL)

For human and mouse kidney analysis, samples were collected and snap-frozen, and then cryosectioned at 8-10 μm thickness. Sections were postfixed with cold acetone (-20°C) or room temperature with 4% paraformaldehyde (PFA), followed by blocking in 5% normal goat serum. For immunofluorescence, cells were grown on fibronectin-coated glass coverslips. For coating, coverslips were incubated with 10 $\mu\text{g}/\text{ml}$ of fibronectin (Invitrogen) for 2 h at room temperature, followed by several washes with PBS. Cells were fixed with 4% PFA for 20 min at room temperature, after which they were permeabilized by incubation with 0.1% Triton X-100/PBS for 5 min, followed by an incubation with 2% BSA/PBS (blocking solution) for 1 h. In some experiments, cells were treated with 0.5% saponin/PBS for 20 min before fixation. After blocking, cells were incubated with primary antibodies for 1 h at RT, washed several times with PBS, and then incubated for 1 h with a suitable secondary antibody. All antibodies were diluted in the blocking solution. Secondary antibody solutions also contained rhodamine-phalloidin and DAPI to stain F-actin and cell nuclei, respectively. For double labeling, incubations were performed sequentially to prevent crossreactions. Photos were taken using Zeiss LSM510 confocal microscope, with 20x, 40x or 63x objectives.

Drug treatments

Transiently transfected human podocytes, HEK293 or NIH3T3 cells were plated on fibronectin-coated coverslips in 24-well plates, and left to adhere and spread for 16 h. Thereafter, cells were incubated for 1 h at 37°C with 10

µg/ml of the actin monomer-sequestering drug latrunculin A (Sigma), 100 nM of wortmannin (Sigma) or LY294002 (Cell signaling), inhibitors of PI3-kinase, diluted from stock solution prepared in DMSO. Control cells were incubated with the vehicle only. After the incubation, cells were fixed, and stained for Myc and F-actin as described above.

Yeast two-hybrid screening (Y2H)

For yeast two-hybrid screening, we used a mouse kidney glomerulus cDNA library custom-generated by Clontech. The library was screened with baits encoding the Gal4 DNA-binding domain fused to full-length Schip1 or Plekhh2 or their deletion variants. Screening was carried out by yeast mating according to the manufacturer's instructions. Diploids were selected through several rounds of culture on minimal synthetic dropout medium. Plasmids from obtained colonies were isolated, sequenced, and analyzed with the BLAST algorithm at the National Center for Biotechnology Information (NCBI).

Western blotting and coimmunoprecipitations

Western blotting was carried out following standard procedures. For coimmunoprecipitations, confluent transiently transfected HEK293 cells were washed twice in cold PBS and lysed in 0.5% Triton X-100, 20 mM Tris-HCl (pH 7.4) and 150 mM NaCl buffer containing protease inhibitor cocktail (Roche) and phosphatase inhibitors (1 mM NaVO₃, 50 mM NaF). Lysates were clarified by centrifugation (14000 x g), incubated with primary antibodies overnight, followed by an incubation with protein A+G agarose beads (Roche Molecular Biochemicals) for 1 h at 4°C. Thereafter the beads were washed 3

times with the lysis buffer, resuspended in 1x SDS-sample loading buffer, and boiled for 10 min. Eluted proteins were analyzed by SDS-PAGE and Western blotting. For subcellular fractionation experiments, cell lysates were fractionated with Qproteome Cell Compartment Kit (Qiagen) prior to gel analysis.

Fluorescent Resonance Energy Transfer (FRET) in fixed cells

A detailed description of the FRET technique can be found elsewhere [150]. We utilized this method to confirm protein interactions discovered by yeast two-hybrid. The Förster constant, R_0 , for the donor-acceptor pairs used in this study, Alexa488 and Alexa568, is 62Å. To determine FRET, we quantified the quenching of donor fluorescence by performing acceptor photobleaching. FRET measurements were performed using a Zeiss LSM510 inverted confocal microscope, apochromat 63x/1.4 NA oil immersion objective and the Zeiss LSM510 software version 2.8. Briefly, fluorophores were excited with 488 and 543 nm laser and images collected separately. The acceptor, Alexa568, was then irreversibly photobleached in a selected adequate region by continuous excitation with a 543 nm laser for about 30 s. Thereafter, residual Alexa568 and Alexa488 image was obtained under same settings as prebleach images, and identical regions on individual cells were outlined in the photobleached area and processed using ImageJ. Ratios between Alexa488 intensities of the selected region, after and before photobleaching, were calculated to quantify FRET. In a typical experiment 15–20 cells were measured for each sample.

Immunoelectron microscopy (iEM)

Samples from human renal cortexes were fixed in 3% PFA in 0.1M Phosphate buffer. After fixation, samples were cut in smaller pieces and dehydrated by stepwise increased concentration of methanol and in each step gradually lowering the temperature down to -40°C in a Leica EMAFS (Leica microsystem) and embedded and polymerized in Lowicryl K11M (Polysciences) at -40°C. Ultrathin sections were cut at room temperature and placed on carbon formvar-coated nickel grids. IEM was performed as described elsewhere, with proteins of interest labeled with 10 and 5 nm gold particles, respectively. For semiquantification by immunoelectron microscopy, six locations per glomerulus (1–2 glomeruli, depending on material) were chosen with a random start at low magnification. Three images were taken from each location. Prints at a final magnification of 52 000x were examined and the number of gold markers (Au) was counted. The area of corresponding compartment was calculated by point counting, using a 1 x 1 cm square lattice, and expressed as μm^2 . The concentration of protein was expressed as the number of gold particles per square micrometer ($\text{Au}/\mu\text{m}^2$). The GBM length and the number of slits were expressed as a ratio $\text{slits}/\mu\text{m}$ to evaluate FPE (less than 1 slit/ μm GBM defined as FPE). Statistical analysis: in comparisons between groups a one-way ANOVA was used followed by Dunnett's test comparing the diseased group means with the control group mean. The Spearman rank order correlation coefficient was used to measure the association between variables within each group. $P < 0.05$ was considered statistically significant.

Cell migration assay

Cell migration ability was assessed in a wound healing scratch assay. Stably expressing GFP-Schip1 HEK293 cells were plated on 24-well culture dishes precoated with 10 μ g/ml of fibronectin. Cells were grown to confluency and serum starved in 0.5% FCS over-night. Next day cells were wounded by manual scratching with a 200- μ l pipette tip, washed with PBS, and incubated at 37°C in complete media or induced by media containing 50 μ g/ml PDGF-BB. At the indicated times, phase contrast images at specific wound sites were captured by Leica microscope and images were analyzed by ImageJ program. Results reported in percent, as size of the wound compared to 0-point and representative of three experiments.

***In vitro* actin assembly assays**

In vitro actin polymerization and depolymerization assays using the Actin Polymerization Kit (Biochem) were employed to study the role of Plekhh2 in the actin assembly processes. The assay relies on the difference between fluorescent signals of pyrene-labeled monomeric G-actin and polymerized pyrene-F-actin (used as positive controls in our experiments). For these assays, we used lysates prepared from 293 cells stably expressing GFP-Plekhh2, and control cells. Cells were plated onto plates coated with 10 μ g/ml of fibronectin, and allowed to adhere overnight in a serum-free media, followed by an overnight treatment with medium containing 10% FCS or 30 μ g/ml of PDGF-BB (Invitrogen). After this, cells were collected and lysed for 3 h at 4°C in a buffer containing 20 mM Tris-Cl, pH 7.5, 20 mM NaCl and protease inhibitors. Lysates were clarified by centrifugation at 14000 rpm for

10 min. The actin polymerization and depolymerization assays were performed according to manufacturer's instructions, and fluorescence kinetic measurements were done with TECAN GENiosPro.

Live cell imaging (paper II, supplementary)

Imaging of GFP-Plekhh2-expressing human podocytes plated on fibronectin-coated glass coverslips was started immediately after cell plating. Imaging was continued overnight, with images being taken every 5 min (Zeiss LSM 510 microscope, 40x objective). They were then processed into a movie with the ImageJ program.

Microarray comparisons of mouse glomerular disease models

Several mouse glomerular disease models were included in this analysis: adriamycin-induced mice nephrotic syndrome model (Nukui M. et al, manuscript), LPS-induced mice nephrotic syndrome model [144] and type II diabetic mice model (Norlin J. et al, manuscript). Mouse glomerular RNA was isolated and hybridized on Affymetrix arrays, and the array data were processed as described before.

4 RESULTS AND DISCUSSION

Results presented in this doctoral thesis are part of a large-scale “glomerulus gene discovery” collaborative project between Prof Karl Tryggvason’s and Prof Christer Betsholtz’s groups. The key for initialization of the project was development of a robust method for kidney fractionation into glomeruli and rest-of-kidney tissue. This was achieved by perfusing mice through the heart with magnetic beads finally ending up in the kidney glomeruli, which can subsequently be isolated with a magnetic particle concentrator [151]. Microarray profiling of glomerular transcriptome led to the generation of the so-called “GlomBase”-a database with over 6000 glomerular genes [57]. After normalization against rest-of-kidney tissue, a group of over 300 genes was found to be specifically upregulated in the glomerulus. Many genes from this group were taken into further more detailed expression analysis and several of the initially analyzed genes were presented in Paper I. Functional characterization performed for two genes, *Plekhh2* and *Schip1*, from the same group of glomerulus-upregulated transcripts, is presented in Papers II and III.

4.1 Expression of novel glomerular genes and proteins (Paper I)

In the first study, detailed expression profile of five glomerulus-upregulated transcripts coding for: *Ehd3*, *dendrin*, *Sh2d4a*, *Plekhh2* and *2310066E14Rik* is presented. Their expression pattern was studied by reverse transcriptase-PCR, Northern blotting, and *in situ* hybridization.

Polyclonal antibodies were raised for studies of proteins distribution in the mouse and human kidney tissue by immunostaining, Western blots and immunoelectron microscopy. We show that these genes have a restricted expression pattern, and in the kidney they are all detected only in the glomerulus.

Ehd3 is a cytosolic protein thought to be associated with endocytic vesicles [152]. Our study identifies it as the first gene ever shown to be expressed exclusively by glomerular endothelial cells. Recently it was shown that the lack of Ehd3 is compensated by upregulation Ehd4 in knockout mice, and that Ehd3/Ehd4 double knockouts exhibit multiple glomerular defects including: proteinuria, thickening of the GBM and loss of endothelial fenestrations [153]. The other four proteins are all localized to glomerular podocytes: **Dendrin** is a cytosolic protein reported to be specific for the dendritic processes of certain neuronal cells of the forebrain [154]. It was shown to interact with cytoskeletal components *in vivo* [155]. In podocytes, it is localized at the cytoplasmic insertion sites of the slit diaphragms. **Sh2d4a** encodes for a novel docking SH2 protein and in podocytes it was found to be diffusely distributed in the cytoplasm of the foot processes. **Plekhh2** is a previously uncharacterized protein with a domain structure resembling that of unconventional myosins, which often localize to actin-rich cellular processes. In kidney immunostaining, the signal for Plekhh2 overlaps that of nephrin, suggesting podocyte foot process localization. **2310066E14Rik** is an unknown intracellular protein, with localization to podocyte cell bodies and major processes.

The glomerular filtration apparatus is extremely specialized and, therefore, many critical glomerular proteins have a very restricted expression pattern, in kidney only in podocytes. Novel glomerular proteins described in this study share these characteristics, which promises that they might also have highly specific roles in glomerulus. We hypothesize that the possible function of dendrin, Sh2d4a and Plekhh2 could be in connecting and/or signaling between actin cytoskeleton and podocyte foot processes/slit diaphragm. Results of this study also emphasize and confirm the power of large-scale transcript profiling efforts from the nephrology standpoint.

4.2 Plekhh2 (Paper II)

One of the interesting proteins that emerged from study I as highly glomerulus-specific was Plekhh2. We decided to characterize the domain structure of this protein, its function in kidney cells, interaction partners network and involvement in human glomerular disease and mouse models of renal disease.

The Plekhh2 polypeptide is predicted to contain several functional domains: a putative α -helical coiled-coil domain at the N-terminus, while the C-terminal half contains two PH domains, a MyTH4 domain, and a FERM domain. Plekhh2 resembles myosin X, a protein shown to have a role in filopodia elongation *via* PIP3 binding to one of its three PH domains [156]. We show that ectopically expressed Plekhh2 localizes to the peripheral regions of lamellipodia in cultured podocytes. Deletion of either PH or FERM domains of full length Plekhh2 is not sufficient to completely abolish Plekhh2 localization

to lamellipodial structures, suggesting that both the PH and FERM domains contribute to the targeting of the protein to this subcellular location. Furthermore, we show that Plekhh2 resides in the membrane and cytoskeletal fractions of cultured human podocytes, suggesting that it is associated to these structures. The Plekhh2 N-terminal half containing the coiled-coil domain (Δ PHPHMyTHFERM truncation variant) was not targeted to lamellipodia but instead localized to the nucleus. However, we are able to show, by coprecipitation and FRET analyses, that this part of the protein indeed mediates Plekhh2 dimerization, as it is predicted for the coiled-coil domains [157]. Analysis of the amino acid sequence of the Plekhh2 PH domains indicated the presence of a PtdIns(3,4,5)P3 (PIP3) consensus binding site in the PH1 domain. Mutation of selected conserved residues, as well as inhibition of PI3-kinase with wortmannin and LY294002, markedly inhibited/abolished Plekhh2 peripheral localization. It is known that although basal cellular levels of PIP3 in cells are low, they are significantly elevated upon PI3-kinase activation by growth factors, such as PDGF [158]. In addition, the lipid is not homogeneously distributed throughout the plasma membrane in polarized cells, but it is concentrated to the basolateral membrane domain [159]. Similarly, distribution of Plekhh2 towards lamellipodia is seen in cultured podocytes plated on fibronectin, and we speculate that this is caused by the low level PIP2 and/or PIP3 activation and integrin signaling.

In order to elucidate the cellular functions of Plekhh2, we employed an unbiased Y2H approach for discovering protein interactions, and screened a mouse kidney glomerular cDNA library with full-length Plekhh2 and its deletion variants. By this screen we identified, and later confirmed, Hic-5, a paxillin-

related focal adhesion protein (TGFB1i1), and β -actin (ActB) as interacting partners of Plekhh2. Furthermore, we are able to colocalize Plekhh2 and Hic5 by IEM in the kidney glomerular filter to podocyte foot processes close to the GBM, within 20 nm distance from each other, suggesting that these two proteins interact not only *in vitro* but also *in situ*. Hic-5 has been shown to interact with the PINCH-ILK- α -parvin complex, which plays a critical role in the control of podocyte adhesion and morphology [160]. Plekhh2 association to Hic5 points that it could participate in the same complex.

Association of Plekhh2 and actin *via* the FERM domain was first observed in Y2H, and then confirmed by yeast mating. It has become evident only during recent years that FERM domains of some proteins are able to directly interact with actin [161-163]. However, the interactions appear generally to have a low affinity. In these studies, these interactions have been demonstrated in cosedimentation assays, and have shown Kd values at the mM level (not measured in every study). Significantly, our study reveals the Plekhh2 FERM domain-actin interaction with a completely unbiased Y2H approach. Plekhh2 and cortical cell actin colocalization data, as well as Plekhh2 detection in the cytoskeletal cell fraction-additionally contribute to the notion that Plekhh2 is indeed associated to actin. Functionally, we show that Plekhh2 stabilizes cortical actin cytoskeleton in cells treated with actin monomer-sequestering drug, probably by attenuating actin depolymerization. Plekhh2 and actin interaction may be weak and present only in certain conditions (e.g. cells extending lamellipodia), or only in cortical actin fractions (and not generally in the cell), but it clearly has implications for maintenance of cellular morphology and migration/adhesion properties.

From our work it appears that, at the sole of podocyte foot processes, Plekhh2 is, very likely in the form of a dimer, part of a multiprotein adhesion complex, involved in linking the complex to the plasma membrane on one side, and to actin filaments on the other, and even contributing to regulation of their dynamics.

Analysis of renal biopsies from patients with perihilar and tip lesion FSGS, which are the most common FSGS subtypes in our patient population, reveals that the Plekhh2 protein is significantly reduced and shows a tendency to relocalization from plasma membrane more centrally into the podocyte foot processes. Also, a comparison of Plekhh2 and its associated proteins, Hic5 and actin, expression in mouse models of glomerular disease revealed parallel changes: upregulation in LPS and downregulation in db/db model. These analyses may indicate that Plekhh2, Hic5 and actin are collectively involved in origin and/or progression of podocyte injury leading to proteinuria. However, the complex underlying mechanisms for this could be very different in various human glomerular diseases and need to be studied further.

4.3 Schip1 (Paper III)

One of the glomerulus-upregulated transcripts encoded for Schip1, a relatively novel protein discovered originally through its interaction with neurofibromatosis type 2 protein (Nf2, Schwannomin, merlin) in the mouse brain [164]. Merlin, the tumor suppressor protein, belongs to a family of ERM proteins (ezrin, radixin, moesin) that function as a regulated link between the cell membrane and the cortical actin cytoskeleton [165]. In brain, Schip1 is

found as a product of a fusion gene named IQCJ-SCHIP1 [166] that localizes to mature nodes of Ranvier and axon initial segments [167]. As it is considered that glomerular podocyte foot processes are similar to neuronal cells extensions [168], it was interesting for us to investigate the expression pattern and function of Schip1 from the kidney point of view.

By use of RT-PCR and Northern blot on a panel of mouse tissues, we observed a wide expression pattern for Schip1 that starts at early embryonic stages, but it was most prominently expressed in brain, kidney and heart. In the kidney glomerulus, it is mostly expressed by glomerular podocytes as shown by RT-PCR from FACS sorted podocytes and rest-of-glomerulus samples. By IFL we also see mainly podocyte staining for Schip1, overlapping with synaptopodin, but we cannot exclude that a small amount of the protein localizes to mesangial cells as well. Electron microscopic analysis of human kidney samples revealed that 67% of labeling for Schip1 localizes to podocyte foot processes *in situ*, where it is found towards the membrane laterally, apically but also basally at the GBM. A portion of Schip1 is localized to endothelial cells of glomerulus (14%).

In cultured human podocytes, Schip1 localizes to lamellipodia at the periphery of plasma membrane, overlapping closely with cortical actin cytoskeleton. Actin disassembly by latrunculin A treatment in Schip1 overexpressing podocytes leaves the protein associated to remnant F-actin, suggesting direct or indirect Schip1 connection with actin cytoskeleton. However, contrary to Plekhh2, Schip1 is not able to increase cortical actin stabilization.

Schip1 knockout mice generated by Schmall et al [169] exhibit skeletal and craniofacial defects and digestive problems, but surprisingly no overt kidney phenotype. However, the loss of one PDGFr β allele is enough for the Schip1-/-PDGFr β +/- mice to show decreased kidney function indicated by swollen and degraded glomeruli and fewer mesangial cells clustered together. It has been suggested that Schip1 is one of the early response genes controlling specific processes downstream of PDGF signaling [169, 170]. Interestingly, we show that a 2h stimulation of Schip1-overexpressing podocytes with PDGF-BB leads to accumulation of cortical cell actin with a significant loss of transversal actin fibers in about 30% of Schip1-transfected cells. In a wound-healing migration assay GFP-Schip1 expressing cells migrated significantly faster than controls when stimulated with PDGF-BB. We propose that Schip1 promotes cell migration in response to PDGF β signaling, probably by cortical actin remodeling.

Yeast two-hybrid screening of glomerulus cDNA library revealed that Schip1 interacts with Nherf2, a component of a well-characterized glomerular protein complex Nherf2/ezrin, which docks actin filaments to the periphery of plasma membrane [65]. We have confirmed interactions of Schip1 with both Nherf2 and ezrin by coprecipitations from transfected cells and FRET, and colocalized these proteins in human podocytes *in vitro* and *in situ*. By co-IEM there was significant colocalization of Schip1 and ezrin proteins in podocytes foot processes, where they were found less than 10 nm apart from each other. Schip1 and Nherf2 colocalized about 30 nm from each other. Interestingly, we also observed that Schip1 and these proteins show a tendency to parallel expression changes in mouse glomerular disease models

underlined with podocyte actin cytoskeleton alterations: downregulation in adriamycin and LPS models, and upregulation in type II diabetes model.

Our results demonstrate that Schip1 plays a role in actin remodeling downstream of PDGF β signaling, very likely due to functional association with Nherf2/ezrin/merlin proteins. This is significant because it has been shown that glomerular epithelial cells, podocytes, express PDGF β receptors already in early stages of diabetic nephropathy and that their levels are much higher than in normal human kidney [171]. Merlin, ezrin and Nherf proteins have already been functionally associated to cortical cell actin and extensively studied not merely as linkers, but also as active modulators of actin cytoskeleton and membrane receptors in subcortical zones of cell extensions, especially in glomerulus [172].

5 CONCLUSIONS AND FUTURE PERSPECTIVES

Knowledge about the gene and protein expression complexity of the kidney glomerulus has been accumulating steadily over the years. This process was especially accelerated with availability of large-scale unbiased techniques for studies of transcriptome profiles and protein interaction networks. Our group has been involved in one of the pioneering projects aiming, not only to have a look into glomerular (*versus* rest of the kidney) transcriptome particularities and its changes in disease and development, but also to take a number of interesting glomerulus-associated genes into further functional analysis.

During a decade of exciting and extensive glomerular research, many novel glomerular genes and proteins were characterized by our group, two of them presented in this thesis work: *Plekhh2* and *Schip1*. We have shown that both of these proteins are normally upregulated in glomerulus (compared to rest-of-kidney tissue) and localized in the podocytes foot processes. Together with their interaction partners, these proteins are parts of complexes involved in cortical actin stabilization at adhesion sites. Furthermore, we have shown that they are also involved in origin and progression of glomerular diseases in human and mouse: *Plekhh2* is significantly downregulated in human FSGS and *Schip1* in LPS-induced model of mouse nephropathy. Here we have concentrated on expression pattern and subcellular localization, interaction partners and cellular functions of these proteins, but clearly more *in vivo* studies are needed to clarify their physiological importance. Nevertheless, results from this thesis can be taken as guidelines and suggestions on how to

interpret future studies involving mouse knockout model challenges or zebrafish knockdown investigations.

In fact, the ultimate ambition of our “glomerular gene discovery project” is to fully characterize novel genes and proteins, from expression data to generation and studies of living models. Having such a perspective has provided us the opportunity to create significant knowledge about glomerular function in normal and disease states, as well as the molecular basis of glomerular pathophysiology. Glomerular failure underlies several fatal kidney diseases and we hope that results of the overall project can be translated to clinical medicine, with possibilities to develop novel diagnostic methods and drug targets for kidney disease.

6 ACKNOWLEDGEMENTS (...and confessions)

To be perfectly honest, this whole PhD-thing has been a struggle for me: I have struggled technically with learning the methodology (for example how to use the microwave...), scientifically to formulate hypotheses and go forward with new findings, psychologically to survive all the downfalls and negative results, and personally trying to organize my life in a foreign country different than my own. Still, here I am at the end of this road, facing one more task that I didn't realize could also be hard: trying to remember everyone who helped me on my way and expressing my gratitude in proper words!

*Well, to start at the beginning, I would not even be here if it wasn't for **Karl** who decided to give a chance to an inexperienced young girl from a country in which this kind of science is certainly underdeveloped. What you saw in me I shall never know, but you have taken me on a journey of a lifetime! Being in "The Matrix" that you created has shaped me not only as a scientist but also as a person, and that is something I can never forget. You are the "*spiritus movens*" and one of those rare*

people in this world that have huge energy and a “spark” to drive things forward and bring changes!

*When it comes to the everyday lab work, discussions, troubleshooting and all that, the first person that springs to my mind is **Timo**. He was my “lab guru”, “proofreading enzyme”, extra pair of eyes and brains and a reality check during my doctoral studies. You have taught me everything about lab work in a kind and patient manner. I wish you all the best in your future life and don’t be sad if The Call never comes (...you now the one in October)!*

*For my projects I also had a lot of help from **Jaakko** and **Mark**, especially in discussions and writing of the manuscripts. Your help was priceless because it came at the right moment when it was most needed!*

*I would like also to thank our collaborators: **Christer Betsholtz**, **Annika Wernerson**, **Kjell Hultenby** and **Jenny Hülkö**, for years of fruitful exchange of ideas and significant contribution to my work.*

*I have been in “The Matrix” for quite some time, so there are quite a few people whose path crossed with mine over the years: I will always remember: **Emma**- my first Swedish friend,*

Stefanía- my shopping soul mate (I still didn't reach 100 pairs of shoes but I am working on it!), Olga and Eyrun- for all our interesting talks, Marko- for being so helpful with computers. Ann-Sofie- for organizing our lab lives so well, Anne-May, Lotta, Bing, Ulla, Susan, Patrícia- our lunch break conversations have been "the highlights" of many gloomy days. Special thanks to Anne-May and Lotta for spicing up the days with delicious homemade pepparkakor and muffins, and to all others for correcting my Swedish. Gigi, we have been struggling together on the same project and I remembered one anecdote from a meeting we had with Jaakko. Disappointed with some results, Jaakko commented: "We are not getting anything out of this project" and you answered "Well, I got myself a nice husband here!" Lwaki, your life energy and positive thinking are an inspiration to me. Anna, I share your love for detective stories. Sergey and Kan, you have been good office mates for many years. Asi, I know you will finish your studies with great results and your ambition will take you far. Juha, I have a feeling you are destined for great discoveries cause science comes like a game to you. To the other dear colleagues and former members of Matrix: Berit, Masa, Sam, Maya,

Elisabeth, Li, Yi Sun, Yunying, Liqun, Ying, Kerstin...you all made my PhD experience special.

Tanja and Dragan are my Serbian friends who have been with me since the second day I set my foot in Sweden, and helped me on many occasions: moving, assembling Ikea furniture...I will always remember that sunny August day you were showing me around Stockholm when I came here for an interview. I knew right away this is where I want to live. Oh, how different it looked when I came back in November! Tanja, thank you for all the PhD commiserations you shared with me over all these years.

The first scientific steps I made in the lab of Prof Sonja Pavlovic in Belgrade, who supervised my master thesis. We were a bunch of girls in the lab then, ambitious and ready to explore the world, with Sonja giving us all the encouragement, freedom and advice. I will remember you always with great emotions: Sonja, Jelena (now in London), Jelena (now in Barcelona), Branka, Natasa.

To my University girls-gang: Marija (Germany), Nadja (Portugal-USA), Marizela (Luxembourg), Jelena (Italy) and Maja (Belgrade), with whom I have studied and shared

exam worries in the best cappuccino places in Belgrade, I wish to send them a message: life has taken us apart but we still need to meet annually and update each other with news!

*I would especially like to remember here two of my Serbian friends, **Ivana** and **Milica**, that I have known since my early childhood. Girls, you deserve special thanks just for being around so many years! We grew up together and even though we had different destinies, we nurtured and guarded our friendships because they are based on similar basic values. Ivana, coffee never tastes the same when I drink it without you and our endless chats! Milica, shall we ever play with Barbie dolls together again? I am so privileged to have such friends as you and I have missed you a lot over all these years!*

Lastly, a few words for those who mean the most to me:

***Voljena moja Mama**, ne mogu ni da zamislim svu zrtvu koju si podnela da nas troje izvedes na put sama. Mozda bi sve bilo drugacije da je tata bio sa nama, tu zalost cu zauvek nositi u sebi. Ne brini, nije bilo uzalud, naci cemo nas troje svoje mesto pod ovim nebom. Zivot je brz i cesto zaboravljam da ti kazem*

*koliko mi značís, ali ovo je pravi trenutak da zastanem: hvala ti sto me nikad nisi sputavala da budem ono sto zelím, ma koliko tebi to bilo tesko! Mojoj braci, **Petru i Dejanu** zelím svetlu budućnost i da uvek budemo jedni uz druge onda kada je to potrebno. **Jelena**, dobrodosla u porodicu!*

*At the very end, how can I ever express in words how much you mean to me, **Nenad**, my dear? Through the best of times and the worst of times you have been my loving partner and understanding friend, and this journey has been easier holding your hand for the past twelve years. Finding you is the best I've ever done, because through you, I found myself. Now, let's look behind the curtain to see what life has in store for us and may the adventure begin!*

*Finally I should say, there were many easier paths but I
am happy I walked this one!*

7 REFERENCES

1. Eckardt, K.U., *Erythropoietin production in liver and kidneys*. Curr Opin Nephrol Hypertens, 1996. **5**(1): p. 28-34.
2. Saxen, L. and H. Sariola, *Early organogenesis of the kidney*. Pediatr Nephrol, 1987. **1**(3): p. 385-92.
3. Bard, J.B., *The development of the mouse kidney--embryogenesis writ small*. Curr Opin Genet Dev, 1992. **2**(4): p. 589-95.
4. Michos, O., *Kidney development: from ureteric bud formation to branching morphogenesis*. Curr Opin Genet Dev, 2009. **19**(5): p. 484-90.
5. Costantini, F., *Renal branching morphogenesis: concepts, questions, and recent advances*. Differentiation, 2006. **74**(7): p. 402-21.
6. Horster, M.F., G.S. Braun, and S.M. Huber, *Embryonic renal epithelia: induction, nephrogenesis, and cell differentiation*. Physiol Rev, 1999. **79**(4): p. 1157-91.
7. Scott, J.E. and M. Renwick, *Antenatal diagnosis of congenital abnormalities in the urinary tract. Results from the Northern Region Fetal Abnormality Survey*. Br J Urol, 1988. **62**(4): p. 295-300.
8. Schedl, A., *Renal abnormalities and their developmental origin*. Nat Rev Genet, 2007. **8**(10): p. 791-802.
9. Cirillo, M., *Evaluation of glomerular filtration rate and of albuminuria/proteinuria*. J Nephrol, 2010. **23**(2): p. 125-32.
10. Jerums, G., et al., *Integrating albuminuria and GFR in the assessment of diabetic nephropathy*. Nat Rev Nephrol, 2009. **5**(7): p. 397-406.
11. Mogensen, C.E., *Microalbuminuria predicts clinical proteinuria and early mortality in maturity-onset diabetes*. N Engl J Med, 1984. **310**(6): p. 356-60.
12. Hudson, B.G., et al., *Alport's syndrome, Goodpasture's syndrome, and type IV collagen*. N Engl J Med, 2003. **348**(25): p. 2543-56.
13. Tryggvason, K., J. Patrakka, and J. Wartiovaara, *Hereditary proteinuria syndromes and mechanisms of proteinuria*. N Engl J Med, 2006. **354**(13): p. 1387-401.
14. Tryggvason, K., et al., *Molecular genetics of Alport syndrome*. Kidney Int, 1993. **43**(1): p. 38-44.
15. Osterholm, A.M., et al., *Genome-wide scan for type 1 diabetic nephropathy in the Finnish population reveals suggestive linkage to a single locus on chromosome 3q*. Kidney Int, 2007. **71**(2): p. 140-5.
16. Thomas, M.C., P.H. Groop, and K. Tryggvason, *Towards understanding the inherited susceptibility for nephropathy in diabetes*. Curr Opin Nephrol Hypertens, 2012. **21**(2): p. 195-202.
17. Franceschini, N., et al., *NPHS2 gene, nephrotic syndrome and focal segmental glomerulosclerosis: a HuGE review*. Genet Med, 2006. **8**(2): p. 63-75.
18. Kestila, M., et al., *Positionally cloned gene for a novel glomerular protein--nephrin--is mutated in congenital nephrotic syndrome*. Mol Cell, 1998. **1**(4): p. 575-82.

19. Gigante, M., et al., *CD2AP mutations are associated with sporadic nephrotic syndrome and focal segmental glomerulosclerosis (FSGS)*. Nephrol Dial Transplant, 2009. **24**(6): p. 1858-64.
20. Kaplan, J.M., et al., *Mutations in ACTN4, encoding alpha-actinin-4, cause familial focal segmental glomerulosclerosis*. Nat Genet, 2000. **24**(3): p. 251-6.
21. Lam, D.W. and D. Leroith, *The worldwide diabetes epidemic*. Curr Opin Endocrinol Diabetes Obes, 2012. **19**(2): p. 93-6.
22. O'Donnell, M.P., et al., *Adriamycin-induced chronic proteinuria: a structural and functional study*. J Lab Clin Med, 1985. **106**(1): p. 62-7.
23. Wang, Y., et al., *Progressive adriamycin nephropathy in mice: sequence of histologic and immunohistochemical events*. Kidney Int, 2000. **58**(4): p. 1797-804.
24. Reiser, J., et al., *Induction of B7-1 in podocytes is associated with nephrotic syndrome*. J Clin Invest, 2004. **113**(10): p. 1390-7.
25. Chen, H., et al., *Evidence that the diabetes gene encodes the leptin receptor: identification of a mutation in the leptin receptor gene in db/db mice*. Cell, 1996. **84**(3): p. 491-5.
26. Sharma, K., P. McCue, and S.R. Dunn, *Diabetic kidney disease in the db/db mouse*. Am J Physiol Renal Physiol, 2003. **284**(6): p. F1138-44.
27. Kreidberg, J.A., *Podocyte differentiation and glomerulogenesis*. J Am Soc Nephrol, 2003. **14**(3): p. 806-14.
28. Obeidat, M. and B.J. Ballermann, *Glomerular endothelium: A porous sieve and formidable barrier*. Exp Cell Res, 2012.
29. Lafayette, R.A., et al., *Nature of glomerular dysfunction in pre-eclampsia*. Kidney Int, 1998. **54**(4): p. 1240-9.
30. Lindahl, P., et al., *Paracrine PDGF-B/PDGF-Rbeta signaling controls mesangial cell development in kidney glomeruli*. Development, 1998. **125**(17): p. 3313-22.
31. Scindia, Y.M., U.S. Deshmukh, and H. Bagavant, *Mesangial pathology in glomerular disease: targets for therapeutic intervention*. Adv Drug Deliv Rev, 2010. **62**(14): p. 1337-43.
32. Jefferson, J.A., C.E. Alpers, and S.J. Shankland, *Podocyte biology for the bedside*. Am J Kidney Dis, 2011. **58**(5): p. 835-45.
33. Patrakka, J. and K. Tryggvason, *Molecular make-up of the glomerular filtration barrier*. Biochem Biophys Res Commun, 2010. **396**(1): p. 164-9.
34. Tryggvason, K., et al., *Type IV collagen in normal and diseased glomerular basement membrane*. Adv Nephrol Necker Hosp, 1993. **22**: p. 1-14.
35. Noakes, P.G., et al., *The renal glomerulus of mice lacking α -laminin/laminin beta 2: nephrosis despite molecular compensation by laminin beta 1*. Nat Genet, 1995. **10**(4): p. 400-6.
36. Zenker, M., et al., *Human laminin beta2 deficiency causes congenital nephrosis with mesangial sclerosis and distinct eye abnormalities*. Hum Mol Genet, 2004. **13**(21): p. 2625-32.
37. Lebel, S.P., et al., *Morphofunctional studies of the glomerular wall in mice lacking entactin-1*. J Histochem Cytochem, 2003. **51**(11): p. 1467-78.

38. Kanwar, Y.S., A. Linker, and M.G. Farquhar, *Increased permeability of the glomerular basement membrane to ferritin after removal of glycosaminoglycans (heparan sulfate) by enzyme digestion*. J Cell Biol, 1980. **86**(2): p. 688-93.
39. Harvey, S.J., et al., *Disruption of glomerular basement membrane charge through podocyte-specific mutation of agrin does not alter glomerular permselectivity*. Am J Pathol, 2007. **171**(1): p. 139-52.
40. Rossi, M., et al., *Heparan sulfate chains of perlecan are indispensable in the lens capsule but not in the kidney*. EMBO J, 2003. **22**(2): p. 236-45.
41. Goldberg, S., et al., *Glomerular filtration is normal in the absence of both agrin and perlecan-heparan sulfate from the glomerular basement membrane*. Nephrol Dial Transplant, 2009. **24**(7): p. 2044-51.
42. Utriainen, A., et al., *Structurally altered basement membranes and hydrocephalus in a type XVIII collagen deficient mouse line*. Hum Mol Genet, 2004. **13**(18): p. 2089-99.
43. Nagata, M., et al., *Cell cycle regulation and differentiation in the human podocyte lineage*. Am J Pathol, 1998. **153**(5): p. 1511-20.
44. Marshall, C.B. and S.J. Shankland, *Cell cycle and glomerular disease: a minireview*. Nephron Exp Nephrol, 2006. **102**(2): p. e39-48.
45. Simons, M., B. Hartleben, and T.B. Huber, *Podocyte polarity signalling*. Curr Opin Nephrol Hypertens, 2009. **18**(4): p. 324-30.
46. Pavenstadt, H., W. Kriz, and M. Kretzler, *Cell biology of the glomerular podocyte*. Physiol Rev, 2003. **83**(1): p. 253-307.
47. Rastaldi, M.P., et al., *Glomerular podocytes contain neuron-like functional synaptic vesicles*. FASEB J, 2006. **20**(7): p. 976-8.
48. Kobayashi, N., *Mechanism of the process formation; podocytes vs. neurons*. Microsc Res Tech, 2002. **57**(4): p. 217-23.
49. Foster, R.R., et al., *Vascular endothelial growth factor and nephrin interact and reduce apoptosis in human podocytes*. Am J Physiol Renal Physiol, 2005. **288**(1): p. F48-57.
50. Bridgewater, D.J., et al., *Insulin-like growth factors inhibit podocyte apoptosis through the PI3 kinase pathway*. Kidney Int, 2005. **67**(4): p. 1308-14.
51. Barisoni, L., et al., *The dysregulated podocyte phenotype: a novel concept in the pathogenesis of collapsing idiopathic focal segmental glomerulosclerosis and HIV-associated nephropathy*. J Am Soc Nephrol, 1999. **10**(1): p. 51-61.
52. Barisoni, L., et al., *Podocyte cell cycle regulation and proliferation in collapsing glomerulopathies*. Kidney Int, 2000. **58**(1): p. 137-43.
53. Meyer, T.W., P.H. Bennett, and R.G. Nelson, *Podocyte number predicts long-term urinary albumin excretion in Pima Indians with Type II diabetes and microalbuminuria*. Diabetologia, 1999. **42**(11): p. 1341-4.
54. Kim, Y.H., et al., *Podocyte depletion and glomerulosclerosis have a direct relationship in the PAN-treated rat*. Kidney Int, 2001. **60**(3): p. 957-68.
55. Frisch, S.M. and H. Francis, *Disruption of epithelial cell-matrix interactions induces apoptosis*. J Cell Biol, 1994. **124**(4): p. 619-26.

56. Ronconi, E., et al., *Regeneration of glomerular podocytes by human renal progenitors*. J Am Soc Nephrol, 2009. **20**(2): p. 322-32.
57. Takemoto, M., et al., *Large-scale identification of genes implicated in kidney glomerulus development and function*. EMBO J, 2006. **25**(5): p. 1160-74.
58. Dreyer, S.D., et al., *Mutations in LMX1B cause abnormal skeletal patterning and renal dysplasia in nail patella syndrome*. Nat Genet, 1998. **19**(1): p. 47-50.
59. Chen, H., et al., *Limb and kidney defects in Lmx1b mutant mice suggest an involvement of LMX1B in human nail patella syndrome*. Nat Genet, 1998. **19**(1): p. 51-5.
60. Rohr, C., et al., *The LIM-homeodomain transcription factor Lmx1b plays a crucial role in podocytes*. J Clin Invest, 2002. **109**(8): p. 1073-82.
61. Quaggin, S.E., et al., *The basic-helix-loop-helix protein pod1 is critically important for kidney and lung organogenesis*. Development, 1999. **126**(24): p. 5771-83.
62. Sadl, V., et al., *The mouse Kreisler (Krml1/MafB) segmentation gene is required for differentiation of glomerular visceral epithelial cells*. Dev Biol, 2002. **249**(1): p. 16-29.
63. Kerjaschki, D., D.J. Sharkey, and M.G. Farquhar, *Identification and characterization of podocalyxin--the major sialoprotein of the renal glomerular epithelial cell*. J Cell Biol, 1984. **98**(4): p. 1591-6.
64. Doyonnas, R., et al., *Anuria, omphalocele, and perinatal lethality in mice lacking the CD34-related protein podocalyxin*. J Exp Med, 2001. **194**(1): p. 13-27.
65. Takeda, T., et al., *Loss of glomerular foot processes is associated with uncoupling of podocalyxin from the actin cytoskeleton*. J Clin Invest, 2001. **108**(2): p. 289-301.
66. Vitureira, N., et al., *Podocalyxin is a novel polysialylated neural adhesion protein with multiple roles in neural development and synapse formation*. PLoS One, 2010. **5**(8): p. e12003.
67. Rops, A.L., et al., *Isolation and characterization of conditionally immortalized mouse glomerular endothelial cell lines*. Kidney Int, 2004. **66**(6): p. 2193-201.
68. Huang, T.W. and J.C. Langlois, *Podoendin. A new cell surface protein of the podocyte and endothelium*. J Exp Med, 1985. **162**(1): p. 245-67.
69. Schacht, V., et al., *T1alpha/podoplanin deficiency disrupts normal lymphatic vasculature formation and causes lymphedema*. EMBO J, 2003. **22**(14): p. 3546-56.
70. Koop, K., et al., *Selective loss of podoplanin protein expression accompanies proteinuria and precedes alterations in podocyte morphology in a spontaneous proteinuric rat model*. Am J Pathol, 2008. **173**(2): p. 315-26.
71. Matsui, K., S. Breiteneder-Geleff, and D. Kerjaschki, *Epitope-specific antibodies to the 43-kD glomerular membrane protein podoplanin cause proteinuria and rapid flattening of podocytes*. J Am Soc Nephrol, 1998. **9**(11): p. 2013-26.

72. Wharram, B.L., et al., *Altered podocyte structure in GLEPP1 (Ptpo)-deficient mice associated with hypertension and low glomerular filtration rate*. J Clin Invest, 2000. **106**(10): p. 1281-90.
73. Ozaltin, F., et al., *Disruption of PTPRO causes childhood-onset nephrotic syndrome*. Am J Hum Genet, 2011. **89**(1): p. 139-47.
74. Christensen, E.I. and H. Birn, *Megalin and cubilin: synergistic endocytic receptors in renal proximal tubule*. Am J Physiol Renal Physiol, 2001. **280**(4): p. F562-73.
75. Prabakaran, T., et al., *Cubilin is expressed in rat and human glomerular podocytes*. Nephrol Dial Transplant, 2012.
76. Adler, S., *Integrin receptors in the glomerulus: potential role in glomerular injury*. Am J Physiol, 1992. **262**(5 Pt 2): p. F697-704.
77. Kreidberg, J.A., et al., *Alpha 3 beta 1 integrin has a crucial role in kidney and lung organogenesis*. Development, 1996. **122**(11): p. 3537-47.
78. Adler, S. and X. Chen, *Anti-Fx1A antibody recognizes a beta 1-integrin on glomerular epithelial cells and inhibits adhesion and growth*. Am J Physiol, 1992. **262**(5 Pt 2): p. F770-6.
79. Dai, C., et al., *Essential role of integrin-linked kinase in podocyte biology: Bridging the integrin and slit diaphragm signaling*. J Am Soc Nephrol, 2006. **17**(8): p. 2164-75.
80. Sachs, N., et al., *Kidney failure in mice lacking the tetraspanin CD151*. J Cell Biol, 2006. **175**(1): p. 33-9.
81. Blumenthal, A., et al., *Morphology and migration of podocytes are affected by CD151 levels*. Am J Physiol Renal Physiol, 2012.
82. Raats, C.J., et al., *Expression of agrin, dystroglycan, and utrophin in normal renal tissue and in experimental glomerulopathies*. Am J Pathol, 2000. **156**(5): p. 1749-65.
83. Williamson, R.A., et al., *Dystroglycan is essential for early embryonic development: disruption of Reichert's membrane in Dag1-null mice*. Hum Mol Genet, 1997. **6**(6): p. 831-41.
84. Durbeej, M. and P. Ekblom, *Dystroglycan and laminins: glycoconjugates involved in branching epithelial morphogenesis*. Exp Lung Res, 1997. **23**(2): p. 109-18.
85. Jarad, G., et al., *Dystroglycan does not contribute significantly to kidney development or function, in health or after injury*. Am J Physiol Renal Physiol, 2011. **300**(3): p. F811-20.
86. Hara, Y., et al., *A dystroglycan mutation associated with limb-girdle muscular dystrophy*. N Engl J Med, 2011. **364**(10): p. 939-46.
87. Lamperti, C., et al., *Congenital muscular dystrophy with muscle inflammation alpha dystroglycan glycosylation defect and no mutation in FKRP gene*. J Neurol Sci, 2006. **243**(1-2): p. 47-51.
88. Wei, C., et al., *Modification of kidney barrier function by the urokinase receptor*. Nat Med, 2008. **14**(1): p. 55-63.
89. Karnovsky, M.J. and S.K. Ainsworth, *The structural basis of glomerular filtration*. Adv Nephrol Necker Hosp, 1972. **2**: p. 35-60.
90. Tryggvason, K., V. Ruotsalainen, and J. Wartiovaara, *Discovery of the congenital nephrotic syndrome gene discloses the structure of the*

- mysterious molecular sieve of the kidney*. Int J Dev Biol, 1999. **43**(5): p. 445-51.
91. Putaala, H., et al., *The murine nephrin gene is specifically expressed in kidney, brain and pancreas: inactivation of the gene leads to massive proteinuria and neonatal death*. Hum Mol Genet, 2001. **10**(1): p. 1-8.
 92. Liu, L., et al., *Defective nephrin trafficking caused by missense mutations in the NPHS1 gene: insight into the mechanisms of congenital nephrotic syndrome*. Hum Mol Genet, 2001. **10**(23): p. 2637-44.
 93. Lenkkeri, U., et al., *Structure of the gene for congenital nephrotic syndrome of the finnish type (NPHS1) and characterization of mutations*. Am J Hum Genet, 1999. **64**(1): p. 51-61.
 94. Schwarz, K., et al., *Podocin, a raft-associated component of the glomerular slit diaphragm, interacts with CD2AP and nephrin*. J Clin Invest, 2001. **108**(11): p. 1621-9.
 95. Huber, T.B., et al., *Nephrin and CD2AP associate with phosphoinositide 3-OH kinase and stimulate AKT-dependent signaling*. Mol Cell Biol, 2003. **23**(14): p. 4917-28.
 96. Verma, R., et al., *Nephrin ectodomain engagement results in Src kinase activation, nephrin phosphorylation, Nck recruitment, and actin polymerization*. J Clin Invest, 2006. **116**(5): p. 1346-59.
 97. Coward, R.J., et al., *Nephrin is critical for the action of insulin on human glomerular podocytes*. Diabetes, 2007. **56**(4): p. 1127-35.
 98. Boute, N., et al., *NPHS2, encoding the glomerular protein podocin, is mutated in autosomal recessive steroid-resistant nephrotic syndrome*. Nat Genet, 2000. **24**(4): p. 349-54.
 99. Roselli, S., et al., *Early glomerular filtration defect and severe renal disease in podocin-deficient mice*. Mol Cell Biol, 2004. **24**(2): p. 550-60.
 100. Wolf, G. and R.A. Stahl, *CD2-associated protein and glomerular disease*. Lancet, 2003. **362**(9397): p. 1746-8.
 101. Kim, J.M., et al., *CD2-associated protein haploinsufficiency is linked to glomerular disease susceptibility*. Science, 2003. **300**(5623): p. 1298-300.
 102. Jones, N., et al., *Nck adaptor proteins link nephrin to the actin cytoskeleton of kidney podocytes*. Nature, 2006. **440**(7085): p. 818-23.
 103. Lehtonen, S., et al., *Cell junction-associated proteins IQGAP1, MAGI-2, CASK, spectrins, and alpha-actinin are components of the nephrin multiprotein complex*. Proc Natl Acad Sci U S A, 2005. **102**(28): p. 9814-9.
 104. Barletta, G.M., et al., *Nephrin and Neph1 co-localize at the podocyte foot process intercellular junction and form cis hetero-oligomers*. J Biol Chem, 2003. **278**(21): p. 19266-71.
 105. Huber, T.B., et al., *The carboxyl terminus of Neph family members binds to the PDZ domain protein zonula occludens-1*. J Biol Chem, 2003. **278**(15): p. 13417-21.
 106. Sellin, L., et al., *NEPH1 defines a novel family of podocin interacting proteins*. FASEB J, 2003. **17**(1): p. 115-7.

107. Donoviel, D.B., et al., *Proteinuria and perinatal lethality in mice lacking NEPH1, a novel protein with homology to NEPHRIN*. Mol Cell Biol, 2001. **21**(14): p. 4829-36.
108. Koda, R., et al., *Novel expression of claudin-5 in glomerular podocytes*. Cell Tissue Res, 2011. **343**(3): p. 637-48.
109. Schneeberger, E.E. and R.D. Lynch, *The tight junction: a multifunctional complex*. Am J Physiol Cell Physiol, 2004. **286**(6): p. C1213-28.
110. Caruana, G., *Genetic studies define MAGUK proteins as regulators of epithelial cell polarity*. Int J Dev Biol, 2002. **46**(4): p. 511-8.
111. Piepenhagen, P.A. and W.J. Nelson, *Differential expression of cell-cell and cell-substratum adhesion proteins along the kidney nephron*. Am J Physiol, 1995. **269**(6 Pt 1): p. C1433-49.
112. Cohen, C.D., et al., *Comparative promoter analysis allows de novo identification of specialized cell junction-associated proteins*. Proc Natl Acad Sci U S A, 2006. **103**(15): p. 5682-7.
113. Reiser, J., et al., *The glomerular slit diaphragm is a modified adherens junction*. J Am Soc Nephrol, 2000. **11**(1): p. 1-8.
114. Mukerji, N., T.V. Damodaran, and M.P. Winn, *TRPC6 and FSGS: the latest TRP channelopathy*. Biochim Biophys Acta, 2007. **1772**(8): p. 859-68.
115. Winn, M.P., et al., *Unexpected role of TRPC6 channel in familial nephrotic syndrome: does it have clinical implications?* J Am Soc Nephrol, 2006. **17**(2): p. 378-87.
116. Winn, M.P., et al., *A mutation in the TRPC6 cation channel causes familial focal segmental glomerulosclerosis*. Science, 2005. **308**(5729): p. 1801-4.
117. Patrakka, J. and K. Tryggvason, *New insights into the role of podocytes in proteinuria*. Nat Rev Nephrol, 2009. **5**(8): p. 463-8.
118. Tsvilovskyy, V.V., et al., *Deletion of TRPC4 and TRPC6 in mice impairs smooth muscle contraction and intestinal motility in vivo*. Gastroenterology, 2009. **137**(4): p. 1415-24.
119. Welsh, G.I. and M.A. Saleem, *The podocyte cytoskeleton--key to a functioning glomerulus in health and disease*. Nat Rev Nephrol, 2012. **8**(1): p. 14-21.
120. Kobayashi, N. and P. Mundel, *A role of microtubules during the formation of cell processes in neuronal and non-neuronal cells*. Cell Tissue Res, 1998. **291**(2): p. 163-74.
121. Drenckhahn, D. and R.P. Franke, *Ultrastructural organization of contractile and cytoskeletal proteins in glomerular podocytes of chicken, rat, and man*. Lab Invest, 1988. **59**(5): p. 673-82.
122. Farquhar, M.G., R.L. Vernier, and R.A. Good, *An electron microscope study of the glomerulus in nephrosis, glomerulonephritis, and lupus erythematosus*. J Exp Med, 1957. **106**(5): p. 649-60.
123. Peti-Peterdi, J. and A. Sipos, *A high-powered view of the filtration barrier*. J Am Soc Nephrol, 2010. **21**(11): p. 1835-41.
124. Togawa, A., et al., *Progressive impairment of kidneys and reproductive organs in mice lacking Rho GDIalpha*. Oncogene, 1999. **18**(39): p. 5373-80.

125. Sharma, R., et al., *Vasoactive substances induce cytoskeletal changes in cultured rat glomerular epithelial cells*. J Am Soc Nephrol, 1992. **3**(5): p. 1131-8.
126. Yao, J., et al., *Alpha-actinin-4-mediated FSGS: an inherited kidney disease caused by an aggregated and rapidly degraded cytoskeletal protein*. PLoS Biol, 2004. **2**(6): p. e167.
127. Kos, C.H., et al., *Mice deficient in alpha-actinin-4 have severe glomerular disease*. J Clin Invest, 2003. **111**(11): p. 1683-90.
128. Mundel, P., et al., *Synaptopodin: an actin-associated protein in telencephalic dendrites and renal podocytes*. J Cell Biol, 1997. **139**(1): p. 193-204.
129. Asanuma, K., et al., *Synaptopodin regulates the actin-bundling activity of alpha-actinin in an isoform-specific manner*. J Clin Invest, 2005. **115**(5): p. 1188-98.
130. Garovic, V.D., et al., *Glomerular expression of nephrin and synaptopodin, but not podocin, is decreased in kidney sections from women with preeclampsia*. Nephrol Dial Transplant, 2007. **22**(4): p. 1136-43.
131. Ghiggeri, G.M., et al., *Genetics, clinical and pathological features of glomerulonephritis associated with mutations of nonmuscle myosin IIA (Fechtner syndrome)*. Am J Kidney Dis, 2003. **41**(1): p. 95-104.
132. Kopp, J.B., et al., *MYH9 is a major-effect risk gene for focal segmental glomerulosclerosis*. Nat Genet, 2008. **40**(10): p. 1175-84.
133. Krendel, M., et al., *Disruption of Myosin 1e promotes podocyte injury*. J Am Soc Nephrol, 2009. **20**(1): p. 86-94.
134. Mele, C., et al., *MYO1E mutations and childhood familial focal segmental glomerulosclerosis*. N Engl J Med, 2011. **365**(4): p. 295-306.
135. Berger, K. and M.J. Moeller, *Cofilin-1 in the podocyte: a molecular switch for actin dynamics*. Int Urol Nephrol, 2011. **43**(1): p. 273-5.
136. Kobayashi, T., et al., *Cortactin interacts with podocalyxin and mediates morphological change of podocytes through its phosphorylation*. Nephron Exp Nephrol, 2009. **113**(3): p. e89-96.
137. Kreisberg, J.I., R.L. Hoover, and M.J. Karnovsky, *Isolation and characterization of rat glomerular epithelial cells in vitro*. Kidney Int, 1978. **14**(1): p. 21-30.
138. Shankland, S.J., et al., *Podocytes in culture: past, present, and future*. Kidney Int, 2007. **72**(1): p. 26-36.
139. Mundel, P., et al., *Rearrangements of the cytoskeleton and cell contacts induce process formation during differentiation of conditionally immortalized mouse podocyte cell lines*. Exp Cell Res, 1997. **236**(1): p. 248-58.
140. Schiwek, D., et al., *Stable expression of nephrin and localization to cell-cell contacts in novel murine podocyte cell lines*. Kidney Int, 2004. **66**(1): p. 91-101.
141. Saleem, M.A., et al., *A conditionally immortalized human podocyte cell line demonstrating nephrin and podocin expression*. J Am Soc Nephrol, 2002. **13**(3): p. 630-8.

142. Gao, S.Y., et al., *Rho-family small GTPases are involved in forskolin-induced cell-cell contact formation of renal glomerular podocytes in vitro*. Cell Tissue Res, 2007. **328**(2): p. 391-400.
143. He, L., et al., *Glomerulus-specific mRNA transcripts and proteins identified through kidney expressed sequence tag database analysis*. Kidney Int, 2007. **71**(9): p. 889-900.
144. Sun, Y., et al., *Glomerular transcriptome changes associated with lipopolysaccharide-induced proteinuria*. Am J Nephrol, 2009. **29**(6): p. 558-70.
145. Teramoto, K., et al., *Microarray analysis of glomerular gene expression in murine lupus nephritis*. J Pharmacol Sci, 2008. **106**(1): p. 56-67.
146. Done, S.C., et al., *Nephrin is involved in podocyte maturation but not survival during glomerular development*. Kidney Int, 2008. **73**(6): p. 697-704.
147. Woroniecka, K.I., et al., *Transcriptome analysis of human diabetic kidney disease*. Diabetes, 2011. **60**(9): p. 2354-69.
148. Hodgins, J.B., et al., *A molecular profile of focal segmental glomerulosclerosis from formalin-fixed, paraffin-embedded tissue*. Am J Pathol, 2010. **177**(4): p. 1674-86.
149. Putaala, H., et al., *Primary structure of mouse and rat nephrin cDNA and structure and expression of the mouse gene*. J Am Soc Nephrol, 2000. **11**(6): p. 991-1001.
150. Uhlen, P., *Visualization of Na,K-ATPase interacting proteins using FRET technique*. Ann N Y Acad Sci, 2003. **986**: p. 514-8.
151. Takemoto, M., et al., *A new method for large scale isolation of kidney glomeruli from mice*. Am J Pathol, 2002. **161**(3): p. 799-805.
152. Pohl, U., et al., *EHD2, EHD3, and EHD4 encode novel members of a highly conserved family of EH domain-containing proteins*. Genomics, 2000. **63**(2): p. 255-62.
153. George, M., et al., *Renal thrombotic microangiopathy in mice with combined deletion of endocytic recycling regulators EHD3 and EHD4*. PLoS One, 2011. **6**(3): p. e17838.
154. Herb, A., et al., *Prominent dendritic localization in forebrain neurons of a novel mRNA and its product, dendrin*. Mol Cell Neurosci, 1997. **8**(5): p. 367-74.
155. Kawata, A., et al., *CIN85 is localized at synapses and forms a complex with S-SCAM via dendrin*. J Biochem, 2006. **139**(5): p. 931-9.
156. Umeki, N., et al., *Phospholipid-dependent regulation of the motor activity of myosin X*. Nat Struct Mol Biol, 2011. **18**(7): p. 783-8.
157. Lavigne, P., et al., *Interhelical salt bridges, coiled-coil stability, and specificity of dimerization*. Science, 1996. **271**(5252): p. 1136-8.
158. Shewan, A., D.J. Eastburn, and K. Mostov, *Phosphoinositides in cell architecture*. Cold Spring Harb Perspect Biol, 2011. **3**(8): p. a004796.
159. Watton, S.J. and J. Downward, *Akt/PKB localisation and 3' phosphoinositide generation at sites of epithelial cell-matrix and cell-cell interaction*. Curr Biol, 1999. **9**(8): p. 433-6.
160. Yang, Y., et al., *Formation and phosphorylation of the PINCH-1-integrin linked kinase-alpha-parvin complex are important for regulation of renal*

- glomerular podocyte adhesion, architecture, and survival.* J Am Soc Nephrol, 2005. **16**(7): p. 1966-76.
161. Brault, E., et al., *Normal membrane localization and actin association of the NF2 tumor suppressor protein are dependent on folding of its N-terminal domain.* J Cell Sci, 2001. **114**(Pt 10): p. 1901-12.
162. Moen, R.J., et al., *Characterization of a myosin VII MyTH/FERM domain.* J Mol Biol, 2011. **413**(1): p. 17-23.
163. Lee, H.S., et al., *Characterization of an actin-binding site within the talin FERM domain.* J Mol Biol, 2004. **343**(3): p. 771-84.
164. Goutebroze, L., et al., *Cloning and characterization of SCHIP-1, a novel protein interacting specifically with spliced isoforms and naturally occurring mutant NF2 proteins.* Mol Cell Biol, 2000. **20**(5): p. 1699-712.
165. James, M.F., et al., *A NHERF binding site links the betaPDGFR to the cytoskeleton and regulates cell spreading and migration.* J Cell Sci, 2004. **117**(Pt 14): p. 2951-61.
166. Kwasnicka-Crawford, D.A., A.R. Carson, and S.W. Scherer, *IQCJ-SCHIP1, a novel fusion transcript encoding a calmodulin-binding IQ motif protein.* Biochem Biophys Res Commun, 2006. **350**(4): p. 890-9.
167. Martin, P.M., et al., *Schwannomin-interacting protein-1 isoform IQCJ-SCHIP-1 is a late component of nodes of Ranvier and axon initial segments.* J Neurosci, 2008. **28**(24): p. 6111-7.
168. Vitureira, N., et al., *Podocalyxin is a novel polysialylated neural adhesion protein with multiple roles in neural development and synapse formation.* PLoS One. **5**(8): p. e12003.
169. Schmahl, J., C.S. Raymond, and P. Soriano, *PDGF signaling specificity is mediated through multiple immediate early genes.* Nat Genet, 2007. **39**(1): p. 52-60.
170. Chen, W.V., et al., *Identification and validation of PDGF transcriptional targets by microarray-coupled gene-trap mutagenesis.* Nat Genet, 2004. **36**(3): p. 304-12.
171. Uehara, G., et al., *Glomerular expression of platelet-derived growth factor (PDGF)-A, -B chain and PDGF receptor-alpha, -beta in human diabetic nephropathy.* Clin Exp Nephrol, 2004. **8**(1): p. 36-42.
172. Theisen, C.S., et al., *NHERF links the N-cadherin/catenin complex to the platelet-derived growth factor receptor to modulate the actin cytoskeleton and regulate cell motility.* Mol Biol Cell, 2007. **18**(4): p. 1220-32.

I

Expression and Subcellular Distribution of Novel Glomerulus-Associated Proteins Dendrin, Ehd3, Sh2d4a, Plekhh2, and 2310066E14Rik

Jaakko Patrakka,^{*,†} Zhijie Xiao,^{*} Masatoshi Nukui,^{*} Minoru Takemoto,^{*} Liquan He,^{*} Asmundur Oddsson,^{*} Ljubica Perisic,^{*} Anne Kaukinen,[‡] Cristina Al-Khalili Szigartyo,[§] Mathias Uhlén,[§] Hannu Jalanko,[‡] Christer Betsholtz,^{*,||} and Karl Tryggvason^{*}

^{*}Division of Matrix Biology, Department of Medical Biochemistry and Biophysics, and ^{||}Department of Medicine, Karolinska Institute, and [§]Department of Biotechnology, Royal Institute of Technology, Stockholm, Sweden; and [†]Electron Microscopy Unit, Institute of Biotechnology, and [‡]Hospital for Children and Adolescents and Biomedicum Helsinki, University of Helsinki, Helsinki, Finland

The glomerular capillary tuft is a highly specialized microcapillary that is dedicated to function as a sophisticated molecular sieve. The glomerulus filter has a unique molecular composition, and several essential glomerular proteins are expressed in the kidney exclusively by glomerular podocytes. A catalog of >300 glomerulus-upregulated transcripts that were identified using expressed sequence tag profiling and microarray analysis was published recently. This study characterized the expression profile of five glomerulus-upregulated transcripts/proteins (ehd3, dendrin, sh2d4a, plekhh2, and 2310066E14Rik) in detail. The expression pattern of these novel glomerular transcripts in various mouse tissues was studied using reverse transcriptase-PCR, Northern blotting, and *in situ* hybridization. For studying the distribution of corresponding proteins, polyclonal antibodies were raised against the gene products, and Western blotting, immunofluorescence, and immunoelectron microscopic analyses were performed. Remarkably, it was discovered that all five transcripts/proteins were expressed in the kidney exclusively by glomerular cells. Ehd3 was expressed only by glomerular endothelial cells. Importantly, ehd3 is the first gene ever shown to be expressed exclusively by glomerular endothelial cells and not by other endothelial cells in the kidney. Dendrin, sh2d4a, plekhh2, and 2310066E14Rik, however, were transcribed solely by podocytes. With the use of polyclonal antibodies, dendrin, sh2d4a, and plekhh2 proteins were localized to the slit diaphragm and the foot process, whereas 2310066E14Rik protein was localized to the podocyte major processes and cell body. This study provides fresh insights into glomerular biology and uncovers new possibilities to explore the role of these novel proteins in the glomerular physiology and pathology.

J Am Soc Nephrol 18: 689–697, 2007. doi: 10.1681/ASN.2006060675

The glomerular capillary tuft of the kidney is a unique micro-organ that is specialized to operate as a sophisticated molecular sieve (1). The filtration barrier is composed of the glomerular endothelial cells (GEC), the glomerular basement membrane (GBM), and the podocyte cells. GEC differ from most other endothelial cells in that they are extraordinarily flattened and fenestrated (2). The fenestrated structure of GEC depends on podocyte-derived vascular endothelial growth factor A (3), but the mechanisms behind their unique structure largely are unknown. The GBM, like all basement membranes (BM), is composed of interconnected collagen type IV and laminin networks, where proteoglycans and other ma-

trix components are attached. The GBM, however, is distinct from most other BM of the body, because it contains a unique composition of collagen type IV and laminin isoforms. The importance of these components is highlighted by the fact that defects in GBM-specific type IV collagen or laminin lead to Alport syndrome and Pierson syndrome, respectively (4–6).

The podocyte foot processes and the slit diaphragm serve as a final filtration barrier in the glomerulus. This filtration machinery contains a number of unique molecular components. Two fundamental molecules of the slit diaphragm, nephrin and podocin, were discovered through studies in human proteinuric kidney diseases (7,8). Absence of NEPH1 and FAT1, two other membrane-spanning proteins of the slit diaphragm, result in massive proteinuria in mice (9,10). Intracellularly, the slit diaphragm is connected to the actin cytoskeleton *via* nck proteins and CD2-associated protein (CD2AP) (11,12). Mice that lack nck proteins from the podocytes and CD2AP knockout mice develop massive proteinuria (12,13). In addition, studies that were carried out in human proteinuric kidney diseases and knockout mice showed the critical importance of podocyte-associated proteins α -actinin-4 (*ACTN4*), synaptopodin, podo-

Received June 29, 2006. Accepted December 7, 2006.

Published online ahead of print. Publication date available at www.jasn.org.

J.P. and Z.X. contributed equally to this work.

Address correspondence to: Dr. Karl Tryggvason, Division of Matrix Biology, Department of Medical Biochemistry and Biophysics, Karolinska Institute, 17177 Stockholm, Sweden. Phone: +46-8-5248-7720; Fax: +46-8-316-165; E-mail: karl.tryggvason@ki.se

calyxin, and glomerular epithelial protein 1 for the glomerular filtration barrier (14–17). Importantly, many of these essential proteins are highly specific for the glomerulus and the podocyte. Nephrin, podocin, NEPH1, FAT1, synaptopodin, α -actinin-4, and glomerular epithelial protein 1, for example, are expressed in the kidney only by podocytes (7,17–21). This emphasizes the unique function and molecular composition of the podocyte foot process and the slit diaphragm.

Recently, we identified >300 glomerulus-upregulated transcripts through large-scale sequencing and microarray profiling of the glomerular transcriptome (22). In our approach, we chose five novel transcripts that were identified in the microarray analyses and characterized their expression profile in detail. We show that four of the transcripts/proteins are expressed exclusively in the kidney by podocytes. Using immunoelectron microscopy, we localize two of these proteins to the slit diaphragm and the foot process. In addition, we show that one of the proteins is expressed in the kidney only by the GEC and, remarkably, not by other endothelial cells. The identification of these novel molecular components provides fresh insights into glomerular biology.

Materials and Methods

Reverse Transcriptase–PCR and Northern Blot

The expression of glomerular-enriched transcripts in a variety of mouse tissues was studied using reverse transcriptase–PCR (RT–PCR) and Northern Blot. Gene-specific oligonucleotides for PCR analysis were designed according to the predicted cDNA sequences (<http://www.ensembl.org>). Primer sequences and sizes of expected PCR products were as follows: Dendrin, left 5′-AATGGAGAGGCCTTGAACCT-3′, right 3′-GGGAAGGCCTAAAAGTGTCC-5′, 502 bp; EHD3, right 5′-CAAGAGCAGGGTTAGGCACT-3′, 5′-CTAATGAACGGGAGGCTGAG-3′, 498 bp; sh2d4a, left 5′-TCTGGGCTGGTCAAGTCTCT-3′, right 5′-GAAGCTGCTTTCCTGGTGAC-3′, 573 bp; plekh2, left 5′-CTGATTCGCACTCTTCACA-3′, right 5′-CGCTGGAGTTGAGAAAGTTC-3′, 353 bp; and 2310066E14Rik, left 5′-GGAGCAGTTCACCATCTTCC-3′, right 5′-TGTCGATGAGCAGACTGTCC-3′, 500 bp). As a template for PCR analysis, we used cDNA libraries that were generated from various adult mouse tissues (Mouse Multiple Tissue cDNA Panel I; Clontech Laboratories, Palo Alto, CA). PCR amplification was carried out with TaqDNA polymerase (Invitrogen, Carlsbad, CA), and the amplified fragments were analyzed on 1.5% agarose gel.

For Northern blots, we used cDNA probes that were obtained from the amplification of cDNA libraries (see previous paragraph). The probes were ³²P-labeled using the Rediprime II random primer labeling system (Amersham Pharmacia Biotech, London, UK), and the probes were hybridized to the blots that contained RNA that were isolated from various mouse organs (Mouse MTN Blot; Clontech Laboratories). Hybridizations also were performed on blots that contained mRNA that was isolated from mouse kidney fractions that contained either only glomerular tufts or the kidney excluding glomeruli. Glomerular fractions were isolated as described previously (23). The hybridizations were performed according to the standard procedures. As a positive loading control, we used glyceraldehyde-3-phosphate dehydrogenase probe (Clontech Laboratories).

In Situ Hybridization

The probes for *in situ* hybridizations were synthesized by subcloning of the PCR products that were obtained from RT–PCR analyses (see

previous section) into the pCR II–TOPO Dual Promoter Vector (Invitrogen). Antisense and sense RNA were prepared by using T7 or SP6 polymerases. *In situ* hybridization experiments with ³⁵S-labeled probes were performed on snap-frozen tissue sections that were collected from newborn mouse kidneys as described previously (24).

Production of Polyclonal Antibodies Directed against Novel Glomerular Proteins

We raised antisera directed against novel glomerular proteins by purifying recombinant proteins with affinity tags and by immunizing NZW rabbits with these antigens using standard protocols (SVA, Uppsala, Sweden; KTH, Stockholm, Sweden). The generation of antigens is described briefly here.

For the production of dendrin and ehd3 antigens, we generated mouse recombinant proteins. Dendrin residues 55 to 384 were cloned into the pET-28a(+) expression vector (Novagen, Madison, WI), whereas ehd3 residues 260 to 424 were cloned into the pGEX 4T-3 vector (Amersham Biosciences). The his-tagged dendrin and the GST-tagged ehd3 recombinant proteins were solubilized from inclusion bodies in 8 M urea. Then, dendrin antigen was purified using sequential S-Sepharose ion exchange and Sephadex S-200 gel filtration columns (Amersham Biosciences), whereas his-tagged ehd3 antigen was purified using G-Sepharose 4B ion exchange column (Amersham Biosciences). Finally, two NZW rabbits were immunized with each prepared antigen.

Human recombinant proteins were generated for production of sh2d4a, plekh2, and 2310066E14Rik antigens. Two sequences were selected for sh2d4a suitable for antigen production: Residues 27 to 150 and 327 to 443. For plekh2 and 2310066E14Rik, selected sequences comprised amino acids 223 to 357 and 845 to 961, respectively. The protein fragments were expressed as recombinant proteins with a dual tag: A hexahistidine tag that enabled purification of the expressed antigen by immobilized metal ion affinity chromatography and an albumin-binding protein fragment of *Streptococcus* protein G with immunopotentiating capabilities (25). Antibodies were raised by immunization of NZW rabbits, and obtained sera were used for purification of monospecific antibodies. Purification was performed using a two-step purification procedure including depletion of tag-specific antibodies and subsequent affinity purification as described previously (26).

Western Blotting

In Western blotting, we compared the extracts of glomerular tufts and kidneys that lacked glomeruli. The glomeruli were isolated from 8- to 12-wk-old adult mice and from human cadaver kidneys that were unsuitable for transplantation (from the IV Department of Surgery of Helsinki, Finland). The isolation methods have been described previously (23,27). The Western blotting was done following standard procedures using polyvinylidene difluoride membrane and horseradish peroxidase-conjugated secondary antibody (Amersham Biosciences). As a positive loading control, we used polyclonal anti- β -actin antibody (Abcam, Cambridge, UK).

Immunohistochemistry

For immunofluorescence stainings, kidney samples were collected from either 4- to 12 wk-old mouse kidneys or adult human cadaver kidneys that were unsuitable for transplantation (from the IV Department of Surgery of Helsinki, Finland). The samples were snap-frozen, and the cryosections (10 μ m) were postfixed with cold acetone (–20°C) followed by blocking in 5% normal goat serum. The primary antibodies were incubated overnight at 4°C, followed by a 1-h incubation with the

secondary antibody. For double-labeling experiments, the incubations were performed sequentially.

The primary antibodies used are described above in Production of Polyclonal Antibodies Directed against Novel Glomerular Proteins. For double-labeling experiments, we used anti-mouse synaptopodin (Progen, Heidelberg, Germany), anti-mouse CD31 (Pharmingen Int., San Diego, CA), anti-mouse collagen type IV $\alpha 5$ (H53; gift from Dr. Sado, Shigei Medical Research Institute, Yamada, Japan), anti-human vimentin (Zymed Laboratories, San Francisco, CA), and anti-human nephrin 50A9 (28) antibodies. DAPI reagent was purchased from Molecular Probe (Eugene, OR). Secondary antibodies were purchased from Jackson ImmunoResearch Laboratories (West Grove, PA). Microscopy was performed with standard Leica confocal laser scanning microscope.

Immunoelectron Microscopy

For immunoelectron microscopy, the samples from mouse and human renal cortexes were fixed in a solution that contained phosphate-buffered 3.5% paraformaldehyde and 0.02% glutaraldehyde. After fixation, the samples were embedded in 10% gelatin, infiltrated with 2.3 M sucrose in PBS, and frozen in liquid nitrogen. Immunolabeling experiments were done as described previously (29).

Ethical Considerations

This study was approved by the ethical committees of the Karolinska Institute and The Hospital for Children and Adolescence of the University of Helsinki.

Results

Dendrin

Dendrin is an intracellular protein without known motifs or function (30,31). RT-PCR and Northern blotting experiments demonstrated the presence of dendrin transcript in brain, kidney, and lung tissues (Figure 1). The size of the transcript

(approximately 3.5 kb) is in agreement with the predicted mouse dendrin cDNA (NCBI cDNA accession no. XM_912147).

Two antisera raised against the mouse dendrin protein gave similar results in our experiments, and the specificity of the antisera was confirmed by transfection of HEK293 cells with the full-length dendrin cDNA (data not shown). In the analysis of kidney fractions, both Northern and Western blotting revealed the presence of dendrin (mRNA and protein) in glomerular tufts, whereas no mRNA or protein was detected in the kidney extract that lacked glomeruli (Figure 2). Using Western blotting, anti-dendrin antisera recognized a protein that was approximately 80 kD (Figure 2). This is in line with the published rat dendrin protein size (81 kD) (30).

The glomerulus specificity of dendrin mRNA was verified using *in situ* hybridization. An antisense probe showed signal exclusively in the glomeruli (Figure 3). With a higher magnification, signal could be localized to the podocytes in newborn mouse kidney (Figure 3, inset). Sense probe gave only background signal (data not shown). In immunofluorescence staining, anti-dendrin antisera gave strong immunoreactivity in glomeruli, whereas the rest of the kidney remained negative (Figure 4). In glomerular tufts, dendrin protein was observed as a linear line around glomerular capillary loops. The staining for dendrin was found on the urinary side of CD31 immunoreactivity, whereas double labeling with COL4a5 revealed nearly overlapping of the two immunoreactivities. However, staining for dendrin was localized mostly on the urinary side of COL4a5 reactivity. Double staining with synaptopodin antibody revealed almost complete overlapping of the two proteins at the light microscopic level. In immunoelectron microscopy, gold

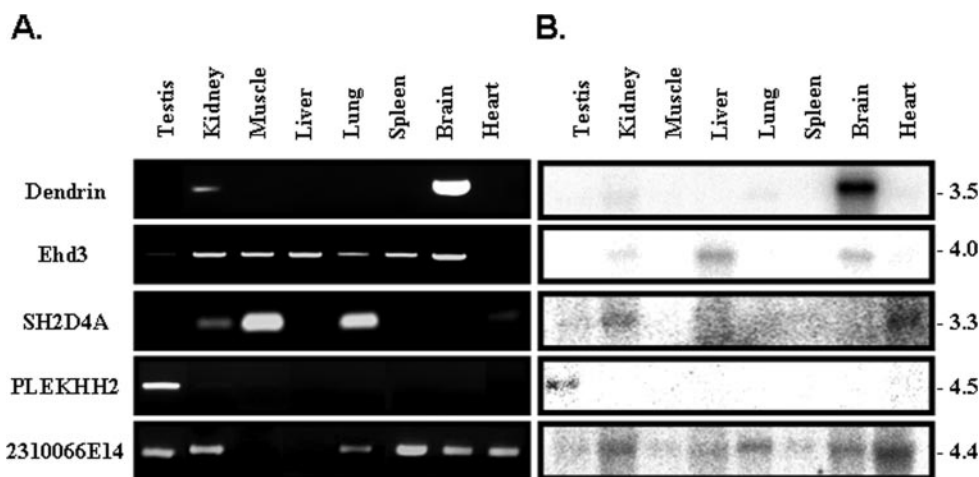


Figure 1. Expression of novel glomerular transcripts in various mouse organs using reverse transcriptase-PCR (RT-PCR; A) and Northern blot (B) analysis. Dendrin mRNA (approximately 3.5 kb) is present abundantly in brain tissue, whereas weaker expression is observed in kidney tissue. In Northern analysis, dendrin probe hybridizes also a weak band in lung mRNA. Ehd3 mRNA is detected in all organs analyzed using RT-PCR, whereas Northern blot reveals the presence of ehd3 mRNA (approximately 3.6 kb) only in kidney, liver, and brain tissues. Sh2d4a mRNA is detected in kidney, muscle, lung, and heart tissues using RT-PCR, whereas in Northern blotting, sh2d4a mRNA (approximately 3.3 kb) is detectable only in kidney and heart tissues. Plekhh2 mRNA (approximately 4.5 kb) is detected only in testis tissue using RT-PCR and Northern blotting. 2310066E14Rik mRNA is detected in testis, kidney, lung, spleen, and heart tissues using RT-PCR, whereas Northern blotting shows the presence of 2310066E14Rik transcript (approximately 4.4 kb) in all organs analyzed.

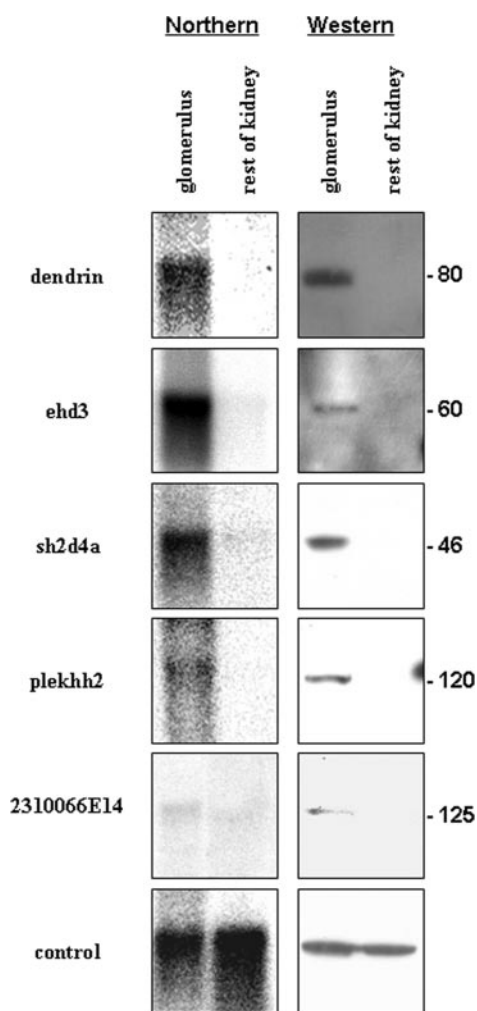


Figure 2. Expression of novel glomerular transcripts/proteins in glomerular and the rest of the kidney fractions as detected using Northern and Western blotting. All of the transcripts (dendrin, ehd3, sh2d4a, plekhh2, and 2310066E14Rik) analyzed with Northern blotting show strong expression in the glomerulus fraction, whereas no expression is detected in the kidney fraction that lacked glomeruli. The sizes of glomerular transcripts are as follows: Dendrin 3.5 kb, ehd3 3.6 kb, sh2d4a 3.3 kb, plekhh2 4.5 kb, and 2310066E14Rik 4.4 kb. Control hybridization with glyceraldehyde-3-phosphate dehydrogenase (GAPDH) probe shows strong signal in both lanes. In Western blotting, the antibodies/antisera directed against dendrin, ehd3, sh2d4a, plekhh2, and 2310066E14Rik give immunoreactivity in glomerular fractions, whereas the rest of the kidney fraction remains negative. The sizes of the proteins detected in Western blotting are as follow: Dendrin 81 kD, ehd3 68 kD, sh2d4a 46 kD, plekhh2 120 kD, and 2310066E14Rik 120 kD. Anti- β -actin antibody, which was used as a loading control, gave similar reactivity in both lanes.

label for dendrin was concentrated at the cytoplasmic insertion sites of the slit diaphragms (Figure 5A).

Ehd3

Ehd3 is predicted to be a cytosolic protein (32). RT-PCR and Northern blotting analyses showed that ehd3 transcripts were present in

many different mouse organs (Figure 1). Using Northern blotting, the strongest expression was observed in kidney, liver, and brain tissues. The size of ehd3 mRNA was approximately 3.6 kb, which is in line with the published transcript size (32).

In the analysis of kidney fractions, both Western and Northern blotting revealed the presence of ehd3 (mRNA and protein) exclusively in the glomerular fractions, whereas no expression was detected in the kidney extract excluding glomeruli (Figure 2). With the use of Western blotting, a protein that was approximately 68 kD in size was detected, which is in line with the predicted ehd3 protein size (Ensembl protein ENSMUSP0000024860).

In situ hybridization of the newborn mouse kidney confirmed the findings because strong signal for ehd3 mRNA was observed solely in glomerular tufts (Figure 3). With higher magnification, the signal for ehd3 mRNA was localized to the GEC in newborn mouse kidney (Figure 3, inset). This is in line with our previous microarray results; ehd3 mRNA showed 11-times upregulation in the nonpodocyte fraction of the glomerulus transcriptome (22). In immunofluorescence stainings, anti-ehd3 antisera gave strong reactivity in glomerular capillary tufts, whereas the rest of the kidney remained negative (Figure 4). In the glomerulus, the staining for ehd3 showed linear staining pattern around glomerular capillary loops. In double labeling with anti-CD31 antibody, the immunoreactivity for ehd3 was found in close proximity of this endothelial marker. The staining for ehd3, however, was localized mostly on the urinary side of CD31 immunoreactivity. The double labeling with COL4A5 and synaptopodin showed partial overlapping of the ehd3 protein with these two proteins. Surprising, the staining for ehd3 was observed occasionally on the urinary side of these two markers. This probably reflects the close proximity of the basal aspects of the GEC, the GBM, and the foot processes. Therefore, we performed immunoelectron microscopy for ehd3, which revealed that this protein was localized to the GEC (Figure 5B). The gold labeling in the GEC was abundant with only minimal background labeling of other kidney cell types and tissue components (data not shown). In the endothelium, the label often was confined to the level of the endothelial foramina.

Sh2d4a

Sh2d4a is a previously uncharacterized cytosolic protein. Expression profiling using RT-PCR and Northern blotting revealed the presence of sh2d4a transcripts in kidney, liver, and heart tissues (Figure 1). The size of the transcript (approximately 3.3 kb) is in line with the predicted transcript size (XM_134197).

Two affinity-purified polyclonal antibodies raised against sh2d4a protein gave similar results in our experiments (data not shown). In the analysis of kidney fractions, sh2d4a mRNA and protein both were detected in the glomerular fraction, whereas no signal was observed in the kidney fraction that lacked glomeruli (Figure 2). In the Western analysis, the antibodies detected a protein size of approximately 46 kD.

In immunofluorescence stainings, strong sh2d4a-specific immunoreactivity was observed in glomeruli, whereas the rest of the kidney was completely negative (Figure 4). Double labeling with nephrin revealed almost complete overlapping of the two proteins in the glomerulus at the light microscopic level (Figure 4). No

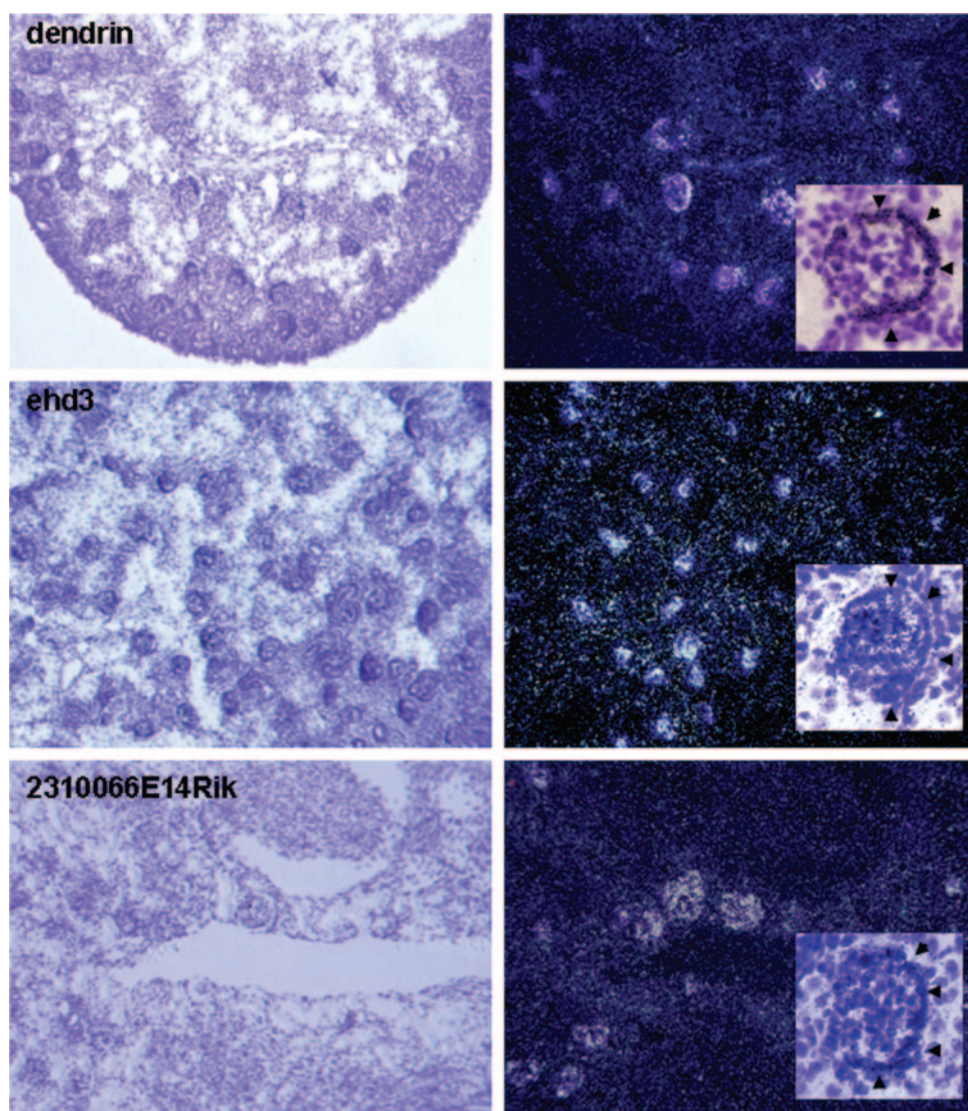


Figure 3. Expression of novel glomerular transcripts in newborn mouse kidneys as revealed by radioactive *in situ* hybridization. Insets show capillary loop stage glomerulus in which podocytes are localized as one row (arrowheads). (A) Strong signal for dendrin mRNA is detected in the glomerular tufts of newborn mouse kidneys, whereas the rest of the kidney remains negative. With a higher magnification, the signal for dendrin mRNA can be localized to the podocytes (inset). (B) Probe for ehd3 gives strong signal in the glomerular tufts, and no signal is detected outside the glomeruli. With higher magnification, ehd3 mRNA can be localized to the vascular cleft in the developing glomerulus, which indicates localization to the glomerular endothelial cells (GEC). (C) Signal for 2310066E14Rik mRNA is detected in the glomeruli, whereas no signal is observed in the rest of the kidney. With higher magnification, the signal can be localized to the podocytes (inset). Magnifications: $\times 50$ in A through C; $\times 300$ in insets.

overlapping was observed in double stainings with anti-vimentin antibody or DAPI stainings. In immunoelectron microscopy, gold label for sh2d4a was found diffusely distributed in the cytoplasm of podocyte foot processes (Figure 5, C and D).

Plekhh2

Plekhh2 is a previously uncharacterized intracellular protein. Using RT-PCR and Northern blotting, we detected the presence of plekhh2 transcript only in testis and kidney tissues (Figure 1). The size of plekhh2 transcript was approximately 4.5 kb.

In the analysis of kidney fractions, both Northern and Western blotting experiments showed the presence of plekhh2

(mRNA and protein) in the glomerulus fraction (Figure 2). Two plekhh2 transcripts were detected in the glomerulus (data not shown). No plekhh2 mRNA or protein was detected in the kidney fraction that lacked glomeruli. Affinity-purified polyclonal antibody recognized a protein of approximately 120 kD.

In immunofluorescence stainings, anti-plekhh2 antibody gave glomerulus immunoreactivity, and no significant signal was observed outside glomeruli (Figure 4). With higher magnification, plekhh2 was detected mainly as a linear line around glomerular capillary loops, indicating localization to the podocyte foot processes. At the light microscopic level, plekhh2 seemed to co-localize partially with nephrin. No overlapping

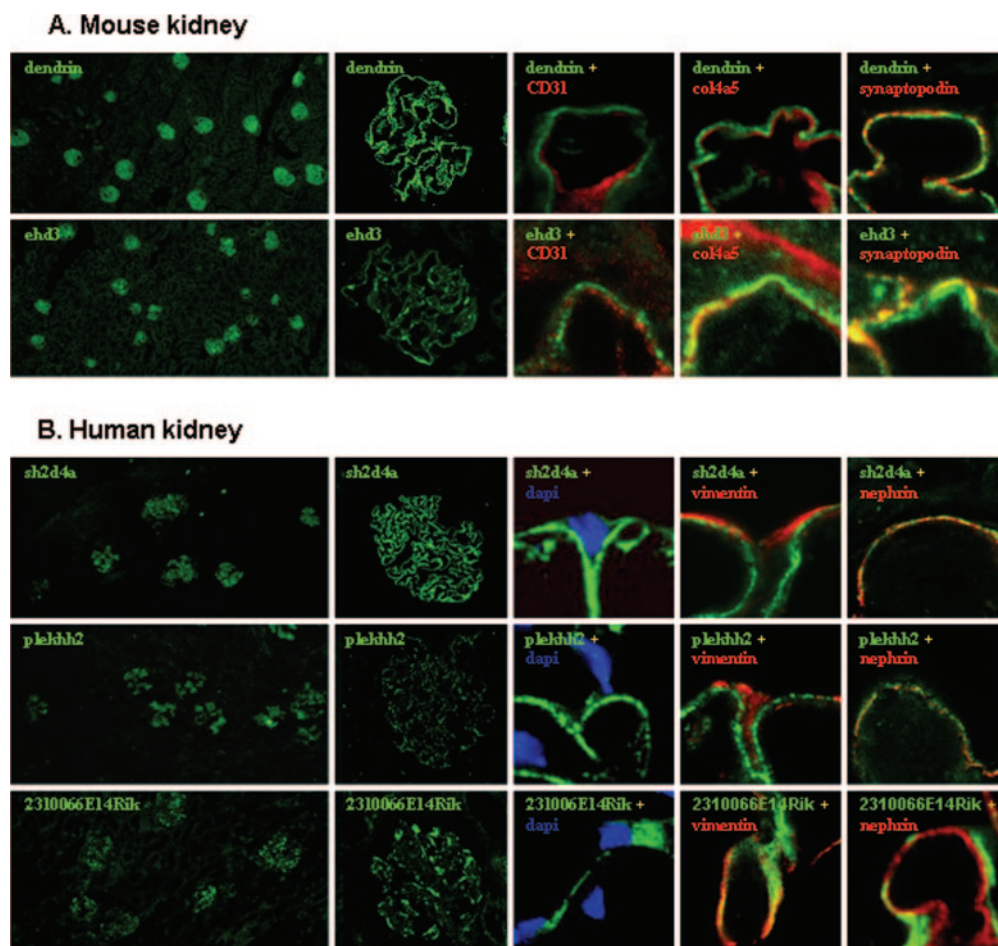


Figure 4. Expression of novel glomerular proteins in adult mouse or human kidneys as detected using double immunofluorescence staining. All antibodies give immunoreactivity exclusively in the glomerular tufts of adult mouse/human kidneys, and no significant signal is detected outside glomeruli. Double immunolabeling experiments were done with CD31, synaptopodin, vimentin, and nephrin (red). DAPI (nuclear) staining is shown in blue. Analysis with high magnification using confocal microscope reveals subcellular localization of the antigens (green) as follows. Dendrin-specific immunofluorescence (green) is found in close proximity of CD31 and COL4A5 proteins (red). The staining for dendrin is found mostly on the urinary side of these two markers. Double labeling with synaptopodin reveals almost complete overlapping (yellow) of dendrin and synaptopodin immunoreactivities. Both proteins are distributed along the glomerular capillary loops as a linear line. Ehd3 immunoreactivity is detected as a linear line in close proximity of CD31 reactivity. The staining for ehd3 is localized mostly on the urinary side of CD31 staining. The double labeling with COL4A5 and synaptopodin shows partial overlapping of ehd3 immunoreactivity with these two markers. Ehd3 immunoreactivity can be observed on both the capillary and the urinary side of the COL4A5 and synaptopodin stainings. The staining for sh2d4a is found as a line surrounding the glomerular capillaries. The immunoreactivity for sh2d4a does not overlap with vimentin or nuclear stainings. Instead, the staining for sh2d4a practically completely overlaps (yellow) with that of nephrin. Plekhh2 protein is observed as a line around the glomerular capillary loops. Double stainings with DAPI and anti-vimentin antibody do not show overlapping. Instead, the staining for nephrin mostly overlaps with plekhh2 immunoreactivity. Staining for 2310066E14 protein was localized to podocytes. Double staining with DAPI does not show co-localization, although diffuse cytoplasmic staining is observed in close proximity of nuclear staining. The staining for vimentin partially overlaps (yellow) with that of 2310066E14Rik. The staining for nephrin does not overlap with 2310066E14Rik immunoreactivity. Magnifications: $\times 80$ in overviews, $\times 400$ in single glomeruli, and $\times 2000$ in blow-ups.

was observed in double stainings with anti-vimentin antibody or DAPI stainings (Figure 4).

2310066E14Rik

2310066E14Rik transcript codes for an unknown intracellular protein. Using RT-PCR and Northern blotting, we observed wide expression of 2310066E14Rik transcript in mouse tissues (Figure 1). In Northern blotting, the probe for 2310066E14R hybridized an mRNA of approximately 4.4 kb.

In the analysis of kidney fractions, both Northern and Western analyses revealed the presence of 2310066E14Rik (mRNA and protein) in the glomerulus fraction, whereas no mRNA or protein was observed in the kidney fraction that lacked glomeruli (Figure 2). Polyclonal antibodies raised against this novel protein detected a protein of approximately 125 kD.

The exclusive glomerulus expression was confirmed using *in situ* hybridization; antisense probe gave strong signal in the glomeruli, and no signal was observed outside glomeruli (Figure 3).

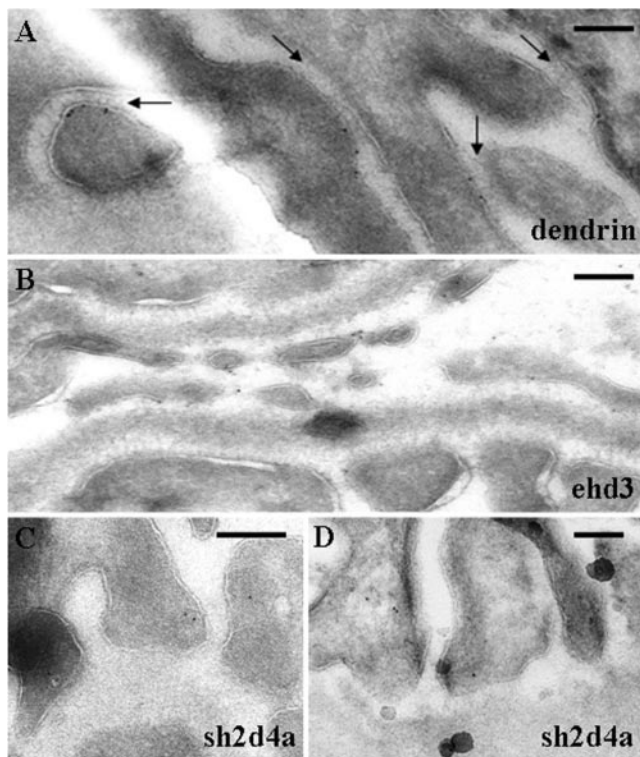


Figure 5. Immunoelectron microscopic localization of dendrin, ehd3, and SH2D4A in mouse and human kidneys. (A) Gold label (10 nm) for dendrin binds to epitopes at the inner leaflet of the foot process plasma membrane in regions where they appose to form slit diaphragms (arrows). (B) Gold label for ehd3 protein is observed in the cytoplasm of endothelial cells. The gold label for ehd3 often is found at the level of endothelial foramina. (C and D) Polyclonal antibodies directed against SH2D4A protein recognize an antigen at the cytosol of podocyte foot processes. Gold label is distributed diffusely in the cytosol of the foot processes. Fp, foot process. Bar = 100 nm.

With a higher magnification, signal for 2310066E14Rik could be localized to the podocytes in newborn mouse kidney (Figure 3, inset). Sense probe showed only background signal (data not shown). In immunofluorescence stainings, strong immunoreactivity was observed in the glomerular tufts, and no staining was observed outside glomeruli (Figure 4). Immunoreactivity was observed on the outer aspects of the glomerular tufts in which diffuse cytoplasmic staining mainly was observed. Double labeling with nephrin antibody showed that the product of 2310066E14Rik gene was localized on the urinary side of nephrin reactivity. Double labeling with anti-vimentin antibody showed partial overlapping reactivity. No overlapping was observed with DAPI stainings, although staining for 2310066E14Rik protein often was localized in close proximity of the nuclear staining. To conclude, the staining results for 2310066E14Rik protein suggest strongly that this protein localizes to the cytoplasm of the podocyte cell bodies and major processes.

Discussion

Recently, we generated a comprehensive catalogue of glomerulus-expressed transcripts (22). Through large-scale ex-

pressed sequence tag sequencing and microarray analyses, we characterized the transcriptome of the mouse glomerulus and identified >300 glomerulus-enriched transcripts. One of the transcripts discovered, a podocyte transcription factor Foxc2, was investigated further through analysis of Fox2 knockout mice. The glomerulogenesis in the mice was arrested before the capillary loop stage of glomerular development, indicating that Fox2 is essential for podocyte development. This example demonstrated that our large-scale approach was a feasible method to discover genes that are critical for normal glomerular function. In this report, we chose five other glomerulus-upregulated transcripts and performed a detailed expression analysis. It is interesting that we discovered that all five transcripts and their protein products were expressed in the kidney only by glomerular cells. Therefore, our results further emphasize the importance of the large-scale transcript profiling effort from the standpoint of nephrology.

The glomerulus filtration apparatus is an extremely specialized micro-organ that is dedicated to function as a sophisticated molecular sieve. The filter is composed of a variety of unique molecules that assist in the orchestration of its specialized function. Therefore, several critical glomerular proteins, such as nephrin, podocin, NEPH1, and FAT1, have very restricted expression pattern. In the kidney, these crucial proteins are expressed exclusively by podocytes. The proteins discovered in this study share this limited expression pattern. This suggests that the novel proteins identified in our study also may have a highly specific role in the glomerulus.

Dendrin is a poorly characterized cytosolic protein with no known function or homology to other proteins or protein domains. Previously, dendrin was reported to be specific for the dendritic processes of certain neuronal cells of the forebrain (30). Particularly, dendrin showed high expression in the regions of the brain that are capable of high synaptic plasticity. Because dendrin is not found in all dendritic processes, it cannot be essential for these structures. We identified dendrin in the kidney glomerulus and localized it to the cytoplasmic face of the podocyte slit diaphragm. Both dendritic processes and foot processes are long, slender cellular extensions, and they share many structural components, such as the actin-rich cytoskeleton (33), and functional features such as plasticity. Because dendrin also is shared by both structures, it could contribute to this plasticity. In the podocyte foot process, the plasticity is required to withstand the continuous filtration pressure (34). However, the localization of dendrin at the cytoplasmic face of the slit diaphragm suggests that dendrin may act as a linker molecule between the slit diaphragm and the actin cytoskeleton. In support of this idea, dendrin was shown recently to interact *in vivo* with two cytoskeletal components, α -actinin and membrane-associated guanylate kinase inverted (35). Recently, dendrin also was shown to interact with the CD2AP homologue CIN85 *in vitro* (36). We have not detected this interaction in the glomerulus by immunoprecipitating glomerulus lysates with CD2AP and dendrin antibodies (data not shown).

Ehd3 belongs to the protein family of eps15 homology domain-containing proteins, which are thought to be associated

with endocytic vesicles (37). With the use of Northern blotting, *ehd3* mRNA was found previously in mouse brain and kidney tissues (32). This is in line with our results because we detected *ehd3* mRNA in brain, kidney, and liver tissues using Northern analysis. More exciting, we discovered that *ehd3* was expressed in the kidney only by GEC. To our knowledge, this is the first protein shown to be expressed only by GEC and not by other endothelial cells in the kidney. This is of critical importance because the use of the *ehd3* promoter enables the generation of a GEC-specific Cre mouse line. Such a mouse line could provide an important tool for future glomerulus research.

Sh2d4a encodes a novel docking protein of SH2 signaling protein family. Members of this protein family probably play a role in intracellular signaling, but no studies have been reported to elucidate their expression or function in mammals. *Plekhh2* encodes for an uncharacterized cytosolic protein with pleckstrin homology, myth4, and band 4.1 domains. Pleckstrin homology domains are implicated in phosphatidylinositol phospholipid signaling (38), the band 4.1 domain is a membrane localization domain that is capable of binding integral membrane proteins (39), and the myth4 domain has no known function. However, the combination of myth4 and band 4.1 domains is found in several unconventional myosin proteins (40), which often are localized to actin-rich processes of the cells. It is interesting that we discovered that both *sh2d4a* and *plekhh2* proteins had a markedly restricted expression pattern in mouse tissues. In the kidney, both proteins were expressed only by podocytes, and at the subcellular level, we localized these cytosolic proteins specifically to the foot processes. *Sh2d4a* protein may be involved in the slit diaphragm signaling. The peculiar domain structure of *Plekhh2* protein suggests, however, that it may be involved in connecting the slit diaphragm to the actin cytoskeleton.

Conclusion

We have identified five novel, highly glomerulus-specific proteins. It is interesting that these proteins share the similar restricted expression pattern with several essential podocyte proteins. Therefore, it is reasonable to speculate that several of these novel glomerular proteins have dedicated roles in glomerulus physiology. This report provides new insights into the biology of the glomerulus and creates numerous possibilities to characterize the role of these novel proteins in the glomerular physiology and pathology.

Acknowledgments

This study was supported by grants from the Knut and Alice Wallenberg Foundation, the Swedish Research Council, Novo Nordisk, Strategic Research, Söderberg and Hedlund foundations, Inga-Britt and Arne Lundberg Foundation, the Juselius Foundation, the Finnish Cultural Foundation, and the program for Postgenomic Research and Technology in South-West Sweden.

We are grateful to Dadi Niu and Satu Kuure for technical assistance.

Disclosures

K.T. is co-founder of and has stock ownership in NephroGenex Inc. C.B. has stock ownership in NephroGenex Inc.

References

1. Tryggvason K, Patrakka J, Wartiovaara J: Hereditary proteinuria syndromes and mechanisms of proteinuria. *N Engl J Med* 354: 1387–1401, 2006
2. Ballermann BJ: Glomerular endothelial cell differentiation. *Kidney Int* 67: 1668–1671, 2005
3. Eremina V, Sood M, Haigh J, Nagy A, Lajoie G, Ferrara N, Gerber HP, Kikkawa Y, Miner JH, Quaggin SE: Glomerular-specific alterations of VEGF-A expression lead to distinct congenital and acquired renal diseases. *J Clin Invest* 111: 707–716, 2003
4. Hudson BG, Tryggvason K, Sundaramoorthy M, Neilson EG: Alport's syndrome, Goodpasture's syndrome, and type IV collagen. *N Engl J Med* 348: 2543–2556, 2003
5. Zenker M, Aigner T, Wendler O, Tralau T, Muntefering H, Fenski R, Pitz S, Schumacher V, Royer-Pokora B, Wuhl E, Cochat P, Bouvier R, Kraus C, Mark K, Madlon H, Dotsch J, Rascher W, Maruniak-Chudek I, Lennert T, Neumann LM, Reis A: Human laminin beta2 deficiency causes congenital nephrosis with mesangial sclerosis and distinct eye abnormalities. *Hum Mol Genet* 2013: 2625–2632, 2004
6. Miner JH, Sanes JR: Molecular and functional defects in kidneys of mice lacking collagen alpha 3(IV): Implications for Alport syndrome. *J Cell Biol* 135: 1403–1413, 1996
7. Boute N, Gribouval O, Roselli S, Benessy F, Lee H, Fuchshuber A, Dahan K, Gubler MC, Niaudet P, Antignac C: NPHS2, encoding the glomerular protein podocin, is mutated in autosomal recessive steroid-resistant nephrotic syndrome. *Nat Genet* 24: 349–354, 2000
8. Kestila M, Lenkkeri U, Mannikko M, Lamerdin J, McCready P, Putaala H, Ruotsalainen V, Morita T, Nissinen M, Herva R, Kashtan CE, Peltonen L, Holmberg C, Olsen A, Tryggvason K: Positionally cloned gene for a novel glomerular protein—nephrin—is mutated in congenital nephrotic syndrome. *Mol Cell* 1: 575–582, 1998
9. Ciani L, Patel A, Allen ND, Ffrench-Constant C: Mice lacking the giant protocadherin mFAT1 exhibit renal slit junction abnormalities and a partially penetrant cyclopia and anophthalmia phenotype. *Mol Cell Biol* 23: 3575–3582, 2003
10. Donoviel DB, Freed DD, Vogel H, Potter DG, Hawkins E, Barrish JP, Mathur BN, Turner CA, Geske R, Montgomery CA, Starbuck M, Brandt M, Gupta A, Ramirez-Solis R, Zambrowicz BP, Powell DR: Proteinuria and perinatal lethality in mice lacking NEPH1, a novel protein with homology to NEPHRIN. *Mol Cell Biol* 21: 4829–4836, 2001
11. Verma R, Kovari I, Soofi A, Nihalani D, Patrie K, Holzman LB: Nephrin ectodomain engagement results in Src kinase activation, nephrin phosphorylation, Nck recruitment, and actin polymerization. *J Clin Invest* 116: 1346–1359, 2006
12. Jones N, Blasutig IM, Eremina V, Ruston JM, Bladt F, Li H, Huang H, Larose L, Li SS, Takano T, Quaggin SE, Pawson T: Nck adaptor proteins link nephrin to the actin cytoskeleton of kidney podocytes. *Nature* 440: 818–823, 2006
13. Shih NY, Li J, Karpitskii V, Nguyen A, Dustin ML, Kana-gawa O, Miner JH, Shaw AS: Congenital nephrotic syndrome in mice lacking CD2-associated protein. *Science* 286: 312–315, 1999
14. Wharram BL, Goyal M, Gillespie PJ, Wiggins JE, Kershaw DB, Holzman LB, Dysko RC, Saunders TL, Samuelson LC, Wiggins RC: Altered podocyte structure in GLEPP1 (Pt-

- pro)-deficient mice associated with hypertension and low glomerular filtration rate. *J Clin Invest* 106: 1281–1290, 2000
15. Doyonnas R, Kershaw DB, Duhme C, Merckens H, Chelliah S, Graf T, McNaghy KM: Anuria, omphalocele, and perinatal lethality in mice lacking the CD34-related protein podocalyxin. *J Exp Med* 194: 13–27, 2001
 16. Asanuma K, Kim K, Oh J, Giardino L, Chabanis S, Faul C, Reiser J, Mundel P: Synaptopodin regulates the actin-bundling activity of alpha-actinin in an isoform-specific manner. *J Clin Invest* 115: 1188–1198, 2005
 17. Kaplan JM, Kim SH, North KN, Rennke H, Correia LA, Tong HQ, Mathis BJ, Rodriguez-Perez JC, Allen PG, Beggs AH, Pollak MR: Mutations in ACTN4, encoding alpha-actinin-4, cause familial focal segmental glomerulosclerosis. *Nat Genet* 24: 251–256, 2000
 18. Barletta GM, Kovari IA, Verma RK, Kerjaschki D, Holzman LB: Nephlin and Neph1 co-localize at the podocyte foot process intercellular junction and form cis hetero-oligomers. *J Biol Chem* 278: 19266–19271, 2003
 19. Inoue T, Yaoita E, Kurihara H, Shimizu F, Sakai T, Kobayashi T, Ohshiro K, Kawachi H, Okada H, Suzuki H, Kihara I, Yamamoto T: FAT is a component of glomerular slit diaphragms. *Kidney Int* 59: 1003–1012, 2001
 20. Mundel P, Heid HW, Mundel TM, Kruger M, Reiser J, Kriz W: Synaptopodin: An actin-associated protein in telencephalic dendrites and renal podocytes. *J Cell Biol* 139: 193–204, 1997
 21. Wang R, St John PL, Kretzler M, Wiggins RC, Abrahamson DR: Molecular cloning, expression, and distribution of glomerular epithelial protein 1 in developing mouse kidney. *Kidney Int* 57: 1847–1859, 2000
 22. Takemoto M, He L, Norlin J, Patrakka J, Xiao Z, Petrova T, Bondjers C, Asp J, Wallgard E, Sun Y, Samuelsson T, Mostad P, Lundin S, Miura N, Sado Y, Alitalo K, Quaggin SE, Tryggvason K, Betsholtz C: Large-scale identification of genes implicated in kidney glomerulus development and function. *EMBO J* 25: 1160–1174, 2006
 23. Takemoto M, Asker N, Gerhardt H, Lundkvist A, Johansson BR, Saito Y, Betsholtz C: A new method for large scale isolation of kidney glomeruli from mice. *Am J Pathol* 161: 799–805, 2002
 24. Putaala H, Sainio K, Sariola H, Tryggvason K: Primary structure of mouse and rat nephrin cDNA and structure and expression of the mouse gene. *J Am Soc Nephrol* 11: 991–1001, 2000
 25. Agaton C, Galli J, Hoiden Guthenberg I, Janzon L, Hansson M, Asplund A, Brundell E, Lindberg S, Ruthberg I, Wester K, Wurtz D, Hoog C, Lundberg J, Stahl S, Ponten F, Uhlen M: Affinity proteomics for systematic protein profiling of chromosome 21 gene products in human tissues. *Mol Cell Proteomics* 2: 405–414, 2003
 26. Nilsson P, Paavilainen L, Larsson K, Odling J, Sundberg M, Andersson AC, Kampf C, Persson A, Al-Khalili Szigyarto C, Ottosson J, Bjorling E, Hober S, Wernerus H, Wester K, Ponten F, Uhlen M: Towards a human proteome atlas: High-throughput generation of mono-specific antibodies for tissue profiling. *Proteomics* 5: 4327–4337, 2005
 27. Tryggvason K, Kouvalainen K: Number of nephrons in normal human kidneys and kidneys of patients with the congenital nephrotic syndrome. A study using a sieving method for counting of glomeruli. *Nephron* 15: 62–68, 1975
 28. Ruotsalainen V, Patrakka J, Tissari P, Reponen P, Hess M, Kestila M, Holmberg C, Salonen R, Heikinheimo M, Wartiovaara J, Tryggvason K, Jalanko H: Role of nephrin in cell junction formation in human nephrogenesis. *Am J Pathol* 157: 1905–1916, 2000
 29. Lahdenkari AT, Lounatmaa K, Patrakka J, Holmberg C, Wartiovaara J, Kestila M, Koskimies O, Jalanko H: Podocytes are firmly attached to glomerular basement membrane in kidneys with heavy proteinuria. *J Am Soc Nephrol* 15: 2611–2618, 2004
 30. Herb A, Wisden W, Catania MV, Marechal D, Dresse A, Seeburg PH: Prominent dendritic localization in forebrain neurons of a novel mRNA and its product, dendrin. *Mol Cell Neurosci* 8: 367–374, 1997
 31. Neuner-Jehle M, Denizot JP, Borbely AA, Mallet J: Characterization and sleep deprivation-induced expression modulation of dendrin, a novel dendritic protein in rat brain neurons. *J Neurosci Res* 46: 138–151, 1996
 32. Galperin E, Benjamin S, Rapaport D, Rotem-Yehudar R, Tolchinsky S, Horowitz M: EHD3: A protein that resides in recycling tubular and vesicular membrane structures and interacts with EHD1. *Traffic* 3: 575–589, 2002
 33. Kobayashi N: Mechanism of the process formation; podocytes vs. neurons. *Microsc Res Tech* 57: 217–223, 2002
 34. Mundel P, Shankland SJ: Podocyte biology and response to injury. *J Am Soc Nephrol* 13: 3005–3015, 2002
 35. Kremerskothen J, Kindler S, Finger I, Veltel S, Barnekow A: Postsynaptic recruitment of dendrin depends on both dendritic mRNA transport and synaptic anchoring. *J Neurochem* 96: 1659–1666, 2006
 36. Kawata A, Iida J, Ikeda M, Sato Y, Mori H, Kansaku A, Sumita K, Fujiwara N, Rokukawa C, Hamano M, Hirabayashi S, Hata Y: CIN85 is localized at synapses and forms a complex with S-SCAM via dendrin. *J Biochem (Tokyo)* 139: 31–39, 2006
 37. Pohl U, Smith JS, Tachibana I, Ueki K, Lee HK, Ramaswamy S, Wu Q, Mohrenweiser HW, Jenkins RB, Louis DN: EHD2, EHD3, and EHD4 encode novel members of a highly conserved family of EH domain-containing proteins. *Genomics* 63: 255–262, 2000
 38. Lemmon MA, Ferguson KM, Abrams CS: Pleckstrin homology domains and the cytoskeleton. *FEBS Lett* 513: 71–76, 2002
 39. Chishti AH, Kim AC, Marfatia SM, Lutchman M, Hanspal M, Jindal H, Liu SC, Low PS, Rouleau GA, Mohandas N, Chasis JA, Conboy JG, Gascard P, Takakuwa Y, Huang SC, Benz EJ Jr, Bretscher A, Fehon RG, Gusella JF, Ramesh V, Solomon F, Marchesi VT, Tsukita S, Tsukita S, Hoover KB: The FERM domain: A unique module involved in the linkage of cytoplasmic proteins to the membrane. *Trends Biochem Sci* 23: 281–282, 1998
 40. Berg JS, Derfler BH, Pennisi CM, Corey DP, Cheney RE: Myosin-X, a novel myosin with pleckstrin homology domains, associates with regions of dynamic actin. *J Cell Sci* 113: 3439–3451, 2000

Plekhh2, a novel podocyte protein downregulated in human focal segmental glomerulosclerosis, is involved in matrix adhesion and actin dynamics

Ljubica Perisic¹, Mark Lal¹, Jenny Hulkko², Kjell Hultenby³, Björn Önfelt⁴, Ying Sun⁵, Fredrik Dunér², Jaakko Patrakka², Christer Betsholtz⁵, Mathias Uhlen⁶, Hjalmar Brismar⁴, Karl Tryggvason¹, Annika Wernerson^{2,7} and Timo Pikkarainen^{1,7}

Q2

¹Division of Matrix Biology, Department of Medical Biochemistry and Biophysics, Karolinska Institutet, Stockholm, Sweden; ²Division of Renal Medicine, Department of Clinical Science, Intervention and Technology, Karolinska Institutet, Stockholm, Sweden; ³Clinical Research Center, Department of Laboratory Medicine, Karolinska Institutet, Stockholm, Sweden; ⁴Cell Physics, Applied Physics, School of Engineering Sciences, Royal Institute of Technology, Stockholm, Sweden; ⁵Vascular Biology Division, Department of Medical Biochemistry and Biophysics, Karolinska Institutet, Stockholm, Sweden and ⁶Department of Biotechnology, Royal Institute of Technology, Stockholm, Sweden

Q3

Pleckstrin homology domain-containing, family H (with MyTH4 domain), member 2 (Plekhh2) is a 1491-residue intracellular protein highly enriched in renal glomerular podocytes for which no function has been ascribed. Analysis of renal biopsies from patients with focal segmental glomerulosclerosis revealed a significant reduction in total podocyte Plekhh2 expression compared to controls. Sequence analysis indicated a putative α -helical coiled-coil segment as the only recognizable domain within the N-terminal half of the polypeptide, while the C-terminal half contains two PH, a MyTH4, and a FERM domain. We identified a phosphatidylinositol-3-phosphate consensus-binding site in the PH1 domain required for Plekhh2 localization to peripheral regions of cell lamellipodia. The N-terminal half of Plekhh2 is not necessary for lamellipodial targeting but mediates self-association. Yeast two-hybrid screening showed that Plekhh2 directly interacts through its FERM domain with the focal adhesion protein Hic-5 and actin. Plekhh2 and Hic-5 coprecipitated and colocalized at the soles of podocyte foot processes *in situ* and Hic-5 partially relocated from focal adhesions to lamellipodia in Plekhh2-expressing podocytes. In addition, Plekhh2 stabilizes the cortical actin cytoskeleton by attenuating actin depolymerization. Our findings suggest a structural and functional role for Plekhh2 in the podocyte foot processes.

Kidney International (2012) **0**, 000–000. doi:10.1038/ki.2012.252

Correspondence: Karl Tryggvason, Division of Matrix Biology, Department of Medical Biochemistry and Biophysics, Karolinska Institutet, Scheeles väg 2, Stockholm 171 77, Sweden.

E-mail: karl.tryggvason@ki.se

⁷These authors contributed equally to this work.

Received 20 December 2011; revised 4 April 2012; accepted 10 May 2012

KEYWORDS: cell biology and structure; cell-matrix interactions; cytoskeleton; podocyte; protein interaction

The kidney glomerulus is a micro-organ comprising a molecular filtration barrier that prevents the loss of blood proteins into the primary filtrate. The capacity of the glomerular filtration barrier to facilitate this function is dependent on the coordinated function of its three constituent layers: the endothelium, the glomerular basement membrane (GBM), and the podocytes. Although each of the three layers contributes to the permselectivity of the glomerular filtration barrier, the podocyte forms the final barrier to filtration. As such, the podocyte is critically positioned to determine the ultimate composition of the primary urine that passes into Bowman's space.¹ The essential role of the podocyte in preventing the filtration of large blood proteins, such as albumin, across the glomerular filtration barrier is provided by genetic studies identifying podocyte genes that, when mutated, result in podocyte dysfunction and nephrotic syndrome.² Focal segmental glomerulosclerosis (FSGS) is one of the most common causes of nephrotic syndrome among adults and is a significant cause of chronic renal failure. It consists of several different categories based on histological features, and recent studies have identified a number of mutations in podocyte-expressed genes that cause podocyte dysfunction and result in some of the hereditary forms of FSGS.

The cytoarchitecture of the glomerular podocyte is defined by three parts: the cell body, the major processes, and the interdigitating foot processes. The foot processes of individual podocytes envelop the capillary and are interconnected with each other via specialized cell junctions, the slit diaphragms,³ whereas their basal domains sit on the GBM. Formation of this highly articulated morphology is stringently dependent on the actomyosin cytoskeleton.

Q4

The actin filament network is the predominant cytoskeletal component of podocyte foot processes and is formed by a unique assembly of linker and adaptor molecules.⁴ The actin cytoskeleton determines proper podocyte foot process structure and provides mechanical support for morphology of glomerular podocytes. Moreover, its dynamic behavior is necessary during podocyte development, in response to injury, for counteraction of the forces that distend the capillary wall and generally for podocyte foot process flexibility. Notably, mutations/deletions in many podocyte genes that result in foot process effacement (FPE) and albuminuria ultimately impact cytoskeletal dynamics. Normally, the podocyte foot process cytoskeleton is organized as highly ordered bundles of parallel actin filaments. When effaced, however, the podocyte cytoskeleton is reorganized and transformed into a dense network.⁵ Podocyte FPE is a common ultrastructural finding in proteinuric diseases where the shape of the foot process is widened and elongated; however, the mechanisms are not yet well understood. Cultured podocytes *in vitro* develop large lamellipodia, which are adhesion and migration structures that may functionally resemble podocyte processes *in vivo*. Lamellipodia are thin, protrusive actin sheets giving rise to ruffles of the plasma membrane at the leading edge of migrating cells or extending cellular processes.⁶

We have identified over 300 glomerulus-upregulated genes using expressed sequence tag profiling and microarray analysis.⁷ Plekhh2, a previously uncharacterized gene, was shown to be most strongly expressed by the testes and the podocyte cells of the kidney glomerulus.⁸ It is a protein of unique domain organization, having a coiled-coil segment at the N terminus followed by two adjoined PH domains, a MyTH domain and a FERM domain at the C terminus (Figure 1a). Here we show that Plekhh2 expression is altered in human FSGS, as well as in two mouse models of glomerular nephropathy. *In vitro* studies of Plekhh2 subcellular localization and interaction partners suggest that Plekhh2 has a role in adhesion structures linking the podocyte foot processes to the GBM. It may also contribute to the connection of actin filaments to these structures and affect the dynamics of the filaments. These findings therefore reveal Plekhh2 as a novel, important component of the podocyte foot processes.

RESULTS

Plekhh2 localizes to the podocyte foot processes and is reduced in FSGS

Immunofluorescence and immunoelectron microscopy (iEM) revealed that in the normal human glomerulus Plekhh2 localizes to the podocyte foot processes where it is mainly found centrally in the foot process cytoplasm (56%) or close to the plasma membrane (within a distance of 100 nm, 28%). Some expression was also seen close to the GBM (12%) but rarely in the slit diaphragm (4%; Figure 1b, c and e).

Analysis of renal biopsies from patients with perihilar and tip lesion FSGS, which are the most common FSGS subtypes

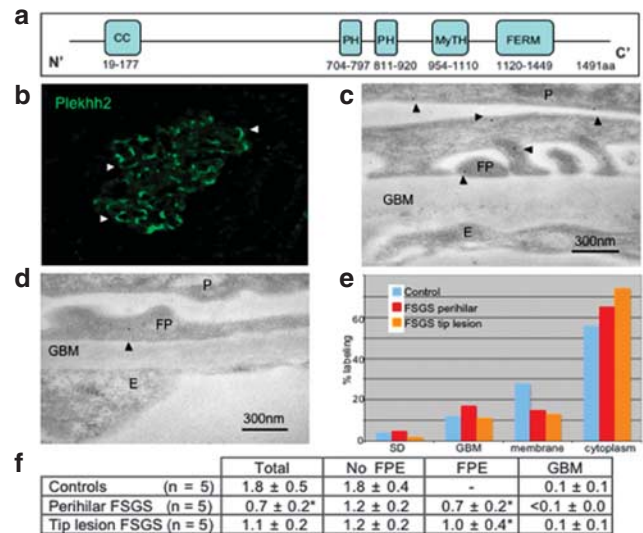


Figure 1 | Plekhh2 localizes to podocyte foot processes and is found in reduced levels in FSGS. (a) Schematic domain structure prediction of Plekhh2 shows the presence of a putative α -helical coiled-coil domain (CC), two adjoined PH domains, a MyTH domain, and a FERM domain. Numbers indicate the location of the domains in the mouse Plekhh2 polypeptide. (b) Plekhh2 localizes to podocyte foot processes giving 'linear' staining in human glomerulus, as shown by immunofluorescence. (c) Immunoelectron microscopy (iEM) analysis of Plekhh2 in the normal glomerulus shows expression centrally in the cytoplasm of the podocyte (P) foot processes (FP, arrowhead), in association with the plasma membrane (arrowhead) or the GBM, but rarely in the slit diaphragm (SD). No expression is detected in the endothelial cells (E). (d) The labeling for Plekhh2 is reduced in areas with foot process (FP) effacement in the perihilar variant of focal segmental glomerulosclerosis (FSGS). (e) Quantification of Plekhh2 localization in the podocytes in control and patient material. Bars represent the percentage of labeling observed in the different compartments of the podocyte foot processes. SD, in the slit diaphragm; membrane, membrane associated; cytoplasm, centrally in the cytoplasm; GBM, adjacent to the glomerular basement membrane. A tendency to redistribution of Plekhh2 from the plasma membrane centrally into the FP was seen in FSGS. (f) Expression of Plekhh2 in human controls and biopsies, based on semiquantitative iEM, expressed as the number of gold particles/ μm^2 (Au/ μm^2). * $P < 0.05$ compared with controls. FPE, foot process effacement.

in our patient population, indicated that there was a significant reduction in total podocyte Plekhh2 expression in perihilar FSGS compared with controls (0.7 ± 0.2 vs. 1.8 ± 0.5 Au/ μm^2 ; Figure 1f; all clinical data presented in Supplementary Table S1 online). However, no correlation between the degree of proteinuria, FPE (measured as slits/ μm GBM), and the amount of Plekhh2 (Au/ μm^2) was found. Low labeling density for Plekhh2 was seen in areas of FPE (Figure 1d) and a tendency toward decreased labeling was also noted in areas without FPE (data not shown). In tip lesion FSGS, we detected reduced levels of Plekhh2 in areas with FPE. As mentioned above, a tendency toward decreased labeling was seen in areas without FPE, but this was not statistically significant. Intriguingly, a tendency for redistribution of Plekhh2 from the plasma membrane to the central parts of the foot process was seen in both FSGS

subtypes, although this was statistically significant only in tip lesion FSGS (Figure 1e). We have also examined renal biopsies from patients with minimal change nephrotic syndrome, membranous nephropathy, and diabetic nephropathy, but found no significant change in the overall amount of Plekhh2 in the podocytes, except for a reduction in areas with FPE in minimal change nephrotic syndrome (data not shown).

Plekhh2 localizes to the peripheral regions of lamellipodia in cultured podocytes

To study the cellular function of Plekhh2, we turned our attention to investigations of its subcellular localization. When expressed heterologously as a Myc-tagged protein in human podocytes, we found that Plekhh2 localized predominantly to the peripheral regions of lamellipodia (Figure 2a). Peripheral lamellipodia staining of Plekhh2 was similarly observed in other cell types expressing the protein either transiently or stably (Supplementary Figure S1 online). Notably, this pattern of staining was confined to those regions of individual subconfluent cells that did not juxtapose neighboring cells, and no Plekhh2 staining of the plasma membrane was otherwise noted in confluent cells that abut against one another (Figure 2b). To exclude the possibility that artificially high expression levels of Plekhh2 accounted for the observed lamellipodial expression, we detergent-treated cells with 0.5% saponin before fixation and immunostaining. This permeabilization strategy results in the removal of the soluble pool of proteins while sparing those that are more stably anchored. Under these conditions, we found that Plekhh2 staining was partially retained, suggesting association with detergent-insoluble cytoskeletal/membrane structures (Supplementary Figure S2a and b online). In addition, subcellular analysis of Plekhh2-expressing podocytes indicated that Plekhh2 is present in the membrane, cytoskeletal, and cytosolic (but not nuclear) fractions (Supplementary Figure S2c online).

We also transiently transfected human podocytes with a construct encoding green fluorescent protein (GFP)–Plekhh2 and followed the localization of the fusion protein in living cells during their attachment, spreading, and migration on fibronectin-coated surfaces. Plekhh2 was found in initial adhesion structures present at the basal aspect of podocytes very soon after cell plating (Supplementary Figure S3a/Supplementary Video a and Figure S3b/Supplementary Video b online). In spreading cells, GFP–Plekhh2 localized to lamellipodia (Supplementary Figure S3d and f/Supplementary Videos d and f online), whereas in migrating podocytes it was detected at the migration front (Supplementary Figure S3c and e/Supplementary Videos c and e online). Supplementary Figure S4 online shows that the construct encoding for GFP–Plekhh2 gives a band of expected size on western blot analysis (170 kDa).

To additionally assess the specificity of the observed Plekhh2 localization, we turned our attention to the various domains of Plekhh2. On the basis of comparative database analysis, Plekhh2 is predicted to contain multiple putative interactive domains including PH and FERM domains that have previously been described as key determinants of protein localization.^{9,10} In the following set of experiments, we examined whether deletion of one or more of the individual domains in the C-terminal half of Plekhh2 affected its subcellular localization (Figure 3). Expression of a truncation mutant lacking the entire C-terminal half (two PH domains, MyTH domain, FERM domain) prevented Plekhh2 lamellipodial expression, and resulted in its nuclear accumulation. Conversely, expression of a Plekhh2 mutant composed solely of its C-terminal half was targeted to the lamellipodia. These studies demonstrate the importance of the MyTH-FERM cassette and/or PH domains in targeting Plekhh2 to lamellipodial structures. Both FERM and PH domains, when singly expressed, demonstrated a propensity to accumulate at lamellipodia. Deletion of either PH or FERM domains of full-length Plekhh2 was not sufficient to completely abolish Plekhh2 localization to lamellipodial structures. This finding suggests that the PH and FERM domains cooperate to ensure the proper localization of Plekhh2.

An analysis of the amino acid sequence of Plekhh2 indicated the presence of a PtdIns(3,4,5)P₃ (PIP₃) consensus binding site in the PH1 domain (Figure 4a). To test the significance of this finding, we mutated the selected conserved residues (K711A and R722C, asterisk) and studied the localization of the protein in podocytes. Although the K711A mutation had no effect on Plekhh2 localization, the double K711A/R722C mutation markedly affected the ‘linear’ lamellipodial localization of Plekhh2, particularly in the case of the mutant lacking the FERM domain. The protein seemed to be transported toward the cell periphery, but the staining was very diffuse (Figure 4b). We also treated Plekhh2-expressing

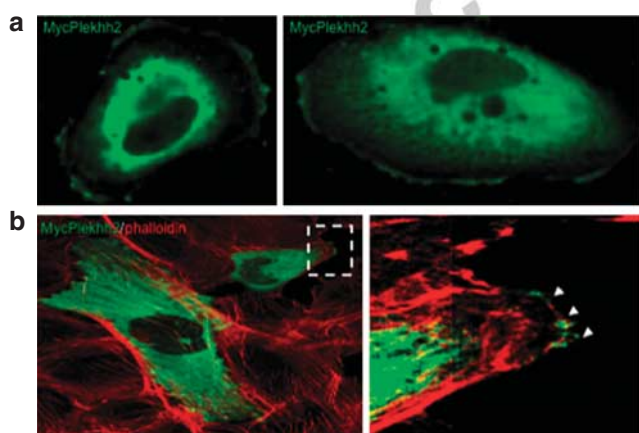


Figure 2 | Plekhh2 localizes to the peripheral region of lamellipodia in cultured human podocytes. (a) Plekhh2 localizes near the lamellipodial plasma membrane in cells spreading on fibronectin. Two cells are shown. (b) Plekhh2 does not localize at the plasma membrane of cells grown to confluence (left panel). Note that Plekhh2 accumulates at the plasma membrane of a cell (left panel, boxed area) extending a lamellipodial extrusion into an empty space (right panel, zoom).

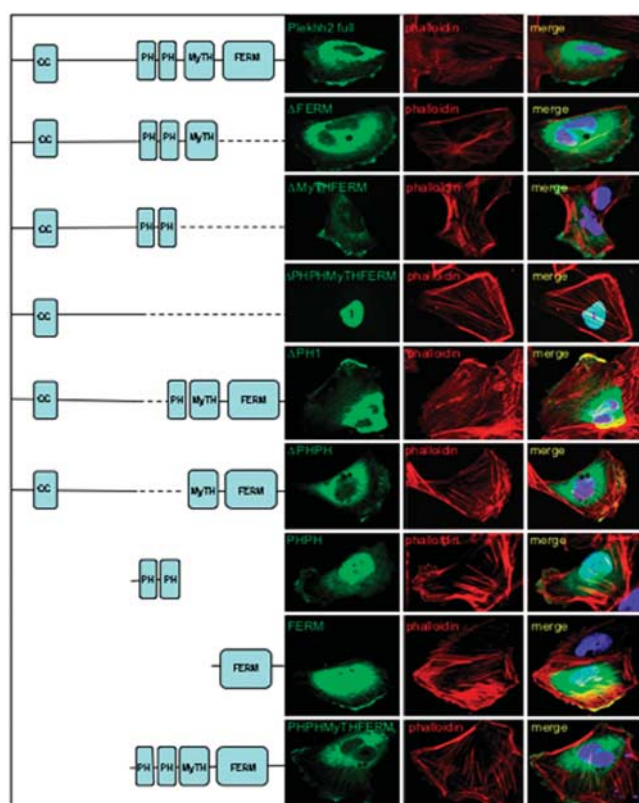


Figure 3 | Localization of truncated Plekhh2 proteins in transfected podocytes. A set of constructs in encoding truncated versions of Plekhh2 and its isolated domains, all containing the Myc-tag at the N terminus, were generated and transfected into human podocytes. Cells were stained with anti-Myc antibody. All Plekhh2 constructs partially directed the expressed protein to the lamellipodial plasma membrane, except for the version lacking the entire C-terminal half that localizes to the nucleus. Deletion of either FERM or PHPH domains is not sufficient to completely prevent Plekhh2 from localizing to lamellipodia, indicating that both domains are important for its peripheral localization. The dashed lines in the schematic drawings indicate the regions of individual constructs that have been deleted. Phalloidin staining used only to demark outer cell borders. CC, coiled-coil domain.

cells with wortmannin or LY294002, potent phosphatidylinositol 3-kinase inhibitors. Both of these treatments markedly reduced Plekhh2 localization to the plasma membrane of lamellipodia (Figure 4c, Supplementary Figure S5 online), with only about 25% of the Plekhh2 signal remaining at this cellular location (Figure 4d). In contrast, Plekhh2 variants composed either of only the PH domains (PHPH) or lacking the FERM domain (Δ FERM) were completely relocalized to the cytosol upon wortmannin or LY294002 treatment (Supplementary Figure S5b and c online). As predicted, localization of the Δ PHPH variant was not altered by either of these two treatments. These findings strongly suggest that interaction of the PH1 domain with PIP3 contributes to Plekhh2 localization to the peripheral regions of lamellipodia, and confirm that the FERM domain at the C terminus of the polypeptide also serves to target Plekhh2 to these sites.

Evidence that Plekhh2 associates with itself

The only recognizable domain within the N-terminal half of the 1491-residue-long Plekhh2 polypeptide is a putative α -helical coiled-coil domain located between amino acids 19 and 177 (Supplementary Figure S6a online). According to the secondary structure prediction by the PSIPRED program,¹¹ this segment folds into a continuous coiled-coil, except for one short interruption (Supplementary Figure S6b online). Coiled-coil domains are common oligomerization domains, the most predominant oligomeric forms being dimers and trimers. Analysis of the segment with the SCORER 2.0 program,¹² which distinguishes parallel dimeric and trimeric coiled-coils, predicts that the coiled-coil domain of Plekhh2 assembles into a dimer. To provide experimental evidence for these predictions, we tested by coimmunoprecipitation whether Plekhh2 self-associates. To this end, HEK293 cells were cotransfected with full-length Plekhh2 tagged with either Myc or hemagglutinin (HA) epitopes, followed by immunoprecipitation with anti-HA antibodies and western blotting with those against the Myc-tag. As shown in Figure 5a, these two full-length versions of Plekhh2 associated with each other. As there is some evidence from structural studies indicating that the FERM domain is capable of forming dimeric structures,¹³ we tested the involvement of this domain in Plekhh2 self-association. However, no interaction was seen when HA-tagged full-length Plekhh2 was coexpressed with the Myc-tagged FERM domain (Supplementary Figure S7 online), indicating that association does not occur through the FERM domain.

We also used fluorescence resonance energy transfer (FRET) to confirm that Plekhh2 self-associates. In this experiment, we coexpressed in human podocytes Plekhh2 proteins tagged at their N termini with either GFP or Myc and measured the change in GFP donor fluorescence following bleaching of the red (Myc) acceptor fluorophore (Figure 5b). Under these conditions, we detected a significant increase in the GFP signal in lamellipodia of the transfected cells (Figure 5c). If the coiled-coil domain located in the N terminus of Plekhh2 is indeed biologically functional, we reasoned that full-length Plekhh2 may be able to alter the nuclear expression pattern of the Plekhh2 mutant that lacks the entire C-terminal half, but that still possesses its coiled-coil domain (the form Δ PHPHMyTH-FERM). Immunofluorescent examination of cells coexpressing these two proteins revealed that the truncated Plekhh2 partially relocalized from the nucleus to the plasma membrane of lamellipodia in the presence of the full-length protein (Figure 5d). Such a partial rescue of Δ PHPHMyTHFERM localization to lamellipodia was not similarly observed in cells overexpressing Ezrin. Altogether, these studies provide evidence that the N-terminal half of Plekhh2, containing the coiled-coil region, is sufficient for the self-association of Plekhh2, which likely assembles into a dimer.

Plekhh2 interacts with Hic-5 and actin, and recruits Hic-5 from focal adhesions to the cell periphery

To predict the cellular function of Plekhh2, we used an unbiased yeast two-hybrid approach for discovering protein

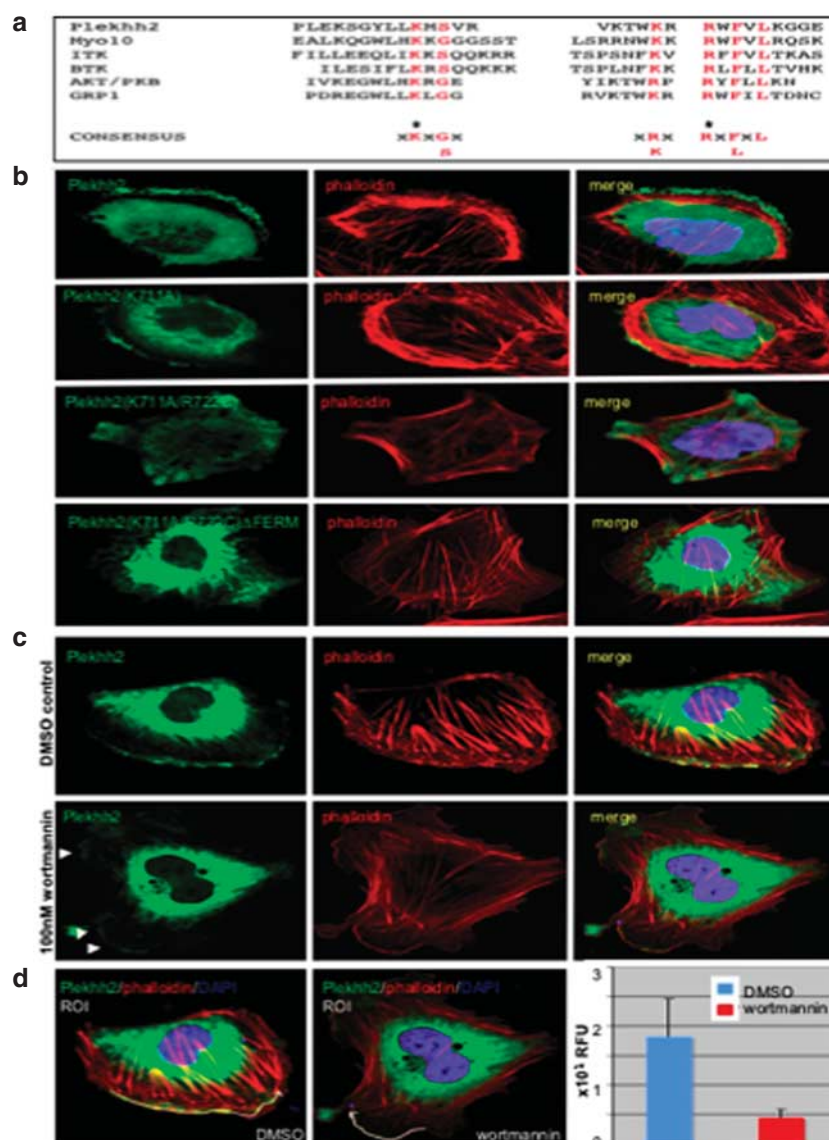


Figure 4 | PI3-K inhibition reduces lamellipodial localization of Plekhh2. (a) Alignment of the mouse Plekhh2 PH1 domain sequence with sequences of various PtdIns(3,4,5)P3 (PIP3)-binding PH domains indicates that this domain of Plekhh2 contains the consensus sequence for PIP3 binding. (b) The Plekhh2 PH1 domain-conserved residues K711 and R722 (marked with asterisk) were mutated in the full-length or Δ FERM protein, and the proteins were localized in the podocytes by staining for the Myc-tag. Double mutation markedly affected the 'linear' lamellipodial localization of Plekhh2, particularly in the case of the variant lacking the FERM domain. (c) Treatment of full-length Plekhh2-expressing podocytes with wortmannin, a potent phosphatidylinositol 3 (PI3)-kinase inhibitor, results in a reduction of Plekhh2 expression at the lamellipodia. (d) Quantification of the intensity of the Plekhh2 signal along the periphery of lamellipodia (left images; white line, region of interest (ROI)) shows a decrease of about 75% following wortmannin treatment ($n > 10$ cells, \pm s.e.m. for each treatment, RFU: relative fluorescence units). DMSO, dimethylsulfoxide.

interactions, and screened a mouse kidney glomerular complementary DNA (cDNA) library with full-length Plekhh2 and its deletion variants. This screen identified Hic-5, a paxillin-related focal adhesion protein (TGFB1i1), and β -actin (ActB) as potential interacting partners of Plekhh2 (Figure 6). Hic-5 was isolated in the screens with full-length Plekhh2, the PHPHMyTHFERM form, and the FERM domain as baits, whereas ActB was identified in the screens with the latter two baits. These findings, which were confirmed in a yeast-mating assay (Figure 6a, Supplementary

Figure S8 online), indicate that it is the FERM domain of Plekhh2 that mediates interaction of Plekhh2 with these two proteins. The interaction of Plekhh2 with Hic-5 was verified in a coimmunoprecipitation assay using HEK293 cells coexpressing HA-tagged Plekhh2 and Myc-tagged Hic-5 (Figure 6b, Supplementary Figure S7 online).

To assess the subcellular relationship between these two proteins, we next examined their spatial distribution in cultured human podocytes. In these cells, endogenous Hic-5 localizes mainly to focal adhesions (Figure 6c, Supplementary

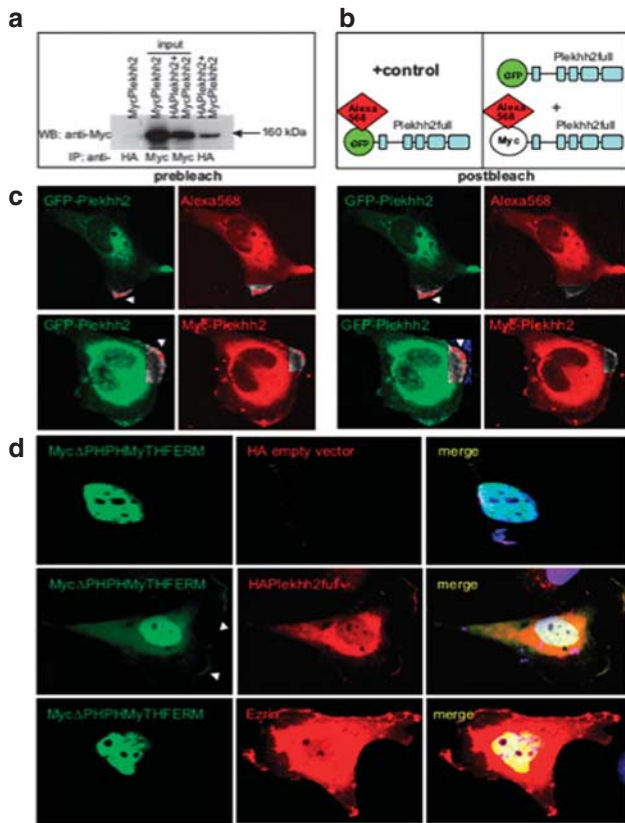


Figure 5 | The N-terminal half of Plekhh2 containing the predicted coiled-coil domain mediates self-association of the protein. (a) Full-length Plekhh2 tagged with either Myc or hemagglutinin (HA) epitopes coimmunoprecipitate from lysates of cotransfected HEK293 cells. (b and c) Green fluorescent protein (GFP)-Plekhh2 signal intensity increases upon Alexa568 bleaching (boxed area shown by arrows) as a result of FRET between the two fluorophores, suggesting association of individual Plekhh2 proteins (lower panel). As a positive control, we used GFP-Plekhh2 stained with anti-GFP- and Alexa Fluor 568-conjugated secondary antibodies (upper panel). (d) Plekhh2 lacking its entire C-terminal half (Δ PHPHMyTHFERM) is partially relocalized from the cell nucleus to the cell periphery by coexpression with full-length Plekhh2, but not by coexpression with Ezrin, a plasma membrane-cytoskeleton linker protein. IP, immunoprecipitation.

Figure S9a online). Following transfection of Plekhh2, endogenous Hic-5 was found to partially relocate to lamellipodial extensions, a response that was observed as a linear staining pattern located at the periphery of lamellipodia, near the plasma membrane (Figure 6c, Supplementary Figure S9b online). This was not due to overall changes in Hic-5 expression (Supplementary Figure S9c online). Consistent with the yeast two-hybrid results, such a relocalization was also seen upon transfection of only the FERM domain of Plekhh2, but not the Δ FERM form.

To examine the location of these two proteins *in situ*, we analyzed human kidney samples by iEM (Figure 7a and b). Hic-5 was occasionally found in the podocyte foot processes, localized close to the GBM. Coimmunolabeling of Plekhh2 and Hic-5 with 10- and 5-nm gold particles, respectively,

indicated that there was significant colocalization of the two proteins and that they are less than 20 nm apart from each other, providing strong evidence that Plekhh2 and Hic-5 interact *in vivo* as well (Figure 7c and d). Glomerular expression of both proteins was also verified by reverse transcription-polymerase chain reaction (PCR; Supplementary Figure S9d online).

Plekhh2 stabilizes lamellipodial cortical actin by slowing down actin depolymerization

Examination of peripheral Plekhh2 by confocal microscopy indicated a significant overlap with the cortical actin cytoskeleton both in the XY- and Z-scan (Figure 8a). Together with the finding that ActB was isolated in the yeast two-hybrid screen with the C-terminal half of Plekhh2, as well as with its FERM domain, and the fact that Plekhh2 is found in the cytoskeletal fraction of podocyte cell lysates, we raised the question that Plekhh2 may regulate the dynamics of the actin cytoskeleton at the cell cortex/lamellipodia. To test this possibility, we compared the response of the actin cytoskeleton to treatment with the actin monomer-sequestering drug latrunculin A in untransfected and Plekhh2-transfected podocytes (Figure 8b, Supplementary Figure S10 online). In the absence of Plekhh2, latrunculin A treatment resulted in a loss of parallel transversal stress fibers, as well as of cortical actin filaments, with a concomitant appearance of phalloidin-positive patches. However, in Plekhh2-expressing cells treated with latrunculin A, actin expression was preserved at the cortical region where it colocalized with Plekhh2. The same response was not observed in cells expressing Δ PHPHMyTHFERM, the truncated Plekhh2 mutant that localizes to the nucleus. In further studies designed to assess the relationship between Plekhh2 and actin dynamics, we examined whether polymerization or depolymerization of exogenous pyrene-labeled actin is differently affected by lysates prepared from 293 cells stably expressing Plekhh2 and control cells. Our results show that Plekhh2 overexpression contributed to stabilization of F-actin by attenuating its depolymerization (Figure 8c).

Plekhh2, Hic-5, and actin show parallel changes in glomerular gene expression in microarray profiles of mouse glomerular disease models

Bioinformatic analysis of Plekhh2 and its associated proteins, Hic-5 and actin, in glomerular microarray profiles from lipopolysaccharide-induced nephrosis and db/db diabetic nephropathy (Figure 9a) revealed that these genes exhibit a coordinated change of expression: downregulation in the lipopolysaccharide model of FPE and significant upregulation in the Type II diabetes model. These analyses may indicate that Plekhh2, Hic-5, and actin are collectively involved in the origin and/or progression of podocyte injury in mice, leading to proteinuria. The complex underlying mechanisms accounting for this could be very different in various human glomerular diseases and need to be studied further.

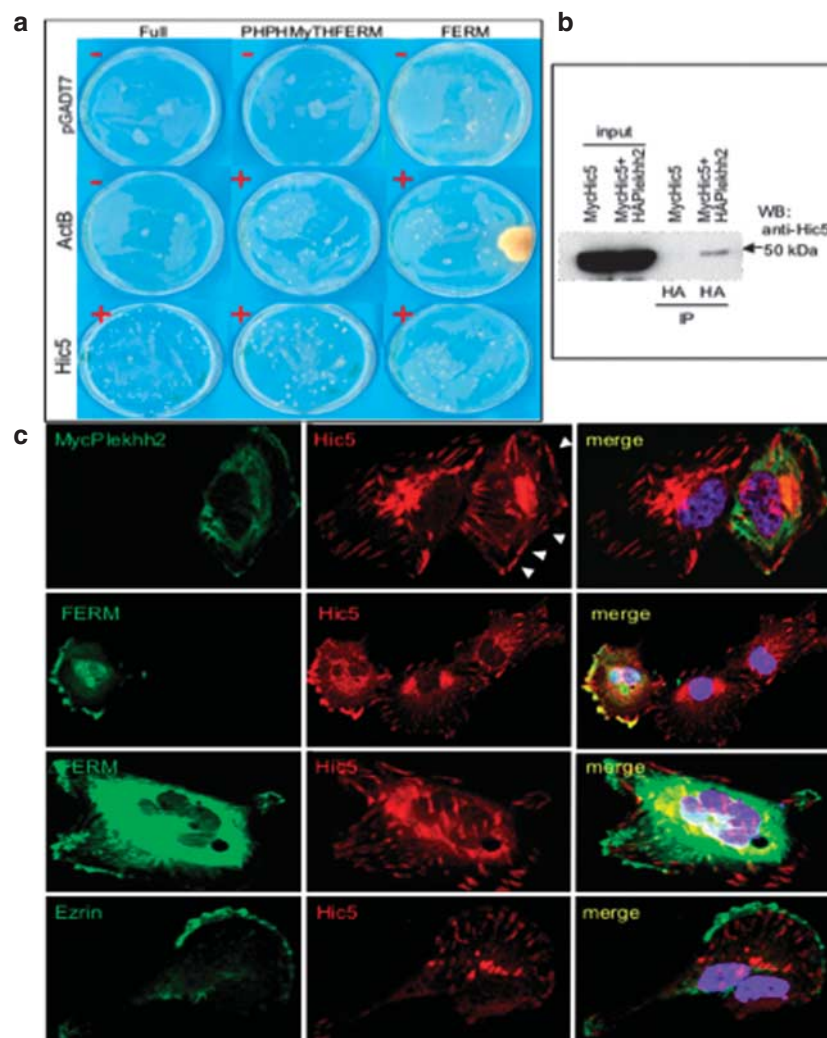


Figure 6 | Plekhh2 interacts with Hic-5 and actin through its FERM domain and recruits Hic-5 to lamellipodia. (a) Yeast two-hybrid screen of a mouse kidney glomerulus cDNA library indicates that Plekhh2 interacts via its FERM domain with Hic-5 and β -actin (ActB). Here, the results were confirmed in a mating assay (+, positive interaction; –, no interaction). Note that ActB does not interact with full-length Plekhh2, but only with the other two baits, the entire C-terminal half and the FERM domain. Hic-5 interacts with all three baits. These findings indicate that the binding sites for Hic-5 and actin on the FERM domain are not identical. (b) Myc-tagged Hic-5 and HA-tagged Plekhh2 coimmunoprecipitate from lysates of cotransfected HEK293 cells. (c) Expression of Plekhh2 causes partial relocalization of endogenous Hic-5 from focal adhesions to lamellipodia (upper panel, arrowheads). The Plekhh2 FERM domain is also sufficient to induce lamellipodial Hic-5 relocalization, whereas Plekhh2 Δ FERM and Ezrin are without effect. HA, hemagglutinin; WB, western blot.

DISCUSSION

In this work, we investigated the function and subcellular localization of Plekhh2, a recently identified scaffold-like protein with high expression levels in the podocytes of the kidney glomerulus. The results shed light on the role of the various domains of Plekhh2, suggest a function for Plekhh2 in adhesion structures linking the podocytes to the underlying GBM, and implicate Plekhh2 as a protein involved in the pathogenesis of kidney disease.

Plekhh2 is one of two previously uncharacterized Plekhh proteins encoded in the mammalian genomes. A Plekhh ortholog has also been described in *Drosophila*, *Caenorhabditis elegans*, and zebrafish. In *C. elegans*, the loss of the protein, termed MAX-1, was found to cause variable axon

guidance defects.¹⁴ It was also shown that a GFP-MAX-1 fusion protein was enriched in neuronal processes in a FERM domain-dependent manner. The reasons for axon guidance defects are not entirely clear, but MAX-1 may at least contribute to the enrichment of a netrin receptor UNC-5 to the growth cone. However, knockdown of the zebrafish MAX-1 was not found to cause apparent defects in neuronal axon guidance, but instead cause defects in intersegmental vessel patterning.¹⁵ Some evidence suggests that the protein might be involved in mediating membrane localization of ephrin proteins that may provide guidance cues for endothelial cell migration.

It is also worth noting that the domain organization within the C-terminal half of Plekhh2 resembles that in the

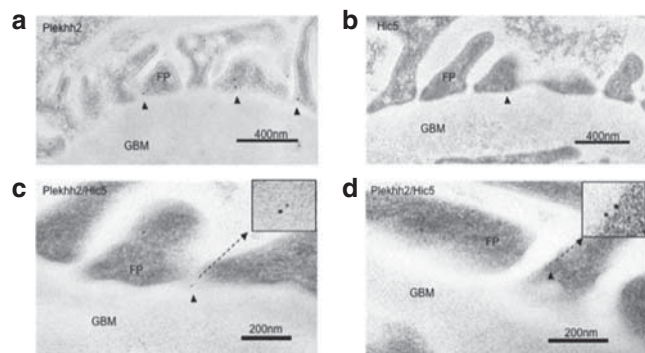


Figure 7 | Plekhh2 and Hic-5 colocalize in podocyte foot processes of the human kidney glomerulus. (a) By immunoelectron microscopy (iEM), Plekhh2 is localized to podocyte foot processes (FP), sometimes close to the glomerular basement membrane (GBM). (b) Hic-5 is also found close to the GBM. (c, d) Double iEM for Plekhh2 (10 nm gold particle) and Hic-5 (5-nm gold particle) indicates that the two proteins colocalize at the same subcellular area in foot processes (dashed arrows), within a distance of 10–20 nm of each other.

tail domains of several unconventional myosins, proteins involved in various cellular functions.¹⁶ It is most similar to myosin X, a protein shown to have a role in filopodia elongation via PIP3 binding to one of its three PH domains, as well as through interaction of its FERM domain with integrins and other cargo that are transported to the filopodial tips.^{16–19} The N-terminal head of myosin X is composed of a motor domain, followed by a neck region containing three IQ motifs and a coiled-coil region, of which the latter segment functions as a dimerization domain. In the case of Plekhh2, secondary structure analysis indicates the presence of a coiled-coil domain near the N terminus of the polypeptide. The sequences of coiled coils are characterized by a heptad repeat (a-b-c-d-e-f-g) comprising mostly hydrophobic residues at positions a and d. The minimum length for the formation of stable coiled coils is reported to be three heptad repeats or 21–23 residues.^{20,21} Plekhh2 is predicted to contain an almost continuous 158-residue-long coiled coil. Our results based on coimmunoprecipitation,

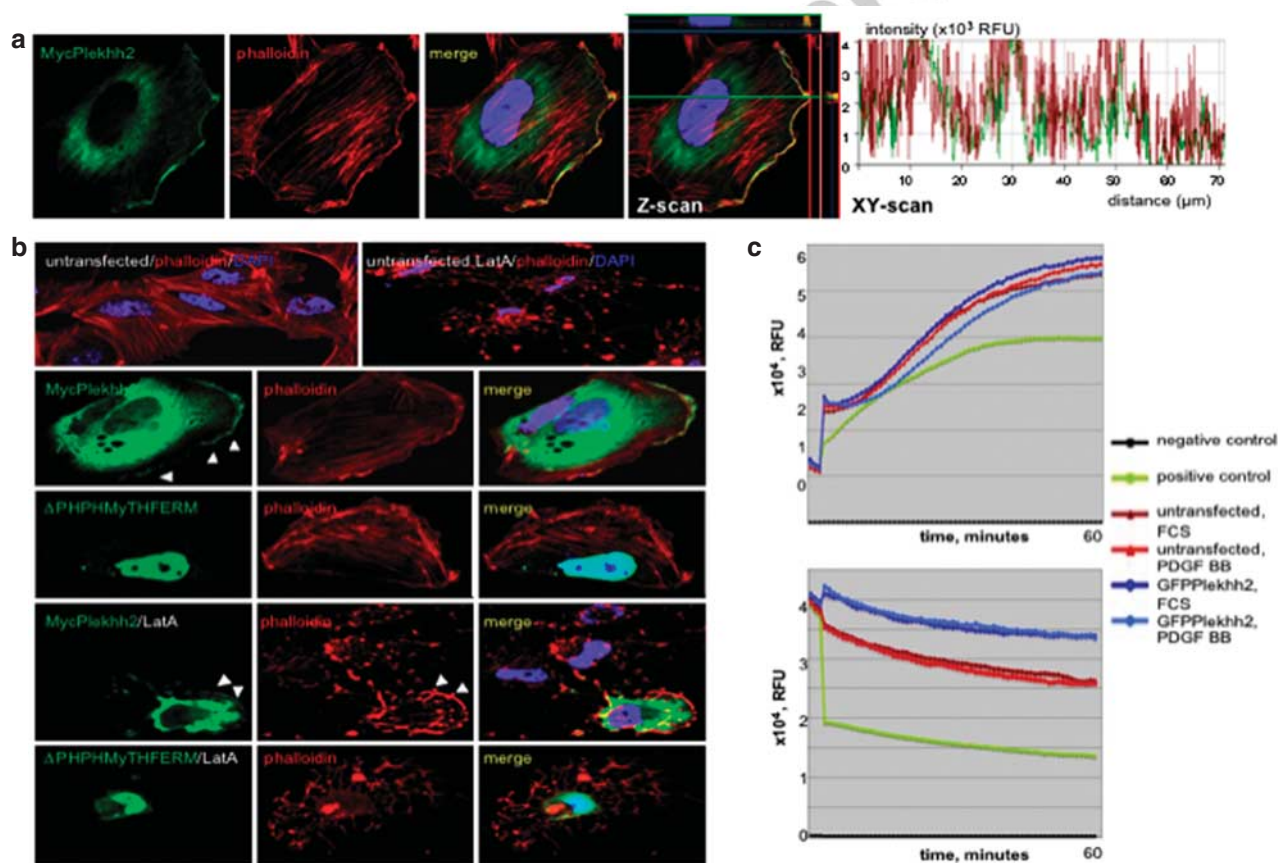


Figure 8 | Plekhh2 colocalizes with cortical actin and contributes to its stabilization by attenuating filamentous actin depolymerization. (a) Plekhh2 colocalizes with cortical filamentous actin in lamellipodia. Both the Z- and XY-scanning indicate considerable signal overlap between Plekhh2 and F-actin along the plasma membrane in cells presenting well-developed lamellipodia. (b) Treatment with latrunculin A, an actin monomer-sequestering drug, results in the complete dissolution of stress fibers in untransfected cells (upper panel), whereas cells expressing Plekhh2 present a partial protection of cortical F-actin expression at the lamellipodia (lower panel, arrowheads). The same is not observed with Δ PHPHMyTHFERM truncation variant that localizes to the nucleus. All stainings are for the Myc-tag. (c) *In vitro* actin polymerization (upper panel) and depolymerization (lower panel) assays with lysates from green fluorescent protein (GFP)-Plekhh2-expressing HEK293 cells and their controls show that Plekhh2 slows down actin depolymerization. Results are representative of three separate experiments. FCS, fetal calf serum; RFU, relative fluorescence units.

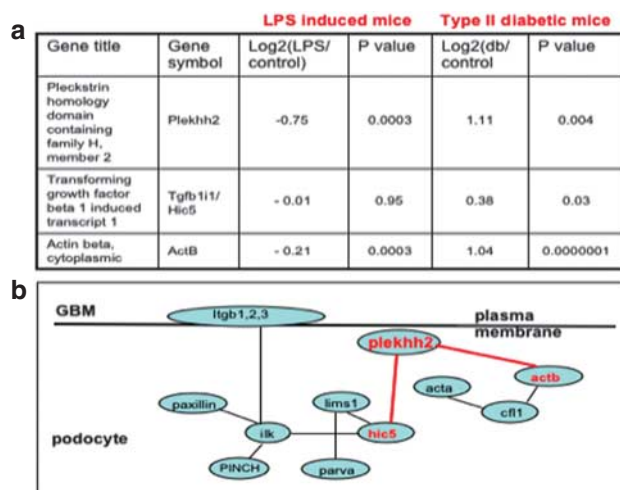


Figure 9 | Microarray comparison of Plekhh2, Hic-5, and actin expression in mouse glomerular disease models and schematic representation of the possible role of Plekhh2 in the podocyte foot processes. (a) Plekhh2 and its interaction partners show parallel expression changes in two mouse models of glomerular disease: downregulation in the lipopolysaccharide (LPS)-induced nephrosis and upregulation in Type II diabetic mice. **(b)** At the base of the foot processes, Plekhh2 is, through Hic-5, linked to a multiprotein complex that is directly associated with the underlying glomerular basement membrane via integrin-ILK interaction. Our findings suggest that Plekhh2 provides another connection to the plasma membrane through binding to PtdIns(3,4,5)P₃, a phospholipid concentrated at the basolateral domain in polarized epithelial cells. Plekhh2 may also contribute to the linkage of actin filaments to cell-matrix contact sites. Both Hic-5 and actin interact with the FERM domain of Plekhh2, but their binding sites are not identical. Novel interactions are highlighted in red; other data (black) are from the GlomNet, a protein-protein interaction network of glomerulus-enriched genes.⁵¹ GBM, glomerular basement membrane.

FRET, and other colocalization studies strongly suggest that this segment is responsible for the self-association of the molecule.

It is well known that the basal cellular levels of PIP₃ in cells are low but significantly elevated upon phosphatidylinositol 3-kinase activation by growth factors, such as PDGF and insulin. However, one has to keep in mind that although overall PIP₃ levels are low in the absence of growth factor stimulation, the existing lipid is not homogeneously distributed throughout the plasma membrane in polarized cells, but it is concentrated to the basolateral membrane domain.²² This very likely reflects high basal levels of phosphatidylinositol 3-kinase activity induced by receptors such as integrins,²³ and enrichment of the lipid phosphatase PTEN, which converts PIP₃ to PIP₂, to the apical domain.²⁴ In light of these facts, it is of considerable significance that Plekhh2 localizes *in situ* to the foot processes, which anchor the podocytes through integrins to the underlying basement membrane. With regard to growth factors and PIP₃ levels, it is known that cell migration and adhesion is promoted by PDGF, a factor present in the serum. In migrating cells, PIP₃ accumulates at the leading edge,²² the location where we can

also find Plekhh2. Furthermore, it is of particular interest to note that podocytes have been shown to be sensitive to insulin.²⁵ In their recent work, Welsh and co-workers²⁶ generated mice lacking the insulin receptor in podocytes, and found that the mice develop significant albuminuria with features such as effacement of the podocyte foot processes and thickening of the GBM. Further studies showed that both the mitogen-activated protein kinase and PIP₃-kinase signaling pathways in response to insulin were abrogated. Moreover, insulin stimulation led to reorganization of the actin cytoskeleton in cultured podocytes. On the basis of our data indicating that PIP₃ contributes to the peripheral localization of Plekhh2, it is interesting to speculate that Plekhh2 localization and function is under the control of insulin signaling.

In transfected cells, we found that the FERM domain is capable of targeting Plekhh2 to the cell periphery. In ERM proteins, the FERM domain is involved in the binding of PIP₂,^{10,27} whose steady-state levels are much higher than those of PIP₃ (40-fold by one estimate²⁸). The binding occurs through a positively charged cleft between two of the subdomains in the FERM domain. However, binding of PIP₂ is not a general feature of FERM domains, as that of myosin X does not possess this positively charged cleft and lacks the conserved PIP₂-interactive residues.²⁹ Moreover, considering the Plekhh2 FERM domain and possible PIP₂ binding, one has to bear in mind that PIP₂ is primarily enriched at the apical membrane domain in polarized epithelial cells.²⁴ Nevertheless, we show in this study that Plekhh2 directly interacts with actin through its FERM domain, suggesting that this domain contributes to Plekhh2 peripheral localization by interacting with the cortical actin cytoskeleton. The observed molecular interaction between the Plekhh2 FERM domain and actin is a novel finding and places Plekhh2 among a limited class of FERM domain-containing proteins that have been shown to possess this capability (merlin,^{30,31} myosin VII,^{32,33} and talin³⁴). Note that in all these cases the interaction was shown in a cosedimentation assay, whereas here we use an unbiased approach. The affinity for the interaction was not measured in case of all these proteins, but when measured the results indicate that it is low. Even if this were the case for Plekhh2, it is possible that the actin concentration at the cell cortex is high enough for the interaction of Plekhh2 with the cortical actin cytoskeleton. Our results obtained using latrunculin A suggest that the Plekhh2-actin interaction appears to protect the cortical actin cytoskeleton by slowing down its depolymerization.

Our findings show that Plekhh2 interacts through its FERM domain not only with actin but also with Hic-5, a transforming growth factorβ1-induced paxillin homolog that localizes to focal adhesions in cultured podocytes. Importantly, Plekhh2 and Hic-5 were also found to colocalize *in vivo*. Hic-5 has been implicated in integrin-mediated signaling by shuttling between the nucleus and focal adhesions.³⁵ There is also evidence of its function in cell

migration,^{36,37} adhesion,³⁸ and epithelial cell differentiation.³⁹ Of significant interest for our study, Hic-5 has been shown to interact with the PINCH-integrin-linked kinase- α -parvin complex, which has a critical role in the control of podocyte adhesion and morphology.^{40–43} Thus, it appears that, at the sole of foot processes, Plekhh2 is, very likely in the form of a dimer, part of a multiprotein adhesion complex, where it may be involved in linking the complex to the plasma membrane. Plekhh2 may also contribute to the connection of the complex to actin filaments, and even contribute to regulation of their dynamics (Figure 9b). With that said, it is of interest to note that in the lipopolysaccharide-induced proteinuria mouse model that is also associated with transient podocyte FPE, glomerular Plekhh2, Hic-5, and actin expression is concomitantly downregulated.⁴⁴ Furthermore, there is some evidence from a genome-wide association study that sequence variants in the Plekhh2 gene region may be associated with diabetic nephropathy, a complication characterized by features such as flattening of the podocyte foot processes and thickening of the GBM.⁴⁵ Other data shown here, using semiquantitative iEM, indicate a reduced Plekhh2 expression and relocalization in FSGS. It is already known that genetic mutations associated with the hereditary form of FSGS, such as α -actinin 4,⁴⁶ CD2AP,⁴⁷ and TRPC6,^{48,49} affect the structure of podocyte cytoskeleton by impairing actin cytoskeleton dynamics.

Finally, recent structural studies demonstrate that the MyTH and FERM domains interact with one another, forming a functional and structural supramodule.^{29,50,51} It remains to be seen whether the MyTH domain of Plekhh2 has FERM domain-independent functions. This appears to be the case in myosin X, where it directly binds to tubulin through a positively charged surface patch.²⁹ It is also worth pointing out that whereas Hic-5 interacted with full-length Plekhh2, the C-terminal half, and the FERM domain in our yeast assays, ActB bound the latter two baits only. These findings indicate that the binding sites of Hic-5 and actin on the FERM domain are not identical, and also that the actin-binding site is hidden in full-length Plekhh2. Thus, it seems that Plekhh2 can exist in at least two conformational states, as is the case for the ERM proteins¹⁰ and several of the unconventional myosins (¹⁸, and references therein).

MATERIALS AND METHODS

Human patients and material

Normal renal tissue was taken from unaffected kidneys surgically removed because of localized carcinoma. Patients who fulfilled the criteria for FSGS clinically and histopathologically were chosen for the study. Biopsies were taken for diagnostic purposes and re-examined to confirm the diagnosis. Biopsy material has been saved prospectively and embedded in a low-temperature resin allowing iEM. The number of cases is thus limited. All materials were used in agreement with the local Board of Ethics.

Expression constructs

Expression constructs were generated by cloning of PCR-amplified fragments into various expression vectors using established

molecular biological methods. Inserts were amplified from kidney cDNA (Mouse MTC Panel I, Clontech Laboratories, Palo Alto, CA) with Long PCR Enzyme Mix (Fermentas International, Burlington, Canada), and sequenced to confirm the absence of PCR-generated mutations. The PCR program used was as follows: 1 cycle of 95°C/4 min, 30 cycles of 95°C/1 min, 51°C/1 min, 72°C/2–10 min, and 1 cycle of 72°C/10 min. For yeast two-hybrid screening, inserts were cloned into the vector pGBKT7 (Clontech Laboratories) in frame with the Gal4 DNA-binding domain. For expression in mammalian cells, cDNAs were cloned into pcDNA3.1 (Invitrogen, Carlsbad, CA), or vectors with various N-terminal tags (pCMV-Myc, pCMV-HA, or pEGFP-C; all from Clontech Laboratories).

Antibodies

The following commercial primary antibodies were used: rabbit anti-Plekhh2 (Sigma Prestige Antibodies, St Louis, MO, AV53218), mouse anti-Hic5 (BD Transduction Labs, San Jose, CA, 611164), mouse anti-c-Myc (Sigma, M4439), rabbit anti-Myc (Sigma, C3956), mouse anti-HA (Sigma, H6908), rabbit anti-GFP (Invitrogen Molecular Probes, A11122), mouse anti-ezrin (Invitrogen, 35-7300), rabbit anti-lamin A/C (Cell signaling, Beverly, MA, 2032), anti-calnexin (Abcam, Cambridge, UK), rabbit anti-actin- β (Abcam), and anti-ERK (Cell signaling). All mouse antibodies were monoclonal. Proteins were visualized with secondary antibodies conjugated to various Alexa Fluor dyes (488, 546, 568; all from Invitrogen) or horseradish peroxidase (GE Healthcare, Piscataway, NJ).

Transient and stable transfections

Human podocytes were grown at 33°C/5% CO₂ in RPMI supplemented with 10% fetal bovine serum (Invitrogen), 1 \times insulin-transferrin-selenium-A supplement (Invitrogen), and antibiotics (100 U/ml penicillin and 100 μ g/ml streptomycin; Invitrogen), as previously described.⁵² HEK293, COS7, and CHO cells were cultured at 37°C/5% CO₂ in Dulbecco's modified Eagle's medium containing the same supplements, except ITS-A. Cells were transiently transfected with Lipofectamine 2000 (Invitrogen) according to the manufacturer's recommendations. For generation of stable GFP-Plekhh2-expressing HEK293 cell clones, cells were selected and maintained in medium containing 500 μ g/ml of G418. Stable transfectants were characterized by immunofluorescence and western blotting for GFP-Plekhh2 expression.

Immunofluorescence

For immunofluorescence, cells were grown on fibronectin-coated glass coverslips. For coating, coverslips were incubated with 10 μ g/ml of fibronectin (Invitrogen, 33010-018) for 2 h at room temperature, followed by several washes with phosphate-buffered saline (PBS). Cells were fixed with 4% paraformaldehyde solution for 20 min at room temperature, after which they were permeabilized by incubation with 0.1% Triton X-100/PBS for 5 min, followed by an incubation with 2% bovine serum albumin/PBS (blocking solution) for 1 h. In some experiments, cells were treated with 0.5% saponin/PBS for 20 min before fixation. After blocking, cells were incubated with primary antibodies for 1 h at room temperature, washed several times with PBS, and then incubated for 1 h with a suitable secondary antibody. All antibodies were diluted in the blocking solution. Secondary antibody solutions also contained rhodamine-phalloidin and 4,6-diamidino-2-phenylindole to stain F-actin and cell nuclei, respectively. For double labeling, incubations

Q9

Q10

Q11

Q12

were performed sequentially to prevent cross-reactions. Photos were taken using Zeiss LSM510 confocal microscope, with $\times 20$, $\times 40$, or $\times 63$ objectives.

Drug treatments

Transiently transfected human podocytes were plated on fibronectin-coated coverslips in 24-well plates, and left to adhere and spread for 16 h. Thereafter, cells were incubated for 1 h at 37°C with 100 nmol/l of wortmannin (Sigma, W1628) or 50 μ mol/l LY294002 (Cell signaling, 9901), inhibitors of phosphatidylinositol 3-kinase, or 10 μ g/ml of the actin monomer-sequestering drug latrunculin A (Sigma, L5163), all diluted from stock solutions prepared in dimethylsulfoxide. Control cells were incubated with the vehicle only. After the incubation, cells were fixed and stained for Myc-tagged Plekhh2 and F-actin as described above.

Western blotting, coimmunoprecipitations, and subcellular fractionations

Western blotting was carried out following standard procedures. For coimmunoprecipitations, confluent transiently transfected HEK293 cells were washed twice in cold PBS and lysed in 0.5% Triton X-100, 20 mmol/l Tris-HCl (pH 7.4), and 150 mmol/l NaCl buffer containing protease inhibitor cocktail (Roche Diagnostics, Mannheim, Germany) and phosphatase inhibitors (1 mmol/l NaVO₃, 50 mmol/l NaF). Lysates were clarified by centrifugation (14,000 g), incubated with primary antibodies overnight, followed by incubation with protein A + G agarose beads (Roche Diagnostics) for 1 h at 4°C. Thereafter, the beads were washed three times with the lysis buffer, resuspended in 1 \times SDS-sample loading buffer, and boiled for 10 min. Eluted proteins were analyzed by sodium dodecyl sulfate-polyacrylamide gel electrophoresis and western blotting. For subcellular fractionation, cell lysates were fractionated with the Qproteome Cell Compartment Kit (Qiagen, Valencia, CA) before sodium dodecyl sulfate-polyacrylamide gel electrophoresis and western blotting.

Fluorescent resonance energy transfer in fixed cells

A detailed description of the FRET technique can be found elsewhere.⁵³ We utilized this method to confirm dimerization of the Plekhh2 protein using human podocytes cotransfected with GFP- and Myc-tagged versions of Plekhh2. The Förster constant, R₀, for the donor-acceptor pair used in this study, Alexa488 and Alexa568, is 62 Å. To determine FRET, we quantified the quenching of donor fluorescence by performing acceptor photobleaching. FRET measurements were recorded using a Zeiss LSM510 inverted confocal microscope, apochromat $\times 63/1.4$ numerical aperture oil immersion objective, and the Zeiss LSM510 software version 2.8. Briefly, fluorophores were excited with 488- and 543-nm lasers and images collected separately. The acceptor, Alexa568, was then irreversibly photobleached in a selected adequate region by continuous excitation with a 543-nm laser for about 30 s. Thereafter, residual Alexa568 and Alexa488 images were obtained under the same settings as prebleach images, and identical regions on individual cells were outlined in the photobleached area and processed using ImageJ. Ratios between Alexa488 intensities of the selected region, after and before photobleaching, were calculated to quantify FRET. In a typical experiment, 15–20 cells were measured for each sample. As a positive control for FRET, we examined GFP-Plekhh2-expressing cells immunostained for the GFP using Alexa568-labeled immunoglobulin-G as a secondary antibody.

Yeast two-hybrid screening

For yeast two-hybrid screening, we used a mouse kidney glomerulus cDNA library custom-generated by Clontech Laboratories. The library was screened with baits encoding the Gal4 DNA-binding domain fused to full-length Plekhh2 or its deletion variants. Screening was carried out by yeast mating according to the manufacturer's instructions. Diploids were selected through several rounds of culture on minimal synthetic dropout medium. Plasmids from obtained colonies were isolated, sequenced, and analyzed with the BLAST algorithm at the National Center for Biotechnology Information. Additional confirmation of interactions was obtained by performing mating of the yeast Y187 and AH109 strains carrying, respectively, a bait and a prey.

Immunoelectron microscopy

Samples from human renal cortexes were fixed in 3% paraformaldehyde in 0.1 mol/l phosphate buffer. After fixation, samples were cut into smaller pieces and dehydrated by stepwise increased concentration of methanol, and in each step gradually lowering the temperature down to -40°C in a Leica EMAFS (Leica Microsystem, Wien, Austria) and embedded and polymerized in Lowicryl K11M (Polysciences, Warrington, PA) at -40°C . Ultrathin sections were cut at room temperature and placed on carbon formvar-coated nickel grids. IEM was performed as described elsewhere,⁵⁴ with Plekhh2 and Hic-5 labeled with 10- and 5-nm gold particles, respectively. For semiquantification by iEM, six locations per glomerulus (1–2 glomeruli, depending on material) were systematically chosen with a random start at low magnification along the glomerular capillaries. Three images were taken from each location, including areas with or without FPE (no sclerotic areas), giving a minimum of 18 images/specimen for semiquantification. Prints at a final magnification of $\times 52,000$ were examined and the number of gold markers (Au) was counted. The area of the corresponding compartment was calculated by point counting, using a 1 \times 1 cm square lattice, and expressed as μm^2 . The concentration of Plekhh2 was expressed as the number of gold particles per square micrometer ($\text{Au}/\mu\text{m}^2$). The GBM length and the number of slits were expressed as a ratio slits/ μm to evaluate FPE (<1 slit/ μm GBM defined as FPE). Statistical analysis: in comparisons between groups, a one-way analysis of variance was used followed by Dunnett's test comparing the diseased group means with the control group mean. The Spearman rank-order correlation coefficient was used to measure the association between variables within each group. $P < 0.05$ was considered statistically significant.

In vitro actin polymerization and depolymerization assays

In vitro actin polymerization and depolymerization assays using the Actin Polymerization Kit (Biochem, Denver, CO; BK003) were used to study the role of Plekhh2 in the actin assembly processes. The assay relies on the difference between fluorescent signals of pyrene-labeled monomeric G-actin and polymerized pyrene/F-actin (used as positive controls in our experiments). For these assays, we used lysates prepared from 293 cells stably expressing GFP-Plekhh2, and control cells. Cells were plated onto plates coated with 10 μ g/ml of fibronectin, and allowed to adhere overnight in a serum-free media, followed by an overnight treatment with medium containing 10% fetal calf serum or 30 μ g/ml of PDGF-BB (Invitrogen, PHG0044). After this, cells were collected and lysed for 3 h at 4°C in a buffer containing 20 mmol/l Tris-HCl, pH 7.5, 20 mmol/l NaCl, and protease inhibitors. Lysates were clarified by centrifugation at 14,000 r.p.m. for 10 min. The actin polymerization and

depolymerization assays were performed according to the manufacturer's instructions, and fluorescence kinetic measurements were recorded with TECAN GENiosPro.

Live-cell imaging

Imaging of GFP-Plekhh2-expressing human podocytes plated on fibronectin-coated glass coverslips was started immediately after cell plating. Imaging was continued overnight, with images being taken every 5 min (Zeiss LSM 510 microscope, $\times 40$ objective). They were then processed into a movie with the ImageJ program.

Gene expression profiling with Affymetrix

Two mouse glomerular disease models were included in this analysis: lipopolysaccharide-induced nephrosis⁴⁴ and Type II diabetes (db/db) (Norlin J, He L, Tryggvason K, Betsholtz C, manuscript in preparation). The mouse glomerular RNA was isolated and hybridized on Affymetrix arrays, respectively, and the array data were processed as previously described.⁵⁵ These data were used for comparative analyses in this study.

DISCLOSURE

All the authors declared no competing interests.

ACKNOWLEDGMENTS

We thank Per Uhlen for advice on FRET experiments, Lwaki Ebarasi for discussions, Sergey Rodin for technical advice, and Ingrid Lindell/Eva Blomen/Anneli Hansson for skillful technical assistance. This work was supported in part by grants from the Knut and Alice Wallenberg Foundation (KT, CB), the Swedish Research Council (KT, CB), the Swedish Foundation for Strategic Research (KT, CB), the Novo Nordisk Foundations (KT, CB), regional agreement on medical training and clinical research (ALF) between Stockholm County Council and Karolinska Institute (AW), the Swedish Association of Kidney Patients (AW), Stig and Gunborg Westman's Foundation (AW), and Magnus Bergvall's Foundation (AW).

SUPPLEMENTARY MATERIAL

Figure S1. Heterologously expressed Plekhh2 localizes to lamellipodia in various cell lines.

Figure S2. Evidence that a fraction of Plekhh2 associates with cytoskeletal/ membrane cell fractions.

Figure S3. in connection to videos. Localization of GFP-Plekhh2 in living podocytes.

Figure S4. Characterization of a HEK293 cell-clone stably expressing GFP-Plekhh2.

Figure S5. PI3K inhibition leads to Plekhh2 relocalization into the cytoplasm.

Figure S6. Plekhh2 contains a α -helical coiled-coil domain in its N-terminus.

Figure S7. Further analysis of the interaction of Plekhh2 with Hic-5 and itself, and the whole blots for Figs. 5a and 6b.

Figure S8. Yeast-mating assays confirm the results of the yeast two-hybrid screen.

Figure S9. Additional evidence that transfection of Plekhh2 causes partial relocalization of endogenous Hic-5 from focal adhesions to lamellipodia.

Figure S10. Additional evidence that overexpression of Plekhh2 stabilizes cortical actin.

Table S1. Clinical data of controls and patients included in the study.

Video a. Localization of GFP-Plekhh2 in living podocytes.

Video b. Localization of Myc-Plekhh2 in fixed podocytes.

Video c. Localization of GFP-Plekhh2 during cell migration.

Video d. Localization of GFP-Plekhh2 during cell spreading.

Video e. Localization of GFP-Plekhh2 during cell migration.

Video f. Localization of GFP-Plekhh2 during cell spreading.

Supplementary material is linked to the online version of the paper at <http://www.nature.com/ki>

REFERENCES

1. Patrakka J, Tryggvason K. New insights into the role of podocytes in proteinuria. *Nat Rev Nephrol* 2009; **5**: 463–468.
2. Tryggvason K, Patrakka J, Wartiovaara J. Hereditary proteinuria syndromes and mechanisms of proteinuria. *N Engl J Med* 2006; **354**: 1387–1401.
3. Pavenstadt H, Kriz W, Kretzler M. Cell biology of the glomerular podocyte. *Physiol Rev* 2003; **83**: 253–307.
4. Takeda T. Podocyte cytoskeleton is connected to the integral membrane protein podocalyxin through Na⁺/H⁺-exchanger regulatory factor 2 and ezrin. *Clin Exp Nephrol* 2003; **7**: 260–269.
5. Oh J, Reiser J, Mundel P. Dynamic (re)organization of the podocyte actin cytoskeleton in the nephrotic syndrome. *Pediatr Nephrol* 2004; **19**: 130–137.
6. Attias O, Jiang R, Aoudjit L et al. Rac1 contributes to actin organization in glomerular podocytes. *Nephron Exp Nephrol* 2010; **114**: e93–e106.
7. Takemoto M, He L, Norlin J et al. Large-scale identification of genes implicated in kidney glomerulus development and function. *EMBO J* 2006; **25**: 1160–1174.
8. Patrakka J, Xiao Z, Nukui M et al. Expression and subcellular distribution of novel glomerulus-associated proteins dendrin, ehd3, sh2d4a, plekhh2, and 2310066E14Rik. *J Am Soc Nephrol* 2007; **18**: 689–697.
9. Lemmon MA. Membrane recognition by phospholipid-binding domains. *Nat Rev Mol Cell Biol* 2008; **9**: 99–111.
10. Fehon RG, McClatchey AJ, Bretscher A. Organizing the cell cortex: the role of ERM proteins. *Nat Rev Mol Cell Biol* 2010; **11**: 276–287.
11. McGuffin LJ, Bryson K, Jones DT. The PSIPRED protein structure prediction server. *Bioinformatics* 2000; **16**: 404–405.
12. Armstrong CT, Vincent TL, Green PJ et al. SCORER 2.0: an algorithm for distinguishing parallel dimeric and trimeric coiled-coil sequences. *Bioinformatics* 2011; **27**: 1908–1914.
13. Kitano K, Yusa F, Hakoshima T. Structure of dimerized radixin FERM domain suggests a novel masking motif in C-terminal residues 295–304. *Acta Crystallogr Sect F Struct Biol Cryst Commun* 2006; **62**: 340–345.
14. Huang X, Cheng HJ, Tessier-Lavigne M et al. MAX-1, a novel PH/MyTH4/FERM domain cytoplasmic protein implicated in netrin-mediated axon repulsion. *Neuron* 2002; **34**: 563–576.
15. Zhong H, Wu X, Huang H et al. Vertebrate MAX-1 is required for vascular patterning in zebrafish. *Proc Natl Acad Sci USA* 2006; **103**: 16800–16805.
16. Sousa AD, Cheney RE. Myosin-X: a molecular motor at the cell's fingertips. *Trends Cell Biol* 2005; **15**: 533–539.
17. Plantard L, Arjonen A, Lock JG et al. PtdIns(3,4,5)P is a regulator of myosin-X localization and filopodia formation. *J Cell Sci* 2010; **123**: 3525–3534.
18. Umeki N, Jung HS, Sakai T et al. Phospholipid-dependent regulation of the motor activity of myosin X. *Nat Struct Mol Biol* 2011; **18**: 783–788.
19. Zhang H, Berg JS, Li Z et al. Myosin-X provides a motor-based link between integrins and the cytoskeleton. *Nat Cell Biol* 2004; **6**: 523–531.
20. Lumb KJ, Carr CM, Kim PS. Subdomain folding of the coiled coil leucine zipper from the bZIP transcriptional activator GCN4. *Biochemistry* 1994; **33**: 7361–7367.
21. Su JY, Hodges RS, Kay CM. Effect of chain length on the formation and stability of synthetic alpha-helical coiled coils. *Biochemistry* 1994; **33**: 15501–15510.
22. Shewan A, Eastburn DJ, Mostov K. Phosphoinositides in cell architecture. *Cold Spring Harb Perspect Biol* 2011; **3**: a004796.
23. Watton SJ, Downward J. Akt/PKB localisation and 3' phosphoinositide generation at sites of epithelial cell-matrix and cell-cell interaction. *Curr Biol* 1999; **9**: 433–436.
24. Martin-Belmonte F, Gassama A, Datta A et al. PTEN-mediated apical segregation of phosphoinositides controls epithelial morphogenesis through Cdc42. *Cell* 2007; **128**: 383–397.
25. Coward RJ, Welsh GI, Yang J et al. The human glomerular podocyte is a novel target for insulin action. *Diabetes* 2005; **54**: 3095–3102.
26. Welsh GI, Hale LJ, Eremina V et al. Insulin signaling to the glomerular podocyte is critical for normal kidney function. *Cell Metab* 2010; **12**: 329–340.
27. Mani T, Hennigan RF, Foster LA et al. FERM domain phosphoinositide binding targets merlin to membrane and is essential for its growth suppressive function. *Mol Cell Biol* 2011; **31**: 1983–1996.
28. Auger KR, Serunian LA, Soltoff SP et al. PDGF-dependent tyrosine phosphorylation stimulates production of novel polyphosphoinositides in intact cells. *Cell* 1989; **57**: 167–175.

29. Hirano Y, Hatano T, Takahashi A *et al.* Structural basis of cargo recognition by the myosin-X MyTH4-FERM domain. *EMBO J* 2011; **30**: 2734–2747.
30. Brault E, Gautreau A, Lamarine M *et al.* Normal membrane localization and actin association of the NF2 tumor suppressor protein are dependent on folding of its N-terminal domain. *J Cell Sci* 2001; **114**: 1901–1912.
31. Xu HM, Gutmann DH. Merlin differentially associates with the microtubule and actin cytoskeleton. *J Neurosci Res* 1998; **51**: 403–415.
32. Moen RJ, Johnsrud DO, Thomas DD *et al.* Characterization of a myosin VII MyTH/FERM domain. *J Mol Biol* 2011; **413**: 17–23.
33. Yang Y, Baboolal TG, Siththanandan V *et al.* A FERM domain autoregulates *Drosophila* myosin 7a activity. *Proc Natl Acad Sci USA* 2009; **106**: 4189–4194.
34. Lee HS, Bellin RM, Walker DL *et al.* Characterization of an actin-binding site within the talin FERM domain. *J Mol Biol* 2004; **343**: 771–784.
35. Shibamura M, Mori K, Kim-Kaneyama JR *et al.* Involvement of FAK and PTP-PEST in the regulation of redox-sensitive nuclear-cytoplasmic shuttling of a LIM protein, Hic-5. *Antioxid Redox Signal* 2005; **7**: 335–347.
36. Avraamides C, Bromberg ME, Gaughan JP *et al.* Hic-5 promotes endothelial cell migration to lysophosphatidic acid. *Am J Physiol Heart Circ Physiol* 2007; **293**: H193–H203.
37. Nishiya N, Tachibana K, Shibamura M *et al.* Hic-5-reduced cell spreading on fibronectin: competitive effects between paxillin and Hic-5 through interaction with focal adhesion kinase. *Mol Cell Biol* 2001; **21**: 5332–5345.
38. Osada M, Ohmori T, Yatomi Y *et al.* Involvement of Hic-5 in platelet activation: integrin α IIb β 3-dependent tyrosine phosphorylation and association with proline-rich tyrosine kinase 2. *Biochem J* 2001; **355**: 691–697.
39. Drori S, Giron GD, Tou L *et al.* Hic-5 regulates an epithelial program mediated by PPAR γ . *Genes Dev* 2005; **19**: 362–375.
40. Shi X, Qu H, Kretzler M *et al.* Roles of PINCH-2 in regulation of glomerular cell shape change and fibronectin matrix deposition. *Am J Physiol Renal Physiol* 2008; **295**: F253–F263.
41. Jung KY, Chen K, Kretzler M *et al.* TGF- β 1 regulates the PINCH-1-integrin-linked kinase- α -parvin complex in glomerular cells. *J Am Soc Nephrol* 2007; **18**: 66–73.
42. Mori K, Asakawa M, Hayashi M *et al.* Oligomerizing potential of a focal adhesion LIM protein Hic-5 organizing a nuclear-cytoplasmic shuttling complex. *J Biol Chem* 2006; **281**: 22048–22061.
43. Yang Y, Guo L, Blattner SM *et al.* Formation and phosphorylation of the PINCH-1-integrin linked kinase- α -parvin complex are important for regulation of renal glomerular podocyte adhesion, architecture, and survival. *J Am Soc Nephrol* 2005; **16**: 1966–1976.
44. Sun Y, He L, Takemoto M *et al.* Glomerular transcriptome changes associated with lipopolysaccharide-induced proteinuria. *Am J Nephrol* 2009; **29**: 558–570.
45. Greene CN, Keong LM, Cordovado SK *et al.* Sequence variants in the PLEKH2 region are associated with diabetic nephropathy in the GoKinD study population. *Hum Genet* 2008; **124**: 255–262.
46. Michaud JL, Chaisson KM, Parks RJ *et al.* FSGS-associated α -actinin-4 (K256E) impairs cytoskeletal dynamics in podocytes. *Kidney Int* 2006; **70**: 1054–1061.
47. Kim JM, Wu H, Green G *et al.* CD2-associated protein haploinsufficiency is linked to glomerular disease susceptibility. *Science* 2003; **300**: 1298–1300.
48. Mukerji N, Damodaran TV, Winn MP. TRPC6 and FSGS: the latest TRP channelopathy. *Biochim Biophys Acta* 2007; **1772**: 859–868.
49. Moller CC, Wei C, Altintas MM *et al.* Induction of TRPC6 channel in acquired forms of proteinuric kidney disease. *J Am Soc Nephrol* 2007; **18**: 29–36.
50. Wu L, Pan L, Wei Z *et al.* Structure of MyTH4-FERM domains in myosin VIIa tail bound to cargo. *Science* 2011; **331**: 757–760.
51. Wei Z, Yan J, Lu Q *et al.* Cargo recognition mechanism of myosin X revealed by the structure of its tail MyTH4-FERM tandem in complex with the DCC P3 domain. *Proc Natl Acad Sci USA* 2011; **108**: 3572–3577.
52. Saleem MA, O'Hare MJ, Reiser J *et al.* A conditionally immortalized human podocyte cell line demonstrating nephrin and podocin expression. *J Am Soc Nephrol* 2002; **13**: 630–638.
53. Sekar RB, Periasamy A. Fluorescence resonance energy transfer (FRET) microscopy imaging of live cell protein localizations. *J Cell Biol* 2003; **160**: 629–633.
54. Duner F, Patrakka J, Xiao Z *et al.* Dendrin expression in glomerulogenesis and in human minimal change nephrotic syndrome. *Nephrol Dial Transplant* 2008; **23**: 2504–2511.
55. He L, Sun Y, Takemoto M *et al.* The glomerular transcriptome and a predicted protein-protein interaction network. *J Am Soc Nephrol* 2008; **19**: 260–268.

Schip1 is a Nherf2 and ezrin interacting podocyte foot process protein involved in regulation of actin dynamics in response to PDGF stimulation

Running title: Schip1 is a novel podocyte protein

Ljubica Perisic¹, Kjell Hultenby², Ying Sun³, Mark Lal¹, Christer Betsholtz³, Mathias Uhlén⁴, Annika Wernerson⁵, Timo Pikkarainen¹, Karl Tryggvason¹, Jaakko Patrakka¹

¹Division of Matrix Biology, Department of Medical Biochemistry and Biophysics, Karolinska Institutet, Stockholm, Sweden

²Clinical Research Center, Department of Laboratory Medicine, Karolinska Institutet, Stockholm, Sweden

³Vascular Biology Division, Department of Medical Biochemistry and Biophysics, Karolinska Institutet, Stockholm, Sweden

⁴Department of Biotechnology, Royal Institute of Technology, Stockholm, Sweden

⁵Division of Renal Medicine, Department of Clinical Science, Intervention and Technology, Stockholm, Sweden

Address for correspondence:

Karl Tryggvason, MD, PhD

Division of Matrix Biology, Department of Medical Biochemistry and Biophysics

Karolinska Institutet, Scheeles väg 2, 171 77 Stockholm, Sweden

E-mail: karl.tryggvason@ki.se

This work was supported by grants from the Knut and Alice Wallenberg Foundation, the Swedish Research Council and the Swedish Foundation for Strategic Research

Abstract

Schip1 is a 465-amino acid protein previously discovered as an interaction partner of schwannomin (merlin) in the mouse brain, where it was localized to neuronal axons. Here we show that Schip1 is a highly expressed glomerular protein found in the podocyte foot processes. In cultured cells, Schip1 localizes to cortical actin-rich regions of lamellipodia near the plasma membrane. Actin disassembly by latrunculin A treatment in Schip1-overexpressing podocytes left the protein associated with remnant F-actin-containing structures, suggesting a connection of Schip1 with the actin cytoskeleton. Interestingly, stimulation of these cells with PDGF-BB (a growth factor shown to induce Schip1 expression), led to marked changes in the actin cytoskeleton, with accumulation of cortical F-actin and dissolution of stress fibers. Schip1 overexpression was also found to promote cell migration in response to PDGF-BB stimulation. Yeast two-hybrid screening revealed that Schip1 interacts with itself and Nherf2, a scaffolding protein whose interaction partners include the PDGFr and ezrin, a well-known plasma membrane-cytoskeleton linker protein. The interactions were confirmed by coimmunoprecipitation. Schip1 and Nherf2 were also found to colocalize both in cultured human podocytes and *in situ*. Similar studies confirmed the interaction of Schip1 with ezrin. Of significant interest, we found that Schip1 and its associated proteins show simultaneous parallel expression changes in several experimental mouse models of glomerular damage. Our results suggest that Schip1 is a scaffolding protein that plays a role in controlling dynamics of actin assembly and chemokinesis in response to PDGF signaling.

Keywords: actin cytoskeleton, ezrin, Nherf2, podocytes, lamellipodia, Schip1

INTRODUCTION

The kidney glomerulus is a knot of specialized capillaries with a fairly high-pressure flow, endowing the ability to filter huge amounts of water and small solutes into the urinary space, while retaining albumin and large proteins (1). The glomerular filtration barrier (GFB) is composed of fenestrated endothelial cells that line the capillary loops, a basement membrane with a unique composition (GBM) and podocytes that sit on the outside of the GBM. The study of these cells has revealed many novel facets of glomerular disease (2). The cytoarchitecture of podocytes is defined by three principal compartments: the cell body, the major processes, and the interdigitating foot processes. In order to withstand high pressure in the capillaries, the podocyte must possess a dynamic contractile apparatus, and to maintain intact and exact filtration properties, the arrangement of the cytoskeleton needs to be precisely and temporally controlled (2). Actin filaments are the predominant cytoskeletal components of podocyte foot processes and this actin network contains a unique assembly of linker and adaptor molecules (3), many of them being specific for glomerular podocytes. Besides acting as a scaffold for submembrane protein complexes, the cortical actin cytoskeleton provides a tensile architectural support for podocyte cellular extensions.

Over 300 kidney glomerulus-enriched transcripts were identified by our group through large-scale sequencing and microarray profiling of the glomerular transcriptome (4). One of these transcripts encoded Schip1, a relatively uncharacterized protein discovered originally through its interaction with neurofibromatosis type 2 protein (Nf2, schwannomin, merlin) in the mouse brain (5). The tumor suppressor protein merlin belongs to a family of ERM proteins (Ezrin, Radixin, Moesin) that function as regulated linkers between the cell membrane and

the cortical actin cytoskeleton (6). Besides Schip1, over 30 other merlin-interacting proteins, including ezrin, paxillin, actin, N-WASP, tubulin, Nherf, and RhoGDI (7), have been discovered, and many of them are expressed in the kidney glomerulus.

Ezrin, Nherf and merlin proteins have been functionally associated to cortical cell actin and extensively studied not merely as linkers, but also as active modulators of the actin cytoskeleton and membrane receptors in the subcortical zones of cell extensions. Several studies have also addressed the role of these proteins in glomerular podocytes (3, 8). A key feature of membrane–cytoskeleton interactions is their ability to be regulated in a highly dynamic fashion. Merlin and ERM proteins play essential roles in many fundamental processes such as determination of cell shape and surface structures, cell-matrix and cell-cell adhesion, cell spreading and motility (9), all mediated through regulation of actin assembly (10). The disorganised cortical actin cytoskeleton observed in *Merlin*^{−/−} cells reflects the ability of merlin to inhibit the cytoskeleton dynamics (11), both *via* Arp2/3 (through interaction with N-WASP) (10) and Rac-induced actin assembly (12). Studies on *Ezrin*^{−/−} mice suggest that remodeling of the actin cytoskeleton is impaired in epithelial cells and this is one of the potential pathways leading to podocyte dysfunction and proteinuria (13). As for Nherf2, it is a multifunctional adaptor protein shown to bind both merlin and activated ERMs (6).

In the brain, Schip1 is found as a product of a fusion gene named IQCJ-SCHIP1. This is the longest isoform of a complex transcriptional unit that bridges two separate genes encoding two distinct proteins, IQCJ, a novel IQ motif containing protein, and Schip1 (14). It has been shown that the fusion protein localizes to mature nodes of Ranvier and axon initial segments, where it possibly contributes to stabilization of multimolecular complexes associated with Nav channels in the axonal membrane

(15). Morphologically, the cytoplasmic extensions of neurons are similar to glomerular podocyte foot processes (16).

Schip1 knockout mice generated by Schmall et al. exhibit skeletal and craniofacial defects and digestive problems, but no overt kidney phenotype. However, the loss of one PDGFr β allele is enough for the Schip1^{-/-}PDGFr β ^{+/-} mice to show decreased kidney function manifested as swollen and degraded glomeruli and an increase in blood urea nitrogen levels. It was suggested that Schip1 is one of the early response genes controlling specific processes downstream of PDGF signaling (17, 18).

In this study we characterized the role of Schip1 in the kidney glomerulus by analyzing its expression profile in detail, investigating its localization in the kidney and in cultured cells, discovering its interaction protein network and by testing the influence of Schip1 on cells during actin disassembly, PDGF stimulation and migration. Our results suggest that Schip1 is a dimeric/oligomeric Nherf2- and ezrin-interacting podocyte foot process protein that plays a role in controlling dynamics of filamentous actin and cell motility in response to PDGF signaling. Moreover, examination of Schip1 and its interaction partners in several mouse glomerular disease models indicated parallel changes in their expression levels, thereby suggesting that altered expression of the proteins may be involved in the pathogenesis of the diseases.

MATERIALS AND METHODS

Expression constructs

Expression constructs were generated by cloning of PCR-amplified fragments into various expression vectors using established molecular biological methods. Inserts were amplified from kidney cDNA (Mouse MTC™ Panel I, Clontech, Palo Alto, CA) with Long PCR Enzyme Mix (Fermentas International Inc, Burlington, Canada), and sequenced to confirm absence of PCR-generated mutations. The PCR program used was: 1 cycle of 95°C/4 min, 30 cycles of 95°C/1 min, 51°C/1 min, 72°C/2-4 min, and 1 cycle of 72°C/10 min. For yeast two-hybrid screening, inserts were cloned into the vector pGBKT7 (Clontech) in frame with the Gal4 DNA-binding domain. For expression in mammalian cells, cDNAs were cloned into pcDNA3.1 (Invitrogen, Carlsbad, CA), or vectors with various N-terminal tags (pCMV-Myc, pCMV-HA, or pEGFP-C; all from Clontech).

Antibodies

Following commercial antibodies were used: rabbit anti-Schip1 (Sigma Prestige Antibodies, St. Luis, MO), mouse polyclonal anti-Schip1 (Abcam Cambridge, UK), rabbit anti-SLC9A3R2 (Nherf2) (Sigma Prestige Antibodies), rabbit polyclonal anti-ezrin (Abcam), mouse monoclonal anti-ezrin (Zymed, San Francisco, CA), monoclonal mouse anti Myc-tag (Sigma), rabbit anti-Myc-tag (Sigma), rabbit polyclonal anti-HA (Sigma), mouse anti-synaptopodin (Progen, Germany), anti-GFP (Invitrogen), anti-calnexin (Abcam), anti- β -actin (Abcam), anti-podocin (Sigma). Proteins were visualized with secondary antibodies conjugated to various Alexa Fluor dyes (488, 546, 568; all from Invitrogen) or HRP (GE Healthcare, Piscataway, NJ, US). Phalloidin and DAPI reagents were purchased from Molecular Probes.

Reverse transcription (RT) and RT-PCR

For generating glomerular and “rest-of-kidney” cDNA, mouse glomeruli and kidney tissue devoid of glomeruli (rest of kidney) were isolated as previously described (4). Fluorescently labeled podocytes were derived by FACS sorting of cells from glomeruli obtained from bitransgenic R26-stop-EYFP mice harboring the Cre transgene driven by the podocin promoter. Total RNA was then isolated by RNeasy mini Kit (Qiagen, Valencia, CA) and 1 µg was reverse transcribed by Superscript III Reverse Transcriptase (Invitrogen). The generated cDNA was diluted 10-fold with Tris-EDTA buffer for storage at -20°C.

For studies on tissue distribution, multiple mouse tissue cDNAs were used as templates for RT-PCR (Mouse MTC™ Panel I, Clontech). The PCR reactions were done by HotStartTaq polymerase (Qiagen) with gene-specific primers to amplify around 500 bp products. The PCR products were analyzed in 1% TBE agarose gel and photographed.

Northern blot

To study tissue distribution at the RNA level, a specific 500 bp PCR product obtained from amplification of glomerular cDNA was used as the probe. The probe was ³²P-dCTP labeled with Prime-It® RmT Random Primer Labeling Kit (Stratagene, La Jolla, CA) and hybridized with Mouse MTN® Blot (Clontech). Hybridizations were also performed on blots containing mRNA isolated from two kidney fractions, either only glomerular tufts or the kidney excluding glomeruli. The blots were exposed to a PhosphorImager SF screen (Molecular Dynamics) and analyzed with ImageQuant software (Molecular Dynamics).

***In situ* hybridization**

In situ hybridizations were performed on paraffin embedded mouse kidney tissue sections (10 μ m). The probes were synthesized by amplifying a 500 bp cDNA fragment corresponding to the 3'UTR-end of the mouse Schip1 gene from a kidney cDNA library, and subcloning this product into the pCR II-TOPO Dual Promoter Vector (Invitrogen). Antisense and sense probes were prepared using T7 and SP6 polymerases.

Transient and stable transfections

Human podocytes were grown at 33°C/5% CO₂ in RPMI supplemented with 10% fetal bovine serum (Invitrogen), 1x insulin-transferrin-selenium-A supplement (Invitrogen), and antibiotics (100 U/ml penicillin and 100 μ g/ml streptomycin) (Invitrogen), as previously described (19). HEK293, COS7 and CHO cells were cultured at 37°C/5% CO₂ in DMEM containing the same supplements, except ITS-A. Cells were transiently transfected with Lipofectamine 2000 (Invitrogen) according to the manufacturer's recommendations. For generation of stable GFP-Schip1-expressing HEK293-cell clones, cells were selected and maintained in medium containing 500 μ g/ml of G418. Stable transfectants were characterized by immunofluorescence (not shown) and Western blotting for GFP-Schip1 expression (Fig. S2).

Immunofluorescence

For human and mouse kidney analysis, samples were collected, snap-frozen, and then cryosectioned at 8-10 μ m thickness. Sections were postfixated with cold acetone (-20°C) or room temperature with 4% paraformaldehyde, followed by blocking in 5%

normal goat serum. For immunofluorescence, cells were grown on fibronectin-coated glass coverslips. For coating, coverslips were incubated with 10 $\mu\text{g/ml}$ of fibronectin (Invitrogen) for 2 h at room temperature, followed by several washes with PBS. Cells were fixed with 4% PFA solution for 20 min at room temperature, after which they were permeabilized by incubation with 0.1% Triton X-100/PBS for 5 min, followed by an incubation with 2% BSA/PBS (blocking solution) for 1 h. In some experiments, cells were treated with 0.5% saponin/PBS for 20 min before fixation. After blocking, cells were incubated with primary antibodies for 1 h at RT, washed several times with PBS, and then incubated for 1 h with a suitable secondary antibody. All antibodies were diluted in the blocking solution. Secondary antibody solutions also contained rhodamine-phalloidin and DAPI to stain F-actin and cell nuclei, respectively. For double labeling, incubations were performed sequentially to prevent crossreactions. Photos were taken using Zeiss LSM510 confocal microscope, with 20x, 40x or 63x objectives.

Drug treatments

Transiently transfected human podocytes, HEK293 or NIH3T3 cells were plated on fibronectin-coated coverslips in 24-well plates, and left to adhere and spread for 16 h. Thereafter, cells were incubated for 1 h at 37°C with 10 $\mu\text{g/ml}$ of the actin monomer-sequestering drug latrunculin A (Sigma) diluted from a stock solution prepared in DMSO. Control cells were incubated with the vehicle only. Alternatively, cells were treated with media containing 50 $\mu\text{g/ml}$ PDGF-BB for 2 h at 37°C. After the incubation, cells were fixed, and stained for Myc-tagged Schip1 and F-actin as described above.

Yeast two-hybrid screening

For yeast two-hybrid screening, we used a mouse kidney glomerulus cDNA library custom-generated by Clontech. The library was screened with baits encoding the Gal4 DNA-binding domain fused to full-length Schip1 or its deletion variant, composed only of its most C-terminal coiled-coil domain. Screening was carried out by yeast mating according to the manufacturer's instructions. Diploids were selected through several rounds of culture on minimal synthetic dropout medium. Plasmids from obtained colonies were isolated, sequenced, and analyzed with the BLAST algorithm at the National Center for Biotechnology Information (NCBI).

Western blotting and coimmunoprecipitations

Western blotting was carried out following standard procedures. For coimmunoprecipitations, confluent transiently transfected HEK293 cells were washed twice in cold PBS and lysed in 0.5% Triton X-100, 20 mM Tris-HCl (pH 7.4) and 150 mM NaCl buffer containing protease inhibitor cocktail (Roche Diagnostics, Mannheim, Germany) and phosphatase inhibitors (1mM NaVO₃, 50 mM NaF). Lysates were clarified by centrifugation (14,000 *g*), incubated with primary antibodies overnight, followed by an incubation with protein A+G agarose beads (Roche) for 1 h at 4°C. Thereafter the beads were washed 3 times with the lysis buffer, resuspended in 1x SDS-sample loading buffer, and boiled for 10 min. Eluted proteins were analyzed by SDS-PAGE and Western blotting.

Fluorescent Resonance Energy Transfer (FRET) in fixed cells

A detailed description of the FRET technique can be found elsewhere (20). We utilized this method to confirm interaction of the Schip1 protein using human

podocytes cotransfected with GFP-Nherf2, pcDNA3.1-ezrin and Myc-tagged Schip1. The Förster constant, R_0 , for the donor-acceptor pair used in this study, Alexa488 and Alexa568, is 62Å. To determine FRET, we quantified the quenching of donor fluorescence by performing acceptor photobleaching. FRET measurements were performed using a Zeiss LSM510 inverted confocal microscope, apochromat ×63/1.4 NA oil immersion objective and the Zeiss LSM510 software version 2.8. Briefly, fluorophores were excited with 488 and 543 nm laser and images collected separately. The acceptor, Alexa568, was then irreversibly photobleached in a selected adequate region by continuous excitation with a 543 nm laser for about 30 s. Thereafter, residual Alexa568 and Alexa488 image was obtained under same settings as prebleach images, and identical regions on individual cells were outlined in the photobleached area and processed using ImageJ. Ratios between Alexa488 intensities of the selected region, after and before photobleaching, were calculated to quantify FRET. In a typical experiment, 15–20 cells were measured for each sample. As a positive control for FRET, we examined GFP-Schip1-expressing cells immunostained for the GFP using Alexa 568-labeled IgG as a secondary antibody.

Immunoelectron microscopy (IEM)

Samples from human renal cortexes were fixed in 3 % PFA in 0.1M phosphate buffer. After fixation, samples were cut in smaller pieces and dehydrated by stepwise increased concentration of methanol and in each step gradually lowering the temperature down to -40°C in a Leica EMAFS (Leica microsystem, Wien, Austria) and embedded and polymerized in Lowicryl K11M (Polysciences, Warrington, United States) at -40°C. Ultrathin sections were cut at room temperature and placed

on carbon formvar-coated nickel grids. IEM was performed with Schip1 and ezrin/Nherf2 antibodies, labeled with 10 and 5 nm gold particles, respectively.

Cell migration assay

Cell migration ability was assessed in a wound healing scratch assay. Stably expressing GFP-Schip1 HEK293 cells were plated on 24-well culture dishes precoated with 10 μ g/ml of fibronectin. Cells were grown to confluency and serum starved in 0.5% FCS overnight. Thereafter, the monolayers were wounded by manual scratching with a 200- μ l pipette tip, washed with PBS and incubated at 37°C in complete media with or without 50 μ g/ml of PDGF-BB. At the indicated times, phase contrast images at specific wound sites were captured by Leica microscope and images were analyzed by ImageJ program. Results are reported in percent, and show the size of the wound compared to the 0-point (right after scratching). They are representative of three experiments.

Gene expression profiling with Affymetrix

Three mouse glomerular disease models were included in these analyses: adriamycin-induced mice nephrotic syndrome model (Nukui M, He L, Patrakka J, Takemoto M, Betsholtz C, Tegner J, Tryggvason K, manuscript in preparation), LPS-induced mice nephrotic syndrome model (21) and Type II diabetic (db/db) mice model (Norlin J, He L, Tryggvason K, Betsholtz C, manuscript in preparation). The mouse glomerular RNA isolation, Affymetrix array hybridization, and data processing were done as described before (4, 22). These data were used for comparative analyses in this study.

RESULTS

Schip1 localizes to the podocyte foot processes

By use of RT-PCR and Northern blotting on a panel of mouse tissues, we observed a wide expression pattern for Schip1 that starts at early embryonic stages (Fig 1a, b, d). It was prominently expressed in brain, kidney, heart and testes tissues. In the kidney glomerulus, Schip1 was mostly expressed by glomerular podocytes, although some weak expression was also seen in the rest-of-glomerulus (ROG) and rest-of-kidney (ROK) fractions (Fig 1c, e, f). This podocyte expression was confirmed by radioactive *in situ* hybridization (Fig 1g). To further localize the Schip1 protein in the kidney, we double immunostained adult mouse and human kidney tissues with anti-Schip1 and anti-synaptopodin antibodies (Fig 1h). Our immunofluorescence stainings localized Schip1 to the glomerulus, where its signal partially overlapped with that of synaptopodin, a protein present in the podocyte foot processes. Electron microscopic analysis of human kidney samples revealed that 67% of labelling for Schip1 was found in podocyte foot processes *in situ*, where it localized towards the membrane laterally, apically but also basally (Fig 1i). A small portion of Schip1 was localized to the endothelial cells of the glomerulus (14%).

Schip1 associates with the cortical actin cytoskeleton and controls actin dynamics and chemokinesis in response to PDGF signaling

We then looked at the subcellular localization of Schip1 in cultured human podocytes. Both endogenous (low expression levels, Fig 2a upper panel, Fig S1a upper panel) and ectopically expressed Myc-tagged Schip1 (Fig 2a, lower panel, fig S1a, lower panel) was observed at the lamellipodial extensions, towards the cellular periphery. Peripheral lamellipodia staining of Schip1 was similarly seen in other cell

types expressing the protein (not shown). To confirm that the lamellipodial localization is correct, we detergent-treated Schip1-expressing cells with 0.5% saponin prior to fixation and immunostaining. This permeabilization strategy results in the removal of the soluble pool of proteins while sparing those that are more stably anchored. Under these conditions, we found that Schip1 staining was partially retained, supporting the association with detergent-insoluble cytoskeletal/membrane structures (Fig. S2a).

Examination of peripheral Schip1 by confocal microscopy indicated a significant overlap with the cortical actin cytoskeleton both in the XY- and Z-scan (Fig 2b). We raised the question that Schip1 may have a role in controlling the dynamics of the actin cytoskeleton at the cell cortex/lamellipodia. To determine the possibility of Schip1 association with the actin cytoskeleton, we treated the cells with latrunculin A, an actin monomer-sequestering drug that distorts actin cytoskeletal structures (Fig 2c, Fig S1b). However, latrunculin A-treatment resulted in a loss of parallel stress fibers as well as of cortical actin filaments in both control and Schip1- transfected cells, with appearance of phalloidin-positive patches and remnant actin fibers. Schip1 signal in transfected cells overlapped with phalloidin staining, supporting the idea that the protein associates with remnant actin fibers. Thus, Schip1 overexpression does not promote stabilization of cortical F-actin, although it seems that proper actin cytoskeleton structure is critically important for the localization of Schip1.

Since Schip1 has been highlighted as an early response gene in the PDGF β signaling cascade (18), it was of interest to test the effect of PDGF stimulation on Schip1-overexpressing cells. In control NIH3T3 cells, PDGF-BB stimulation caused formation of large lamellipodial structures, with retention of parallel actin stress fibers in the cell body (Fig 3a, upper panels). In contrast to this, a 2-h stimulation of Schip1-

transfected cells with PDGF-BB led to accumulation of cortical cell actin with a significant loss of parallel actin stress fibers in about 30% of cells (Fig 3a middle and lower panels, Fig S1c).

In order to investigate whether this PDGF stimulation had Schip1-dependent functional consequences, we performed migration assays with Schip1-overexpressing cells and their controls plated on fibronectin (Fig 3b, c). The cell populations exhibited similar migration rates in media containing 10% FCS. In contrast, when stimulated with PDGF-BB, GFP-Schip1-expressing cells migrated significantly faster than the controls. Therefore, we conclude that Schip1 promotes cell migration in response to PDGF signaling, probably through its effects on the actin cytoskeleton rearrangement.

Schip1 interacts with Nherf2 and ezrin, which together form a complex linking the actin cytoskeleton to the plasma membrane

To further investigate Schip1 function, we performed a yeast two-hybrid screen with a mouse glomerular cDNA library to identify its protein interaction network. In the screen using the Schip1 most C-terminal coiled-coil domain as a bait (amino-acids 398-459), we identified Nherf2 as a potential interacting partner of Schip1. Coimmunoprecipitation from transfected HEK293 cells confirmed the interaction between Schip1 and Nherf2 (Fig 4a, upper panel). As Nherf2 is known to form a complex with ezrin in podocytes, we tested whether Schip1 interacts also with this linker between the cortical actin cytoskeleton and the plasma membrane. As we suspected, Schip1 and ezrin coimmunoprecipitated from transfected cells (Fig 4a, lower panel).

To validate these results, we next examined the localization of these proteins in cultured podocytes. In these cells, all three proteins localized at the lamellipodia periphery (Fig. 4b), although colocalization of Schip1 with Nherf2 was only partial. Furthermore, we used FRET to study the interactions of Schip1 in fixed cotransfected human podocytes fully spread on fibronectin (Fig 4c). In this experiment, we co-expressed Schip1, ezrin and Nherf2 proteins tagged at their N-termini with either GFP or the Myc-tag, and measured the change in green donor fluorescence following bleaching of the red acceptor fluorophore. Significant FRET signal was detected between Schip1 and ezrin in the cellular lamellipodia. Furthermore, a measurable (although weak) signal restricted to areas of partial colocalization, was detected between Schip1 and Nherf2. These results again supported the idea that these proteins interact.

Next, we analyzed whether these proteins colocalize in the glomerulus. By immunofluorescence we observed a partial overlap of Schip1 with ezrin and Nherf2 signals in the glomerulus (Fig 5a). Immuno (Fig 5b) and coimmuno (Fig 5c) electron microscopic studies of Schip1 and ezrin/Nherf2 (labeled with 10 nm and 5 nm gold particles, respectively) indicated significant colocalization of Schip1 and ezrin within 10 nm of each other. Schip1 and Nherf2 colocalized about 30 nm from each other. Altogether, our results provide evidence for the interaction of Schip1 with Nherf2 and ezrin *in vivo*.

Schip1 and its associated proteins show parallel changes of expression in microarray profiles of mouse glomerular disease models

Based on our data and the finding that Schip1 knockout mice show susceptibility to decreased kidney function upon genetic challenge (17), we suspected that Schip1

expression might be affected in various mouse models of glomerular diseases. Thus, we analyzed the expression of Schip1 and its associated proteins in microarray profiles from the adriamycin- and LPS-induced mouse proteinuria models, as well as the db/db model for type II diabetic nephropathy (Fig 6). Interestingly, Schip1 and these proteins often show a similar trend in the regulation of their expression: downregulation in adriamycin and LPS models, and upregulation in type II diabetes model. These analyses suggest that Schip1, Nherf2 and ezrin are possibly involved in the initiation and/or progression of glomerular injury leading to proteinuria, even though the complex underlying mechanisms could be very different in various glomerular diseases.

Schip1 associates with itself

Yeast two-hybrid screen with the full-length Schip1 revealed that the protein potentially interacts with itself, in the form of homodi(oligo)mers. According to the secondary structure prediction, the C-terminal half of Schip1 contains multiple coiled-coil segments (Fig 7a), which are common motifs for oligomerization. Analysis with the SCORER 2.0 program (23), which distinguishes parallel dimeric and trimeric coiled-coils, predicts that the first and the third coiled-coil domains of Schip1 assemble into a trimer, whereas the second one folds into a dimer (Fig 7b). To provide experimental evidence for these predictions, we tested by coimmunoprecipitation whether Schip1 self-associates. To this end, HEK293 cells were co-transfected with full-length Schip1 tagged with either Myc or HA epitopes, followed by immunoprecipitation with anti-HA antibodies and Western blotting with those against the Myc-tag. As shown in Fig 7c, these two full-length versions of Schip1 interacted with each other. Furthermore, by immuno-EM on human kidney sections Schip1-

labelled gold particles can occasionally be seen very close to each other (as in the form of homooligomers) in the podocyte foot processes (Fig 7d), suggesting that Schip1 oligomerization is physiologically possible and important.

DISCUSSION

In our studies, Schip1 emerged as a protein highly expressed in glomerular podocyte foot processes. Schip1 colocalized with Nherf2 and ezrin, and interacted with both of these proteins. Nherf2 and ezrin are proteins bound to the highly conserved cytoplasmic tail of podocalyxin in podocytes, thereby linking this apical membrane protein to the actin cytoskeleton (3, 8). During glomerulogenesis, podocytes undergo extensive morphological changes necessary for the creation of the glomerular filter, including polarization, branching of interdigitating foot processes and formation of slit diaphragms. These structures require complex machinery for normal maintenance. It is known that podocalyxin plays one of the major roles in both development and maintenance of podocytes thanks to antiadhesive properties of its ectodomain (24). Recently, a protein called CLIC5A was proposed as a new component of podocalyxin-Nherf2-ezrin complex (25). From our work it seems that Schip1 could be another novel component of the same complex and may play an important role in the connection between podocalyxin and the actin cytoskeleton. Importantly, podocyte damage seen after protamine-sulfate, sialidase or PAN treatment in rats, and in CLIC5A knockout mice, is caused by the disruption of this complex (8, 25, 26). It is of interest to note that in the adriamycin- and LPS-induced proteinuria mouse models associated with transient podocyte foot process effacement (FPE), glomerular Schip1 expression is downregulated simultaneously with its interaction partners and other functionally associated proteins. Furthermore, a significant downregulation of Schip1 was seen in glomeruli from human patients with diabetic nephropathy (27), a disease also characterized by podocyte foot process effacement. Although the number of samples in this study was small, the results point

to the fact that expression of many genes controlling actin cytoskeleton formation and maintenance is disturbed. Taken together, our results suggest that Schip1 and proteins associated with it may participate in normal podocyte foot process cytoskeleton architecture and have a role in the development of foot process effacement and proteinuria.

In cultured cells, we demonstrated that Schip1 concentrates in cortical actin-rich zones of lamellipodia, where it also associates with the actin cytoskeleton. The formation of cortical actin-enriched lamellipodia, membrane ruffles and filopodia in cultured cells, downstream of RacGTPase activation, are cellular features characteristic of PDGF receptor stimulation (28). In fact, we observed that Schip1 overexpression promoted F-actin rearrangement in PDGF-treated cells, as well as stimulated cell migration in response to the growth factor. Similar results have previously been reported by Schmall et al. (17), as they showed that *Schip1*^{-/-} mice embryonic fibroblasts exhibit significantly decreased migration in response to PDGF β activation. Collectively, results from Schmall et al. and us suggest that Schip1 indeed acts in regulation of actin remodeling downstream of PDGF β signaling.

How is PDGF β signaling linked to Schip1? Through an unbiased yeast two-hybrid screening with a mouse glomerular library, we identified Nherf2 as an interaction partner of Schip1. Nherf2 has been shown to interact directly with the intracellular tail of PDGFr β (6), to potentiate receptor activity upon stimulation with PDGF (29) and to play a role in subsequent actin reorganization (6). Theisen et al. (30) have shown that Nherf also links N-cadherin/catenin complex localized in adherens-junctions, to PDGFr and actin cytoskeleton, which is important in regulation of cell motility. This is interesting as it has been shown that the expression of PDGF β receptors in podocytes is upregulated during the development of diabetic nephropathy (31). Thus,

we speculate that Schip1 can be involved in the pathogenesis of diabetic nephropathy through its interaction with Nherf2.

In conclusion, we propose that Schip1 is a novel multimeric, scaffolding and adaptor protein in kidney podocytes, where it may be involved in linking the actin cytoskeleton to the podocyte foot process plasma membrane, as part of the ezrin/Nherf2/merlin actin-modulating complex. Further studies are needed to dissect the exact mechanism of these interactions.

DISCLOSURE

Authors declare no conflict of interest.

ACKNOWLEDGMENTS

We thank Per Uhlen for advice on FRET experiments. This work was supported by grants from the Knut and Alice Wallenberg Foundation (KT, CB), the Swedish Research Council (KT, CB), the Swedish Foundation for Strategic Research (KT, CB).

FIGURE LEGENDS:

Figure 1: Schip1 is a novel protein expressed in glomerular podocytes

(a, b) RT-PCR from embryonic (E-embryonic day) and adult mouse tissue cDNA panels shows wide expression of Schip1 throughout the development and tissues. (c) In the kidney, Schip1 is expressed by both the glomerulus and the kidney fraction lacking glomeruli. In the glomerulus, the expression is mostly detected in FACS-sorted podocytes. As an internal control, expression levels of GAPDH were measured. ROG-rest of glomerulus, ROK-rest of kidney. (d) Northern blotting on a mouse tissue panel shows the presence of two Schip1 mRNA transcripts enriched in the brain, heart, testes and kidney tissues. (e) Northern blotting on glomerulus and rest-of-kidney tissue shows Schip1 expression in the glomerulus. (f) By Western blotting, the Schip1 protein is detected mostly in the glomerulus. Podocin was used as a positive control for the glomerular fraction, β -actin as a loading control. (g) Schip1 mRNA is localized to podocytes by radioactive ISH on mouse kidney sections. (h) Immunofluorescence on mouse and human kidney sections shows a glomerulus specific signal that partially overlaps with a podocyte foot process marker synaptopodin. (i) By immuno-EM, Schip1 localizes to the glomerular podocyte foot processes (FP).

Figure 2. Schip1 localizes to cell lamellipodia and associates with the cortical actin cytoskeleton

(a) Both endogenous (arrowheads, upper panel) and ectopic (arrowheads, lower panel) Schip1 localize to lamellipodia in cultured human podocytes. (b) Schip1 colocalizes with cortical filamentous actin in the podocyte lamellipodia. Both the Z-

and XY-scanning indicate considerable signal overlap between Schip1 and F-actin along the plasma membrane in cells presenting well-developed lamellipodia. **(c)** Treatment with latrunculin A, an actin-monomer sequestering drug, results in the dissolution of actin fibers in untransfected and Schip1-transfected podocytes. Schip1 remains associated with disturbed F-actin remnants.

Figure 3: Schip1 overexpression promotes cortical F-actin accumulation, dissolution of stress fibers and motility in PDGF-BB-stimulated cells

(a) Schip1 is localized to the periphery of lamellipodia in the NIH3T3 cells. In Schip1-transfected cells PDGF-BB causes marked actin cytoskeleton rearrangement with cortical actin accumulation and dissolution of the actin stress fibers (box, zoom). **(b)** GFP-Schip1-expressing and control HEK293 were stimulated with 10% FCS or PDGF-BB, scratched, and left to migrate for 24 h (the wound healing assay). GFP-Schip1 cells exhibit similar migration rate as the controls in medium supplemented with 10% FCS, but migrate significantly faster in the presence of PDGF-BB. **(c)** Microscopic images of control and Schip1-overexpressing cell monolayers 18 or 24 h after wound scratching.

Figure 4: Schip1 interacts and colocalizes with Nherf2 and ezrin

(a) Yeast two-hybrid screening with a bait composed of the most C-terminal coiled-coil domain (amino- acids 398-459) revealed that Schip1 interacts with Nherf2. Myc-tagged Schip1 and Flag-tagged Nherf2 coimmunoprecipitate from lysates of cotransfected HEK293 cells (upper panel). MycSchip1 also interacts with ezrin, a protein known to be in a complex with Nherf2, in cotransfected HEK293 (lower panel). **(b)** Schip1 colocalizes with ezrin and Nherf2 in cultured human podocytes to

cortical actin zones and lamellipodia. Schip1 and ezrin show very close overlap (arrowheads, boxed area, zoom), whereas Schip1 and Nherf2 colocalize partially (boxed area, zoom). **(c)** MycSchip1 signal intensity increases upon Alexa 568 bleaching (boxed area shown by arrows) as a result of FRET between the two fluorophores suggesting associations of Schip1 with ezrin and Nherf2 proteins. As a positive control, we used GFP-Schip1 stained with anti-GFP- and Alexa Fluor 568-conjugated secondary antibodies (upper panel). We detected about 40% FRET signal increase between Schip1 and Ezrin. Lower FRET signal increase of about 10% was detected between Schip1 and Nherf2 (n=20 ROIs tested in each experiment).

Figure 5: Schip1, ezrin and Nherf2 colocalize in the podocyte foot processes of the human kidney glomerulus

(a) Immunofluorescence on human kidney sections shows partial colocalization of Schip/ezrin and Schip/Nherf2 in the glomerulus. **(b)** By IEM, Schip1 is localized to the podocyte foot processes (FP), often to the apical, but also to the basolateral side. Similar localization is seen for ezrin and Nherf2 (arrowheads). **(c)** Double IEM for Schip1 (10 nm gold particle) and ezrin or Nherf2 (5 nm gold particle) indicates that the proteins colocalize at the same subcellular area in the foot processes, with the Schip1-ezrin distance being about 10 nm and that between Schip1 and Nherf2 about 30 nm (arrows).

Figure 6: Comparison of Schip1 and its associated proteins expression in microarray profiles from mouse glomerular disease models

Schip1 expression is significantly downregulated in adriamycin-induced mouse nephrosis and LPS-induced model of glomerular damage, whereas it is significantly

upregulated in type II diabetes model. Interestingly, Schip1-interacting partners and other functionally associated proteins exhibit a tendency to simultaneous and parallel changes of expression levels.

Figure 7: Predicted coiled-coil domains mediate Schip1 self-association

(a) Schematic domain structure prediction of Schip1 shows the presence of several putative coiled-coil domains (CC). Numbers indicate the location of the domains in the mouse Schip1 polypeptide. **(b)** Two different algorithms, MARCOIL and PSIPRED (not shown) predict with high confidence the presence of α -helical coiled-coil segments in the C-terminus of Schip1. Moreover, the SCORER 2.0 algorithm predicts that two of these segments assemble into a trimer and one into a dimer. **(c)** Yeast two-hybrid screening of a mouse glomerulus cDNA library with the full-length Schip1 bait indeed revealed that Schip1 can self-associate (data not shown). As a confirmation, full-length Schip1 tagged with either Myc or HA epitopes were coimmunoprecipitated from lysates of cotransfected HEK293 cells. **(d)** By immunoprecipitation (IP) on human kidney sections, Schip1-labelled gold particles are occasionally seen very close to each other (as in the form of homooligomers) in the podocyte foot processes (arrow, zoom box).

Figure S1: Additional evidence for Schip1 cell localization, actin association upon latrunculin A treatment and response to PDGF-BB stimulation

(a) Schip1 localizes to peripheral lamellipodia regions near the plasma membrane. This is shown both for the endogenously (arrowheads, upper panel) and exogenously (arrowheads, lower panel) expressed protein in human podocytes. **(b)** MycSchip1-transfected podocytes that have been treated with latrunculin A before cell fixation

and staining with anti-Myc antibodies and rhodamine-phalloidin show Schip1 association with disturbed F-actin fibers (arrowheads). **(c)** Two more fields of MycSchip1-transfected NIH3T3 cells, stimulated by PDGF-BB. Schip1 overexpression induced actin reorganization in response to PDGF-BB: cortical actin accumulation and transversal parallel fibers actin dissolution (pointed by arrowheads).

Figure S2: Peripheral Schip1 expression is partially resistant to detergent extraction before cell fixation and additional control Western blots

(a) In this experiment, transiently transfected human podocytes were treated with the standard procedure (fixation and Triton X-100 permeabilization, upper panel), or incubated with saponin prior to cell fixation and staining for MycSchip1 (lower panel). Peripheral Schip1 expression is partially retained after saponin treatment, indicating association of the protein with detergent-insoluble cytoskeletal/plasma membrane structures. **(b)** WB showing expression levels of endogenous Schip1, ezrin and Nherf2 in cultured human podocytes (HPC), NIH3T3 and HEK293 cells. Immunoblotting for calnexin is used as a loading control. **(c)** Control WB showing expression of GFP-Schip1 in stably transfected HEK293 cells. **(d)** Control WB confirming expression of Schip1 in MycSchip1 transfected HEK293 cells, characterized by anti-Myc-tag and anti-Schip1 antibodies.

REFERENCES:

- 1 Russo LM, Bakris GL, Comper WD. Renal handling of albumin: a critical review of basic concepts and perspective. *Am J Kidney Dis* 2002; 39(5):899-919.
- 2 Welsh GI, Saleem MA. The podocyte cytoskeleton-key to a functioning glomerulus in health and disease. *Nat Rev Nephrol*; 8(1):14-21.
- 3 Takeda T. Podocyte cytoskeleton is connected to the integral membrane protein podocalyxin through Na⁺/H⁺-exchanger regulatory factor 2 and ezrin. *Clin Exp Nephrol* 2003; 7(4):260-269.
- 4 Takemoto M, He L, Norlin J, Patrakka J, Xiao Z, Petrova T, et al. Large-scale identification of genes implicated in kidney glomerulus development and function. *EMBO J* 2006; 25(5):1160-1174.
- 5 Goutebroze L, Brault E, Muchardt C, Camonis J, Thomas G. Cloning and characterization of SCHIP-1, a novel protein interacting specifically with spliced isoforms and naturally occurring mutant NF2 proteins. *Mol Cell Biol* 2000; 20(5):1699-1712.
- 6 James MF, Beauchamp RL, Manchanda N, Kazlauskas A, Ramesh V. A NHERF binding site links the betaPDGFR to the cytoskeleton and regulates cell spreading and migration. *J Cell Sci* 2004; 117(Pt 14):2951-2961.
- 7 Scoles DR. The merlin interacting proteins reveal multiple targets for NF2 therapy. *Biochim Biophys Acta* 2008; 1785(1):32-54.
- 8 Takeda T, McQuistan T, Orlando RA, Farquhar MG. Loss of glomerular foot processes is associated with uncoupling of podocalyxin from the actin cytoskeleton. *J Clin Invest* 2001; 108(2):289-301.
- 9 Mangeat P, Roy C, Martin M. ERM proteins in cell adhesion and membrane dynamics. *Trends Cell Biol* 1999; 9(5):187-192.
- 10 Manchanda N, Lyubimova A, Ho HY, James MF, Gusella JF, Ramesh N, et al. The NF2 tumor suppressor Merlin and the ERM proteins interact with N-WASP and regulate its actin polymerization function. *J Biol Chem* 2005; 280(13):12517-12522.
- 11 Curto M, McClatchey AI. Nf2/Merlin: a coordinator of receptor signalling and intercellular contact. *Br J Cancer* 2008; 98(2):256-262.
- 12 Pelton PD, Sherman LS, Rizvi TA, Marchionni MA, Wood P, Friedman RA, et al. Ruffling membrane, stress fiber, cell spreading and proliferation abnormalities in human Schwannoma cells. *Oncogene* 1998; 17(17):2195-2209.

- 13 Li Y, Kang YS, Dai C, Kiss LP, Wen X, Liu Y. Epithelial-to-mesenchymal transition is a potential pathway leading to podocyte dysfunction and proteinuria. *Am J Pathol* 2008; 172(2):299-308.
- 14 Kwasnicka-Crawford DA, Carson AR, Scherer SW. IQCJ-SCHIP1, a novel fusion transcript encoding a calmodulin-binding IQ motif protein. *Biochem Biophys Res Commun* 2006; 350(4):890-899.
- 15 Martin PM, Carnaud M, Garcia del Cano G, Irondelle M, Irinopoulou T, Girault JA, et al. Schwannomin-interacting protein-1 isoform IQCJ-SCHIP-1 is a late component of nodes of Ranvier and axon initial segments. *J Neurosci* 2008; 28(24):6111-6117.
- 16 Vitureira N, Andres R, Perez-Martinez E, Martinez A, Bribian A, Blasi J, et al. Podocalyxin is a novel polysialylated neural adhesion protein with multiple roles in neural development and synapse formation. *PLoS One*; 5(8):e12003.
- 17 Schmahl J, Raymond CS, Soriano P. PDGF signaling specificity is mediated through multiple immediate early genes. *Nat Genet* 2007; 39(1):52-60.
- 18 Chen WV, Delrow J, Corrin PD, Frazier JP, Soriano P. Identification and validation of PDGF transcriptional targets by microarray-coupled gene-trap mutagenesis. *Nat Genet* 2004; 36(3):304-312.
- 19 Saleem MA, O'Hare MJ, Reiser J, Coward RJ, Inward CD, Farren T, et al. A conditionally immortalized human podocyte cell line demonstrating nephrin and podocin expression. *J Am Soc Nephrol* 2002; 13(3):630-638.
- 20 Uhlen P. Visualization of Na,K-ATPase interacting proteins using FRET technique. *Ann N Y Acad Sci* 2003; 986:514-518.
- 21 Sun Y, He L, Takemoto M, Patrakka J, Pikkarainen T, Genove G, et al. Glomerular transcriptome changes associated with lipopolysaccharide-induced proteinuria. *Am J Nephrol* 2009; 29(6):558-570.
- 22 He L, Sun Y, Patrakka J, Mostad P, Norlin J, Xiao Z, et al. Glomerulus-specific mRNA transcripts and proteins identified through kidney expressed sequence tag database analysis. *Kidney Int* 2007; 71(9):889-900.
- 23 Armstrong CT, Vincent TL, Green PJ, Woolfson DN. SCORER 2.0: an algorithm for distinguishing parallel dimeric and trimeric coiled-coil sequences. *Bioinformatics*; 27(14):1908-1914.
- 24 Nielsen JS, McNagny KM. The role of podocalyxin in health and disease. *J Am Soc Nephrol* 2009; 20(8):1669-1676.
- 25 Wegner B, Al-Momany A, Kulak SC, Kozłowski K, Obeidat M, Jahroudi N, et al. CLIC5A, a component of the ezrin-podocalyxin complex in glomeruli, is a determinant of podocyte integrity. *Am J Physiol Renal Physiol*; 298(6):F1492-1503.

- 26 Pierchala BA, Munoz MR, Tsui CC. Proteomic analysis of the slit diaphragm complex: CLIC5 is a protein critical for podocyte morphology and function. *Kidney Int*; 78(9):868-882.
- 27 Baelde HJ, Eikmans M, Doran PP, Lappin DW, de Heer E, Bruijn JA. Gene expression profiling in glomeruli from human kidneys with diabetic nephropathy. *Am J Kidney Dis* 2004; 43(4):636-650.
- 28 Hall A. Rho GTPases and the actin cytoskeleton. *Science* 1998; 279(5350):509-514.
- 29 Maudsley S, Zamah AM, Rahman N, Blitzner JT, Luttrell LM, Lefkowitz RJ, et al. Platelet-derived growth factor receptor association with Na(+)/H(+) exchanger regulatory factor potentiates receptor activity. *Mol Cell Biol* 2000; 20(22):8352-8363.
- 30 Theisen CS, Wahl JK, 3rd, Johnson KR, Wheelock MJ. NHERF links the N-cadherin/catenin complex to the platelet-derived growth factor receptor to modulate the actin cytoskeleton and regulate cell motility. *Mol Biol Cell* 2007; 18(4):1220-1232.
- 31 Uehara G, Suzuki D, Toyoda M, Umezono T, Sakai H. Glomerular expression of platelet-derived growth factor (PDGF)-A, -B chain and PDGF receptor- α , - β in human diabetic nephropathy. *Clin Exp Nephrol* 2004; 8(1):36-42.

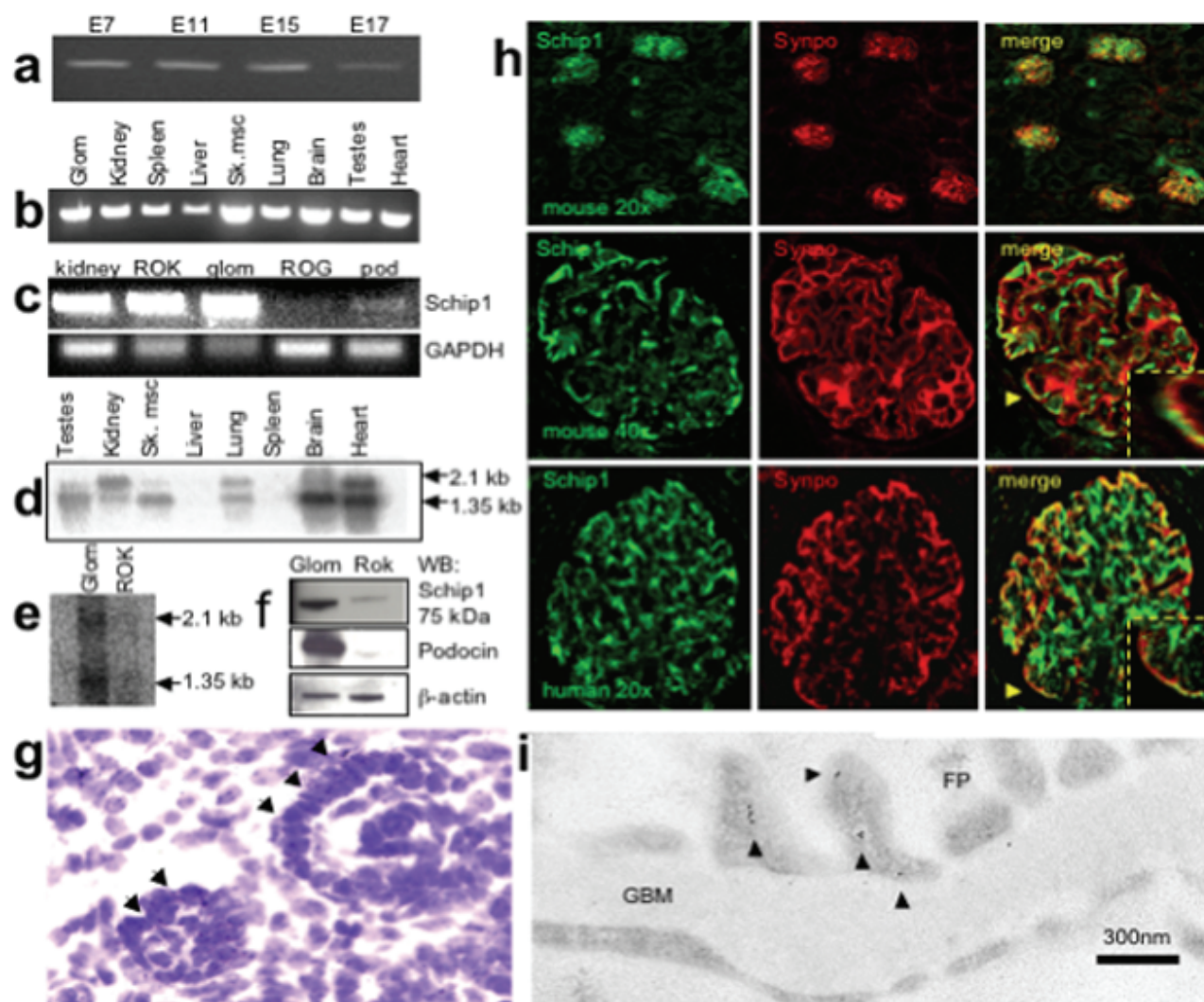


Figure 1

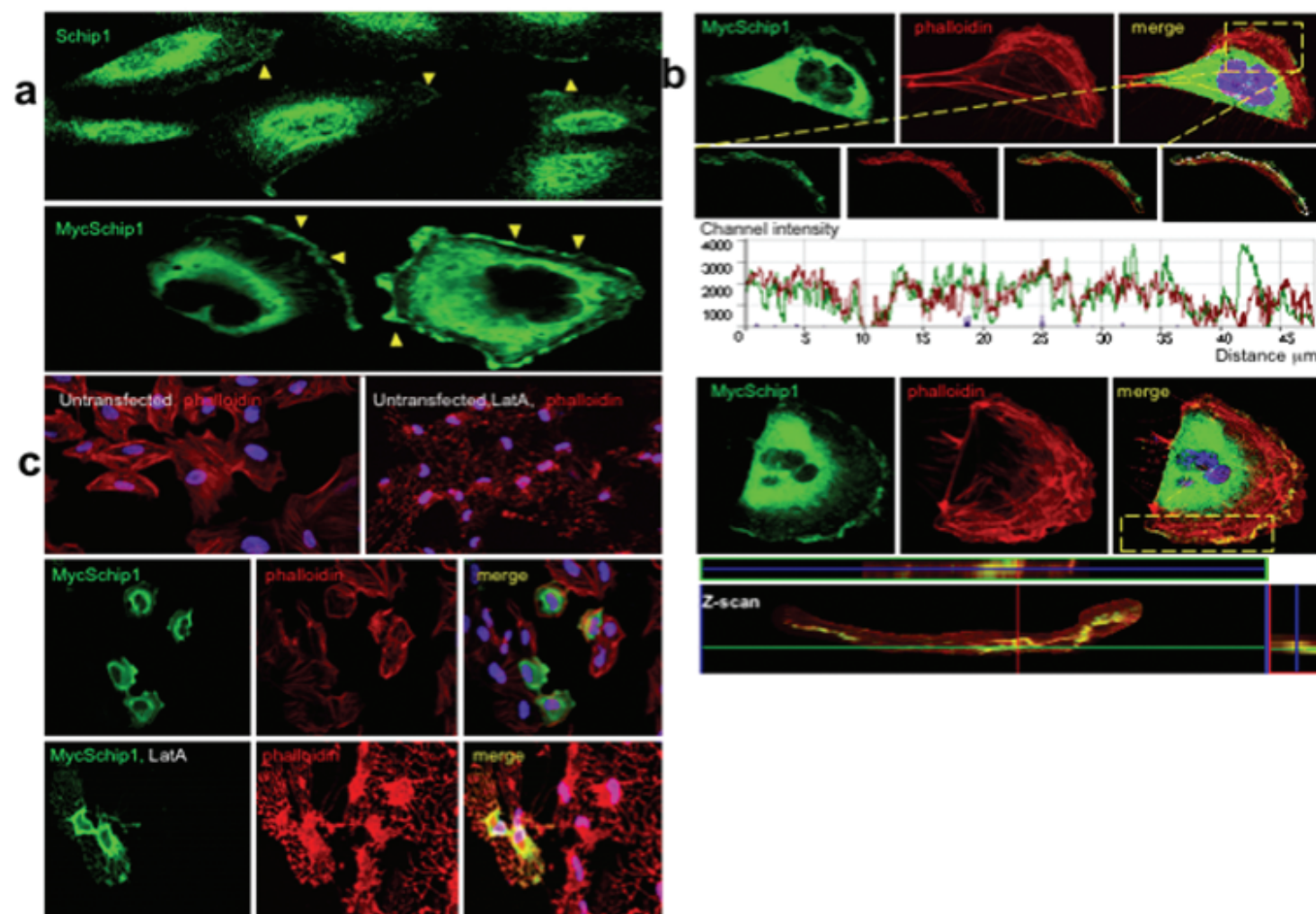


Figure 2

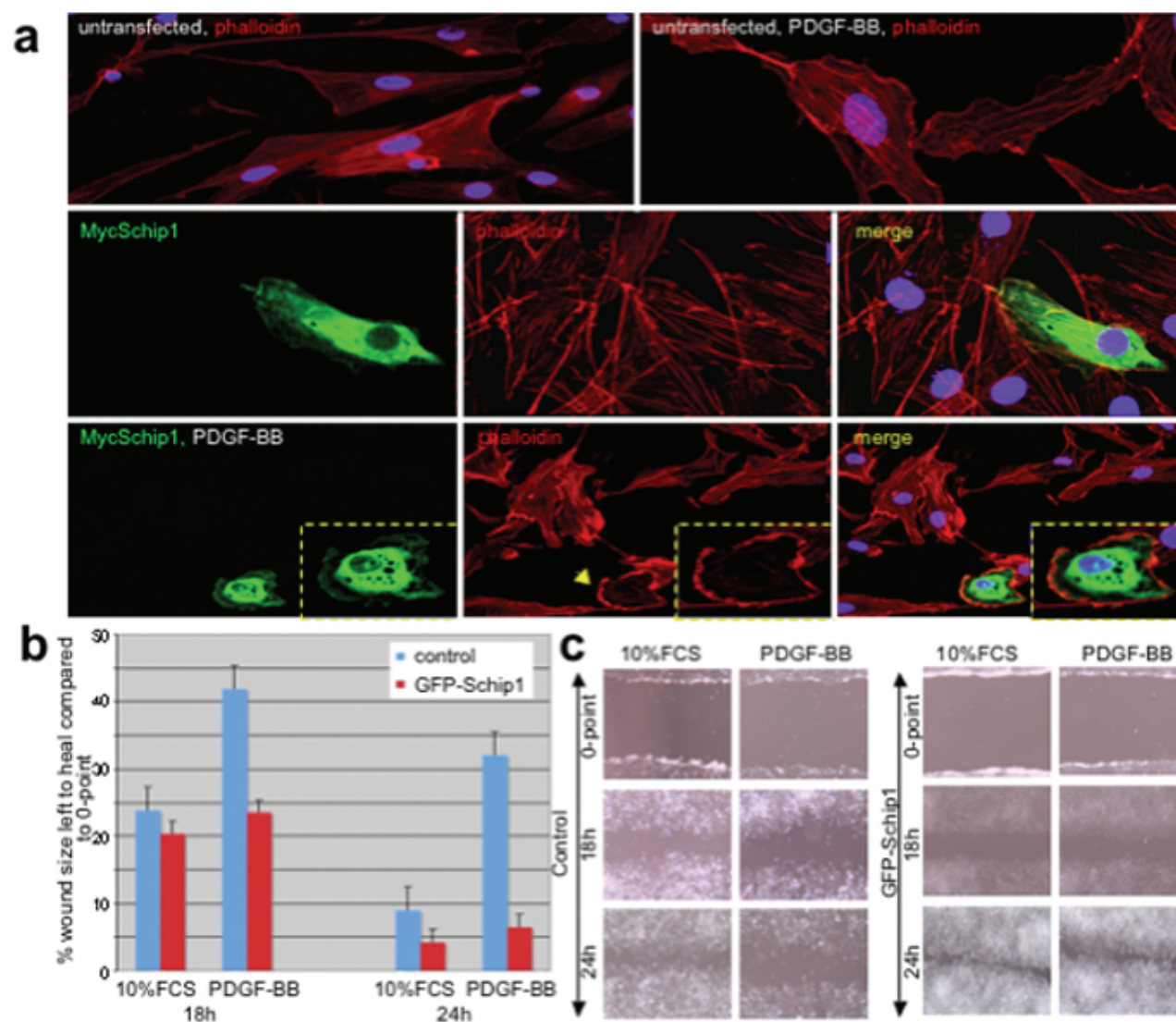


Figure 3

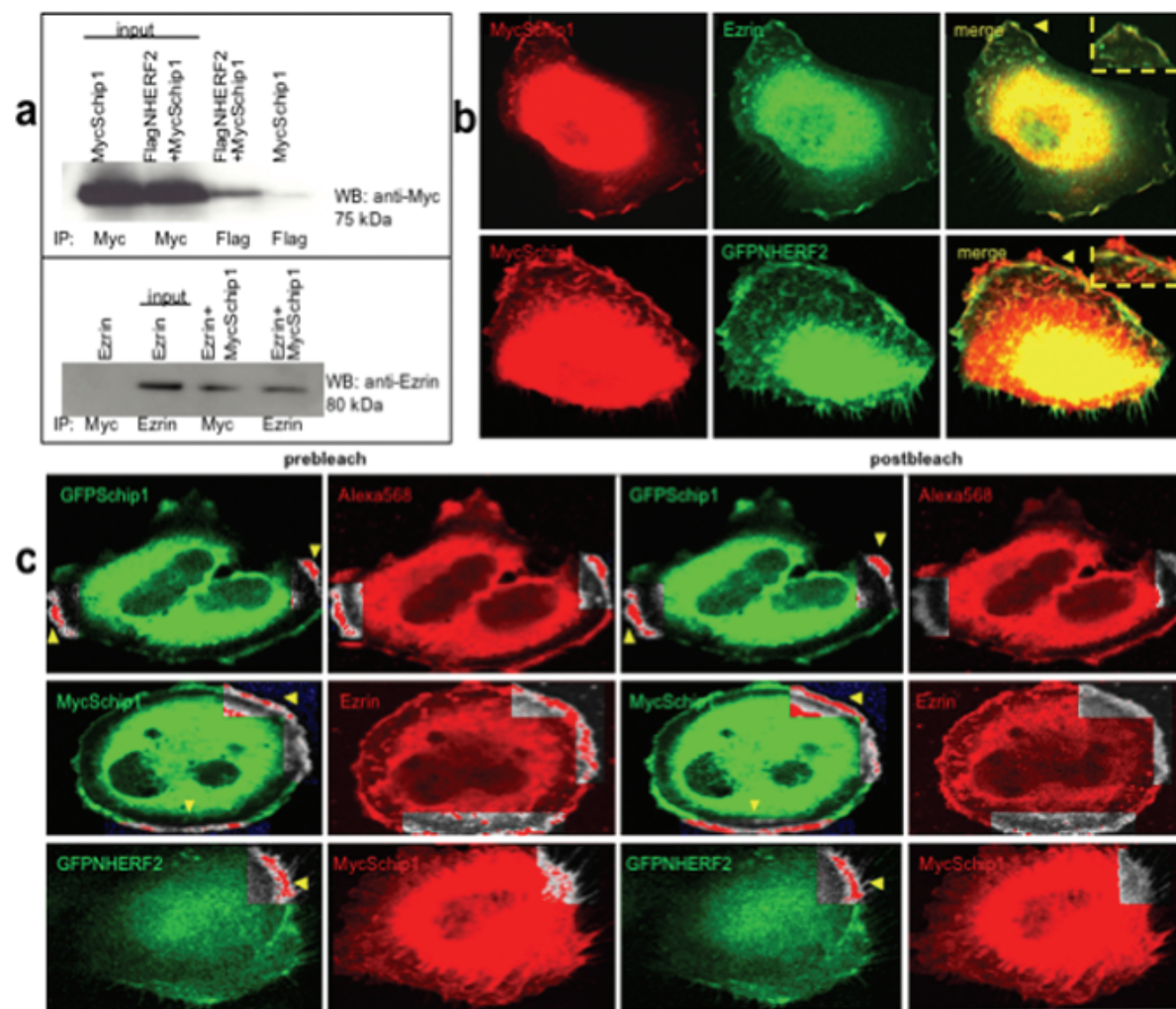


Figure 4

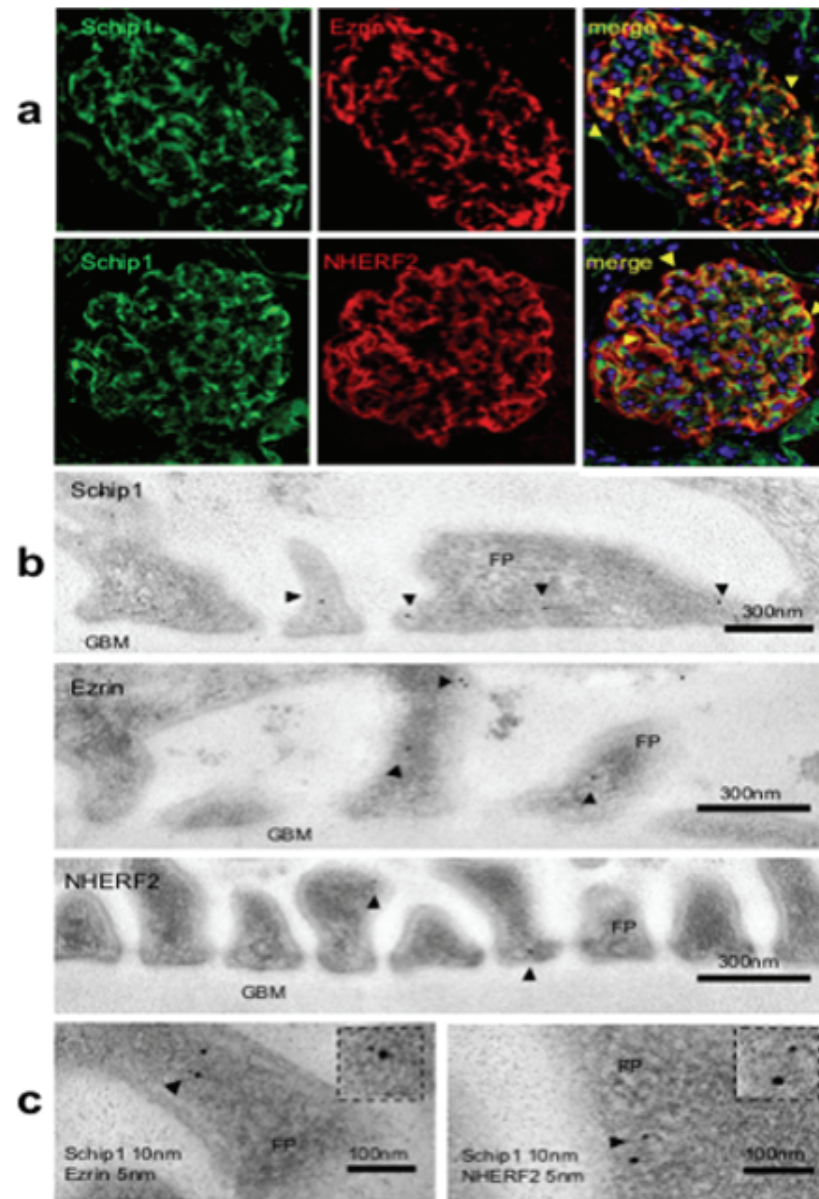


Figure 5

Gene Symbol	Gene Title	Adriamycin induced nephrosis		LPS induced model		Type II DB mice	
		log2(1weekADM/control)	Pvalue	log2(LPS/PBS)	Pvalue	log2(db/control)	Pvalue
Schip1	schwannomin interacting protein 1	-0.56	0.03	-0.13	0.09	1.10	0.0002
Ezr(villin)	ezrin	-0.22	0.26	-0.84	0.00	-0.01	0.930
Slc9a3r2(nherf2)	solute carrier family 9, isoform 3 regulator 2	0.015	0.96	-0.434	0.01	1.029	0.0004
Slc9a3r1(nherf1)	solute carrier family 9, isoform 3 regulator 1	-0.281	0.35	-0.265	0.03	0.614	0.004
ActB	actin, beta, cytoplasmic	0.14	0.26	-0.21	0.00	1.04	0.00
Nf2(merlin)	neurofibromatosis 2	-0.31	0.10	-0.17	0.03	0.32	0.016
Podxl	podocalyxin-like	-1.149	0.01	-1.023	0.00	0.499	0.026
Pdgfrb	platelet derived growth factor receptor beta	-0.594	0.13	-0.303	0.06	0.051	0.843

Figure 6

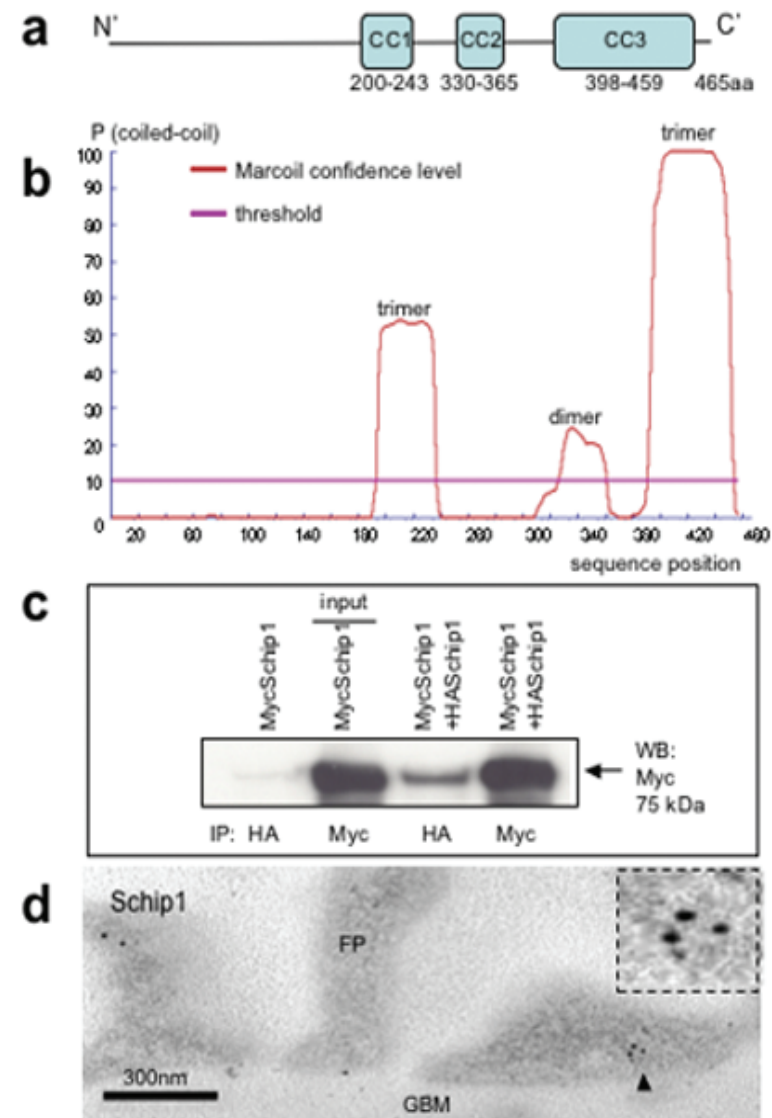


Figure 7

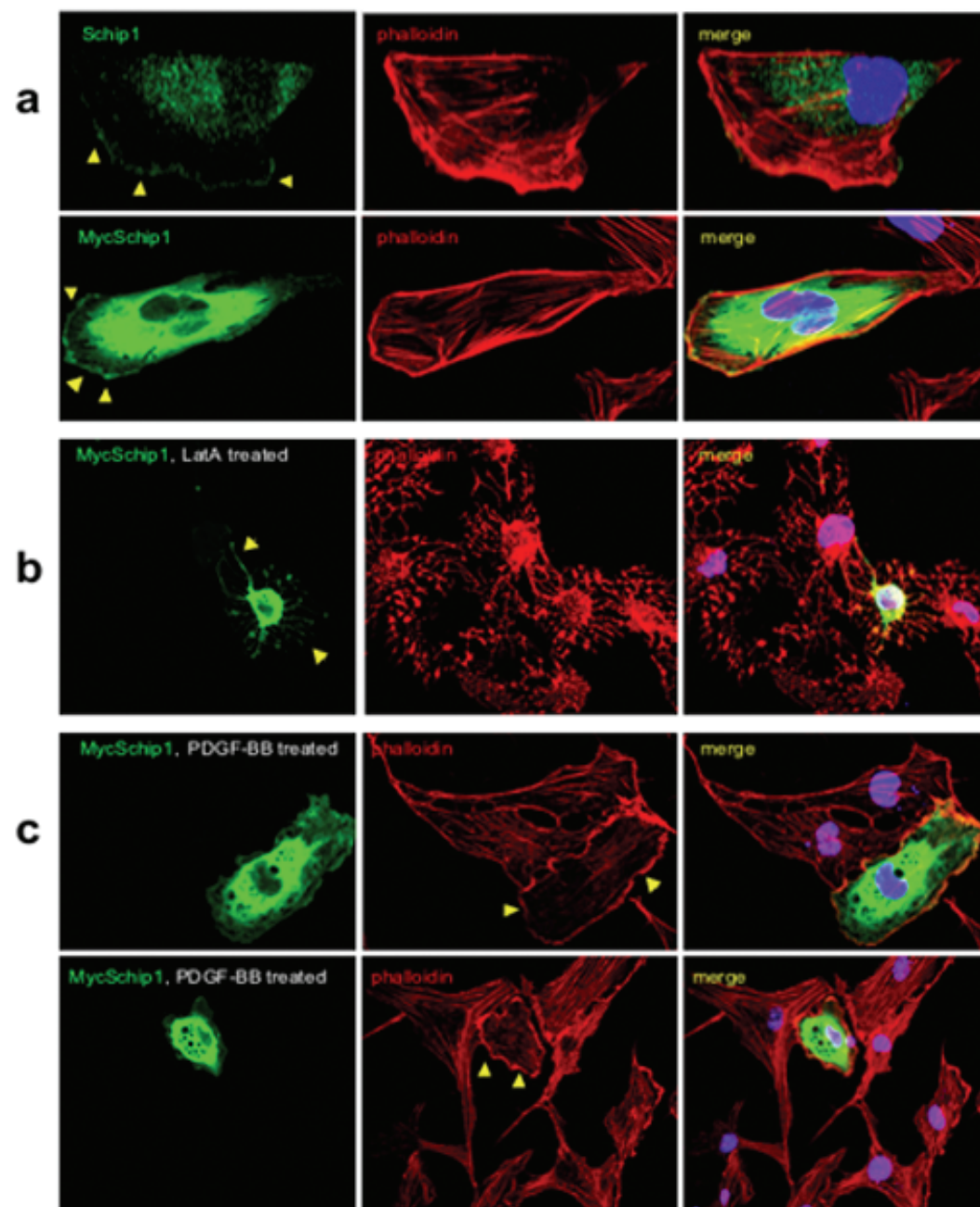


Figure S1

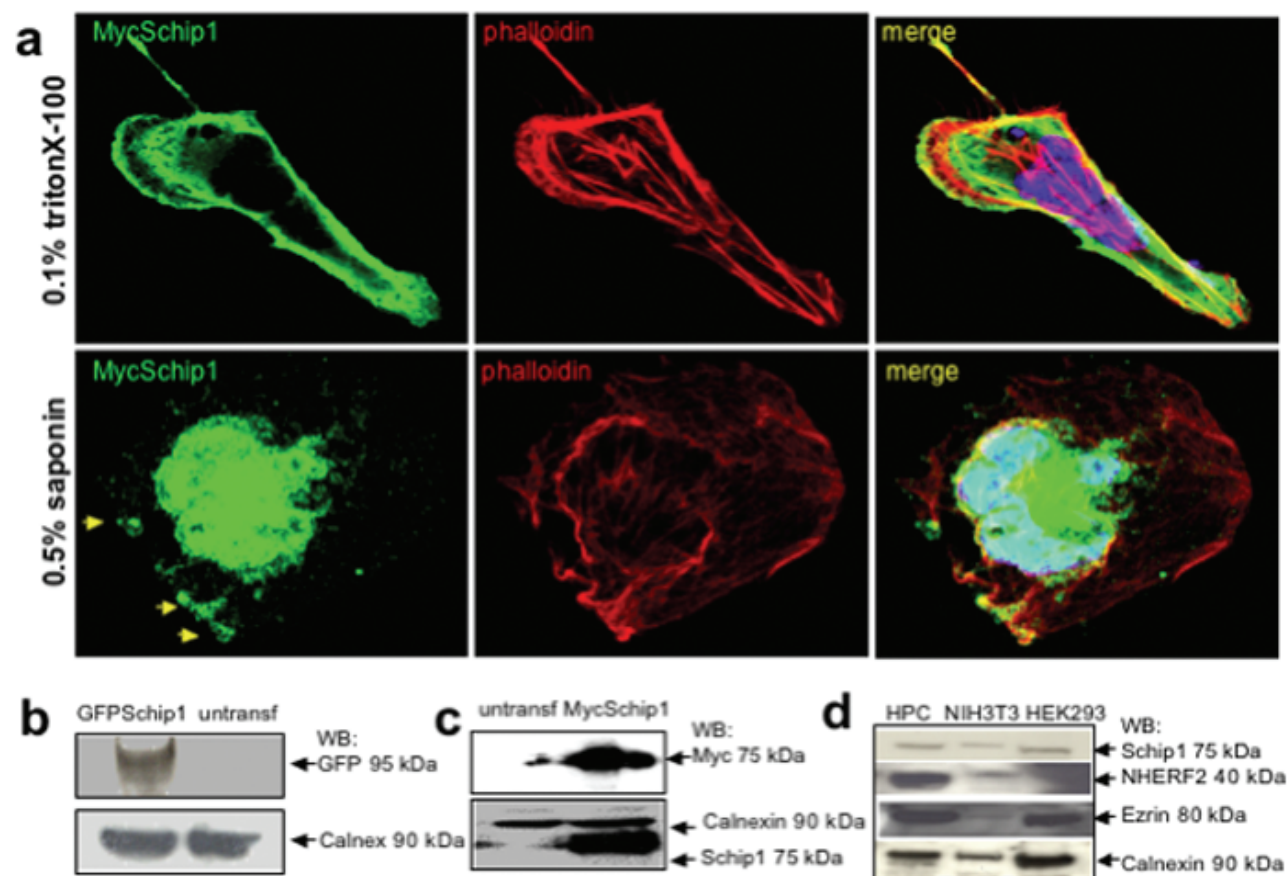


Figure S2